**Title**
Global analysis of biomineralization genes in magnetotactic bacteria



**Author**
McCausland, Hayley Catherine

**Publication Date**
2021

Peer reviewed|Thesis/dissertation

# Global analysis of biomineralization genes in magnetotactic bacteria

by

Hayley C McCausland

A dissertation submitted in partial satisfaction of the

requirements for the degree of

Doctor of Philosophy

in

Molecular and Cell Biology

in the

Graduate Division

of the

University of California, Berkeley

Committee in charge:

Professor Arash Komeili, Chair
Professor Michi Taga
Professor Sarah Stanley
Professor Daniel Portnoy

Summer 2021

Abstract

Genetic analysis of magnetotactic bacteria in changing environments

by

Hayley Catherine McCausland

Doctor of Philosophy in Molecular and Cell Biology

University of California, Berkeley

Professor Arash Komeili, Chair

Magnetotactic bacteria (MTB) are a phylogenetically diverse group of bacteria remarkable for their ability to biomineralize magnetite ($Fe_3O_4$) or greigite ($Fe_3S_4$) in organelles called magnetosomes. MTB can account for up to 30% of the microbial biomass in a an aquatic habitat [1]. MTB also take up large amounts of iron from the environment in order to form magnetosomes—they are estimated to take up anywhere from ~1-50% of dissolved iron inputs into the ocean [2]. However, relatively little is known about the ecology of MTB, other than species diversity in sampled habitats [3]. On the contrary, much is known about the genetics and cell biology of MTB. The majority of genes required for magnetosome formation are encoded by a magnetosome gene island (MAI) and many of their functions are known. However, no previous studies have involved unbiased genetic analysis of biomineralization genes. This work expands the genetic toolset for studying MTB in the lab and identifies novel genes—or functions of genes—that have an impact on biomineralization. Importantly, this dissertation also lays the groundwork to bridge the gap between genetic and environmental studies of MTB.

The first chapter of this dissertation, a published review article, covers the work that has been done on the genetics of MTB and where the field is headed. We focus on the genetics behind the formation of magnetosomes and biomineralization. Then, we cover the history of genetic discoveries in MTB and key insights that have been found in recent years and provide a perspective on the future of genetic studies in MTB.

The second chapter of this dissertation, a published primary research article, takes an unbiased approach to study genes, both inside and outside the MAI, needed for magnetosome formation under different growth conditions. First, we developed the use of random barcoded transposon mutagenesis (RB-TnSeq) in *Magnetospirillum magneticum* AMB-1 and generated a library of tens of thousands of unique mutant strains. The RB-TnSeq library allowed us to determine the essential gene set of AMB-1 under standard growth conditions. We also performed magnetic selection screen in varied growth conditions to uncover novel genes required for biomineralization in high iron and anaerobic growth conditions. We discovered more nuanced functions for the MAI gene *mamT* and several ex-MAI genes that may be important for biomineralization.

The third chapter of this dissertation, a published review article written in collaboration with Dr. Andy Tay, covers the potential uses for microfluidics devices for studying MTB from separating cells based on magnetic properties to directed evolution to single cell analysis. Being able to study magnetotactic bacteria in highly controlled, quantifiable environments will be a boon to the

field. Additionally, using microfluidics devices to mimic natural environments will be valuable for linking the cell biology and genetics of MTB to their ecology. I end the dissertation with a concluding chapter on the future prospects for employing genetics to understand the molecular mechanisms of biomineralization in a variety of environmental contexts.

Table of Contents

CHAPTER 1

# Magnetic genes: Studying the genetics of biomineralization in magnetotactic bacteria

Hayley C McCausland[a] and Arash Komeili[a,b]

Department of Molecular and Cell Biology, University of California, Berkeley, USA[a]; Department of Plant and Microbial Biology, University of California, Berkeley, USA[b]

This chapter has been adapted from following, with permission:
McCausland HC and Komeili A. Magnetic genes: Studying the genetics of biomineralization in magnetotactic bacteria. PLOS Genetics. 2020. 16(2): e1008499.

**Abstract:**

Many species of bacteria can manufacture materials on a finer scale than those that are synthetically made. These products are often produced within intracellular compartments that bear many hallmarks of eukaryotic organelles. One unique and elegant group of organisms is at the forefront of studies into the mechanisms of organelle formation and biomineralization. Magnetotactic bacteria (MTB) produce organelles called magnetosomes that contain nanocrystals of magnetic material, and understanding the molecular mechanisms behind magnetosome formation and biomineralization is a rich area of study. In this Review, we focus on the genetics behind the formation of magnetosomes and biomineralization. We cover the history of genetic discoveries in MTB and key insights that have been found in recent years and provide a perspective on the future of genetic studies in MTB.

**Introduction:**

Bacteria, according to the canonical definition, do not have subcellular compartments for organization or specialized functions. Yet microbiologists are becoming increasingly aware that many bacteria do have organelles, some of which are capable of manufacturing biomaterials with specialized functions [4]. Magnetotactic bacteria (MTB) present a particularly elegant example of the biological behaviors that are mediated by intracellular compartments [5]. MTB are a group of bacteria spanning multiple phyla that can be found in aquatic environments all over the world [1,3,6], where they inhabit low oxygen environments, and are most often found at the oxic-anoxic interface in the water column or sediments [7]. MTB are characterized by their ability to form organelles called magnetosomes, which are lipid-bounded compartments in which biomineralization of magnetic crystals of magnetite ($Fe_3O_4$) and/or greigite ($Fe_3S_4$) occurs [3]. Magnetosomes align in one or multiple chains along the cell, creating a magnetic dipole that allows MTB to passively align along Earth's magnetic field lines [8]. This is thought to help MTB perform more efficient chemotaxis and aerotaxis in the water column as their swimming behavior is restricted to one dimension, instead of a three dimensional run and tumble search; a process called magnetoaerotaxis [7]. The regulated process of biomineralization has made MTB an attractive area of study in basic and applied biology, geochemistry, and physics alike. A greater understanding of the molecular processes needed to form magnetosomes will enhance studies in each of these fields, as knowledge of what is occurring on a molecular scale can lend greater precision to technical applications and provide systems-level information for studying the large scale impacts of MTB.

The ecological impact of MTB is one rising area of research in the field. In recent years our understanding of the diversity of MTB has expanded greatly. In the process of biomineralization of magnetite or greigite, MTB take up large amounts of dissolved iron from the surrounding environment and sequester it in magnetosomes as iron crystals. As such, the role that MTB play in iron cycling in both freshwater bodies and the ocean is potentially quite large [2,6]. Conservative estimates from Amor et al. indicate that estuarine and oceanic MTB may take up anywhere from ~1-50% of dissolved iron inputs (~$9x10^8$ kg/year) in their environments [2]. Having a greater understanding of the iron regulation strategies encoded within the genomes of magnetotactic bacteria, as well as how iron is taken up and distributed to magnetosomes, is important for a more accurate picture of the role of MTB in their aquatic environments.

In this same vein, fossils of magnetosomes can help us understand the environmental conditions that were present when MTB originated and the evolution of life on Earth. Magnetofossils—currently dating back to ~1.9Ga —may reflect changes that occurred in sediments and the water column and have the potential to serve as an indicator of redox and oxygen levels in ancient environments [9]. Based on phylogenetic analyses, the origins of

biomineralization may have occurred much earlier, in the mid-Archaean (~3Ga), where the ability to biomineralize may have provided an advantage in coping with reactive oxygen species, avoiding harmful UV radiation, and/or navigating ferrous iron gradients [10,11]. Understanding the genetic factors behind the formation of magnetosomes that are common across modern MTB can provide insight into the conditions and processes that were present when the first MTB originated [12]. Genetic analysis may uncover unknown functions of magnetosomes. And a greater understanding of how magnetosomes form can hint at the conditions that were needed to produce ancient magnetosomes.

Additionally, the use of magnetotactic bacteria in various biotechnological applications is promising. Magnetosomes are currently being developed for use as magnetic resonance imaging (MRI) contrast agents, drug delivery systems, hyperthermic and photothermic treatments for cancer, bioremediation of heavy metals, and other nanotechnologies [13–15]. In order to efficiently produce the large numbers of magnetosomes required in these applications, it is critical to understand how magnetosomes are produced.

Taking up iron from the environment for biomineralization, producing phospholipid membranes of a specific size, and aligning magnetosomes in a chain is a complex, tightly controlled process—one that is interesting in itself, but also provides insight into the precise formation of organelles more generally. Magnetotactic bacteria encode the genes necessary for these processes in magnetosome gene clusters (MGCs) [16,17]. The MGCs in the most well-studied model organisms—*Magnetospirillum magneticum* AMB-1, *M. gryphiswaldense* MSR-1, and *Desulfovibrio magneticus* RS-1 (Fig. 1)—are structured as magnetosome gene islands (MAIs). In both AMB-1 and RS-1, the MAI is defined by repeat regions on either side of the large chromosomal region [18,19]. Across related species, there is a large amount of genetic homology in the MAI [20]. The functions of many of the genes within MGCs have been investigated, but much remains unknown in each of the model organisms, and there is even more to be discovered about other species and phyla of MTB.

In this review, we lay out the history of landmark genetic discoveries in revealing important insights into the process of magnetosome and biomineral formation by MTB. We also dive into more nuanced views of genetics that have come out in recent years, in step with advances in genetic techniques. Finally, we will address the next directions that the field is taking to learn more about the genetics of MTB.

## Section 1: Genetics in *Magnetospirilla*

The discovery of MTB [8] fueled broad interest in understanding, and exploiting, the process of organelle formation and biomineralization. Development of genetic systems greatly accelerated the discovery of the molecular basis of magnetosome formation at a refined level. *M. magnetotacticum* MS-1 was the first magnetotactic bacterium to be isolated in pure culture [21]. However, MS-1 did not become a major model system for genetics since conditions that support colony growth on solid media have not been identified. Subsequently, AMB-1 and MSR-1 were successfully cultured and established as model organisms in the lab, making it possible to manipulate and investigate their genomes [22–24].

### 1.1 Early studies of MTB genetics

The first genetic studies in MTB involved transposon mutagenesis coupled with magnetic selection and transmission electron microscopy (TEM). Matsunaga et al. (1992) performed mutagenesis in AMB-1 with the Tn5 transposon [22]. They identified several genomic fragments involved in magnetosome synthesis by picking out mutant cultures that no longer responded to a magnet under a light microscope. After confirming the mutants were deficient in magnetosome formation with electron microscopy, they used restriction mapping to narrow down the location of each insertion site in the genome. One of these mutants carries a transposon insertion in

*magA*, a gene encoding a cation efflux pump proposed to function in iron transport [25]. Importantly, this study also demonstrated that it was possible to transfer plasmid DNA to AMB-1 using conjugation.

Large strides were made in understanding MTB genomes in the early 2000s. Wahyudi et al. (2001) also isolated Tn5 transposon mutants in AMB-1 and found colonies with defects in biomineralization by looking at colony color, which is thought to be an indicator of how much magnetite has accumulated in the cell [26]. They concluded that at least 10, and up to 60, genes could be involved in magnetosome formation. The publication of the genome sequences of MS-1 and *Magnetococcus marinus* MC-1 also opened the door to genome level studies [27,28]. Grünberg et al. (2001) compared protein sequences isolated from MSR-1 magnetosomes to those in the MS-1 and MC-1 genomes and found two gene clusters containing genes (*mamA, mamB, mamC,* and *mamD*) we now know to be critical for magnetosome formation [29].

The key genomic region needed for magnetosome formation, the MAI, was discovered when spontaneous non-magnetic mutants of MSR-1 were isolated from a wild-type population of cells [17]. It was characterized as a 130kb region containing multiple insertion sequence (IS) elements [18]. The AMB-1 gene island was described as a 98kb region flanked by two 1.1kb repeat sequences [16]. A study of transcription of MAI genes indicated that while magnetosome genes are organized in operons, they are constitutively expressed [30]. Identifying the MAI narrowed down the pool of genes to investigate and provided a foundation for more targeted genetic studies.

In addition to defining the MAI, the establishment of MSR-1 and AMB-1 as model systems allowed for more detailed molecular and genetic analyses [31,32]. A transposon mutagenesis screen by Komeili et al. (2004) used a magnetic selection to enrich for non-magnetic mutants [33]. Colonies were then grown in 96-well plates and screened for magnetic response using a 24-pin magnetic plate (Fig. 2A). In this study, transposon insertions within the *mamAB* gene cluster of the MAI resulted in nonmagnetic mutants. This work proved to be a great complement to proteomic studies that had found the same MAI-encoded proteins associated with magnetosomes [34].

Transposon mutagenesis studies proved to be a key turning point in using genetics to understand the process of biomineralization in MTB. However, much like many other genetic studies, their interpretation and broader utility were complicated by several confounding factors. First, due to homologous recombination between repeated sequences or potential action of transposases, the MAI is unstable and can be lost spontaneously, an event that is more likely to occur under stress conditions [18]. If transposition occurs in a bacterium that has lost its MAI, or if the MAI is lost following transposition, otherwise neutral events may appear linked to changes in the magnetic phenotype. Screening potential mutants for the presence of the MAI proved essential in isolating mutations in the *mamAB* region [33].

Second, many magnetosome genes contain functional paralogs that play redundant roles. In AMB-1, three genes (*mamQ, mamR,* and, *mamB*) from the *mamAB* operon are perfectly duplicated in another segment of the MAI [35]. Additionally, the AMB-1 genome contains a magnetosome gene islet, a region outside of the MAI, which includes several homologs of *mamAB* genes [36,37]. As a result, the absence of a distinct phenotype when any of the duplicated genes are deleted individually does not rule out the possibility that they play a role in magnetosome formation. Thus, in many cases, multiple genes must be deleted to understand the function of a specific gene and its interactions with other genes. Additionally, complementing deletions becomes critical for the evaluation of gene function.

Third, magnetosome genes are often organized as operons and transposon insertions result in the polar loss of expression for all downstream genes. Thus, it is difficult to link a specific phenotype to the loss of one single gene. Finally, by necessity, these studies used the magnetic phenotype as a quick screening method to find relevant mutants. The secondary screens of transposon mutants were important for establishing which step in the magnetosome formation

process was affected by a particular mutation and allowed for assigning more specific functions to genes (Fig. 2B). For example, a non-magnetic mutant might make magnetosome membranes but not form crystals, indicating the interrupted gene was likely involved in crystal formation. Or a non-magnetic mutant might not make membranes at all, suggesting the site of transposon insertion is a key part of magnetosome membrane formation.

### 1.2 Dissecting *Magnetospirillum* genomes

Obtaining the full genome sequences of the primary model organisms (MSR-1 and AMB-1) propelled genetic investigations of MTB forward [32,38]. Previous studies provided limited functional detail about any particular gene, at times involved looking at large deletions of multiple genes, and had complicating factors, as mentioned above. Deleting individual genes was necessary for a more complete picture of magnetosome formation.

Murat et al. (2010) used previously developed methodology to thoroughly dissect the MAI in AMB-1 by creating targeted deletions of genes and operons [35]. They began with the observation that the loss of the MAI results in complete absence of both magnetosome membranes and magnetic particles. Using a double recombination method for generating nonpolar deletions, they first made mutants lacking larger subsections of the MAI [33]. Next, they focused on the regions that showed dramatic phenotypes such as small particles or complete loss of the magnetosome membrane. Finally, they deleted individual genes within these flagged regions and used a suite of secondary screens to assign specific functions to the genes. Various electron microscopy techniques were used to visualize the magnetosome membrane as well as the size, morphology, and subcellular arrangement of magnetic particles. GFP fusions to model magnetosome proteins were used to monitor protein localization.

Through multiple layers of analysis, Murat et al. described the possible functions of many of the key magnetosome formation genes in AMB-1, like *mamE, mamN, mamM, mamO, mamI, mamL, mamQ,* and *mamB*. Lohße et al. (2011, 2014) dissected the MAI in MSR-1 [39,40] and found similar results, except that *mamI* and *mamN* were not essential for magnetosome formation in MSR-1. This discrepancy might be due to the particular growth conditions used obscuring more subtle differences between the two species. It may also reflect broader divergence between the two organisms. Heterologous expression of the *mamAB* and *mms6* operons, plus *mamGFDC* and *mamXYZ* was found to be sufficient to produce magnetosomes in the non-magnetic $\alpha$-proteobacterium *Rhodospirillum rubrum* [41], highlighting both the importance of these operons in magnetosome formation and the minimal gene set needed to make magnetosomes under laboratory conditions.

These studies of the AMB-1 and MSR-1 islands provided a broad overview of the functions of genes in the MAI. Further studies dove into investigating the functions of individual genes in magnetosome formation and their mechanisms of action. The general framework that magnetosome genes are important for either membrane formation (Fig.3E) [42–44] or biomineralization (Fig.3C-D) [45–52] holds true. A third category of genes that are involved in chain organization has become an important area of study in recent years [37,53–58](Fig.3A-B). At the center of the chain arrangement process is an actin-like protein called MamK. Dynamic polymerization behavior of MamK is required for the integrity and proper segregation of the chain during cell division [53–57,59,60]. The proteins MamJ and MamY are also key components of chain formation. MamJ acts as a link between MamK filaments and magnetosomes [53]. MamY is a cytoplasmic membrane protein that works to align the magnetosome chain along the cell's motility axis, which likely improves the efficiency of magnetotaxis [58]. To add nuance to the broad categories, more specific functions of genes involved in each stage of the process are being discovered as techniques and tools improve. More detailed summaries of the genes and proteins responsible for magnetosome formation can be found in previously published review articles (Fig.3F) [61–63].

In addition to the limits of techniques used in genetic analysis, the growth conditions of MTB are an important factor to consider when examining the phenotype of particular genes. Genes both inside and outside the MAI have been found to have important roles in biomineralization, but only under certain conditions. For example, within the MAI Δ*mamX*, Δ*mamZ*, Δ*mamH*, and Δ*ftsZm* strains only show defects in biomineralization when MSR-1 is grown with ammonium in place of nitrate, indicating that the use of oxygen instead of nitrate as the terminal electron acceptor is detrimental to magnetosome formation [64–66]. Genes outside the island, like the *nap* operon encoding nitrate reductase genes [67] and the cytochrome *c* oxidase *cbb3* [68] are also key in the biomineralization process, again highlighting the importance of redox processes in magnetosome formation [69]. It is possible that these metabolic pathways generate an overall redox balance within the cell that is compatible with biomineralization, which requires both ferric and ferrous iron to be present. Alternatively, they may participate directly in generating a redox-balanced iron pool that will allow for magnetite biomineralization.

Another key environmental factor to consider in magnetosome formation is the availability of iron. Unsurprisingly, genes involved in regulating the uptake of iron have been connected to biomineralization. MSR-1 contains a gene that is homologous to the ferric uptake regulator (*fur*) genes common among bacteria [70]. This *fur*-like gene affects magnetosome size and number—potentially due to reduced incorporation of iron into magnetite and an increase in cytoplasmic iron concentrations—as well as transcription levels of several key MAI genes, including the *mamGFDC* and *mms6* operons [71]. Deletion of *feoB1*—which is involved in transport of ferrous iron into the cell—in MSR-1 resulted in fewer and smaller magnetosomes, as well as decreased uptake of iron [72]. In AMB-1, the *feoAB* operon showed increased levels of transcription under iron-rich conditions and was associated with an increase in intracellular iron levels, suggesting that it is a component of iron uptake in AMB-1 [73]. Ferric iron transporters were downregulated in the same high iron conditions. While the *feoAB1* operon is within the MAI, it is not a magnetosome-associated protein and thus its regulation of magnetosome formation is indirect. MS-1 also expresses *feoB*, indicating that iron uptake systems are conserved across species of MTB [74]. The iron response regulator IrrB was shown to be important for magnetosome formation in MSR-1 and deletion affected the transcription of several genes involved in the regulation of iron uptake [75]. These studies taken together indicate that iron availability is an important factor to consider in magnetosome formation and genetic regulation.

**Section 2: Genetics and genomics of diverse MTB**

As described above, work in the model organisms MSR-1 and AMB-1 has identified many of the genes that are important for the formation and positioning of magnetosomes. However, MSR-1 and AMB-1 are both α-proteobacteria species and MTB are an incredibly diverse group of organisms with strains found in several classes of Proteobacteria, as well as Nitrospirae and the candidate division OP3 [3]. Little is known about the formation of magnetosomes in non-model organisms. The genetic studies in MSR-1 and AMB-1 have been used as jumping off points for the newer model system *Desulfovibrio magneticus* RS-1, as well as uncultured species of MTB like those from other classes of proteobacteria and the phyla Nitrospirae [20]. Additionally, improved sequencing technologies have allowed the field to study the phylogeny of MTB using more relevant magnetosome genes, instead of standard housekeeping genes.

**2.1 The magnetosome gene island in *Desulfovibrio magneticus* RS-1.**

The establishment of the δ-proteobacterium RS-1 as a model system has opened up the field to studying the genetic diversity of magnetosome formation. In the phylogeny of proteobacteria, the δ-proteobacteria class is deeply branching, relative to α-proteobacteria. As such, research into δ-proteobacteria can provide valuable insight into the origins of MTB. Through the study of

RS-1 it has been found that, in addition to a core set of genes required across all magnetotactic bacteria, different types of MTB have distinct genes for magnetosome formation. Presumably the genes evolved to adapt to the diverse lifestyles of each organism.

Comparative genome analysis of a variety of δ-proteobacteria revealed that many of the genes required for magnetosome formation in α-proteobacteria are shared by the δ-proteobacteria, though some of the genes in the *mamAB* operon and the entire *mamGFDC* operon are missing [19]. It was discovered in the same study that the δ-proteobacteria and Nitrospirae MTB have a separate set of class-specific genes termed the *mad* genes, which are likely involved in the production of bullet-shaped magnetite crystals. Additionally, Nitrospirae MTB have another set of genes, the *man* genes, that may be involved in the processes of magnetosome formation and/or chain arrangement that are particular to Nitrospirae [76]. The magnetosome gene sets that appear in different phyla provide a convincing link between genetic differences and the clear phenotypic differences seen across MTB. Model organisms from the δ-proteobacteria and Nitrospirae are necessary to study the functions of *mad* and *man* genes.

In 1993, RS-1 was discovered as a sulfate-reducing MTB [77] and later identified as a *Desulfovibrio* species [78]. RS-1 is an obligate anaerobe that synthesizes bullet-shaped magnetite crystals, as opposed to the cubo-octahedral crystals produced by the α-proteobacteria MTB species. While RS-1 was successfully cultured in the lab, attempts to delete individual genes were unsuccessful at first. Rahn-Lee et al. got around this problem with a classic forward genetic screen using random chemical and UV mutagenesis followed by whole genome sequencing of non-magnetic mutants of RS-1 [79]. Both *mam* genes and *mad* genes were found to be important in biomineralization, as were several novel MAI genes, including the ion transport genes *tauE* and *kup*. Genetic tools for deleting specific genes in RS-1 were only recently developed. Using suicide vectors for targeted gene deletion—as is commonly done in other bacterial systems—does not work in RS-1 due to low transconjugation and recombination rates. Grant et al. developed a strategy using replicative plasmids that carry positive and negative selectable markers to replace the gene of interest with an antibiotic resistance gene [80].

The study of magnetosome formation in RS-1 also identified a novel organelle consisting of iron-phosphorous granules surrounded by a membrane [81]. Byrne et al. showed that these granules are separate organelles and not precursors to the formation of magnetite with a pulse chase experiment using different stable isotopes of iron. This conclusion was further solidified by the finding that the deletion of the entire MAI of RS-1 had no impact on the formation of the iron-rich granules [79]. The genetics of these novel bacterial organelles is a rich area for future investigation.

### 2.2 The MAI in non-model/uncultured MTB

The genetic differences that have already been found between MSR-1, AMB-1, and RS-1 highlight the need to study diverse MTB species in order to more fully understand magnetosome formation and function(s). The rapid improvements in sequencing technologies in recent years—in addition to the elegant method for isolating MTB using an external magnetic field—have made it possible to study uncultured organisms in greater detail [82]. The genomes of many uncultured MTB have been sequenced and analyzed in detail [19,27,41,76,83–85], revealing that MTB belong to a wide variety of bacterial phyla. Metagenomic analyses are also contributing greatly to our knowledge of the diversity of MTB and their evolutionary history [10,20].

In the realm of non-model organisms, greigite-producing strains provide an interesting case to study the evolution of MTB. Work by DeLong et al. analyzing 16S rRNA gene sequences suggested that greigite-producing strains and magnetite-producing strains evolved separately

[86]. However, a later analysis by Abreu et al. found that the greigite-producing strain *Candidatus* Magnetoglobus multicellularis has some of the *mam* genes that magnetite-producing strains require to produce magnetosomes, suggesting a monophyletic origin for MTB [87]. Lefèvre et al. (2011) discovered the δ-proteobacteria *Desulfamplus magnetovallimortis* BW-1 and found that it is capable of producing both magnetite and greigite [85]. Interestingly, the BW-1 genome has *mam* genes in two separate magnetosome gene clusters (MGCs). Proteins encoded in one cluster are closely related to proteins found in magnetite-producing species, while those in the second cluster are more closely related to the proteins encoded in the MGCs of greigite producers. The simplest hypothesis emerging from these genomic insights is that each cluster is responsible for producing a chemically distinct magnetic mineral. Lefèvre and colleagues used the unique MGCs of BW-1 to examine phylogenetic differences between magnetite-producing and greigite-producing strains [19]. Genes required for producing magnetite-containing magnetosomes are clustered together, as are those required for producing greigite-containing magnetosomes, suggesting that there are separate sets of genes (and proteins) involved in forming each type of crystal. However, the *mad* genes, which are needed to form bullet-shaped magnetosomes, are present in both clusters. It is still unclear if *mad* genes were lost during the evolution of magnetite-producing strains that do not form bullet-shaped crystals or if they were acquired separately by δ-proteobacteria and Nitrospirae strains of MTB. Analysis of the α-proteobacteria PR-1 also indicated that evolution of MTB likely involved both vertical inheritance and horizontal gene transfer (HGT) or duplication events [84].

Looking further into the origins of MTB, Lefèvre et al. (2013) compared phylogenies of several α, δ, and γ-proteobacteria and one Nitrospirae MTB species. They constructed phylogenetic trees using either 16S rRNA gene sequences and housekeeping genes or common Mam proteins [88]. They found that both trees showed a similar pattern of divergence, leading to the conclusion that all modern day Proteobacteria and Nitrospirae had a magnetotactic common ancestor, though they did not rule out the possibility of an ancient HGT event. Two recent studies from Lin *et al.* analyzed metagenomic data to gain insight into the origins of MTB [10,20]. The first study analyzed the genomes of multiple magnetotactic Nitrospirae strains and found that the gene content and order in the magnetosome gene clusters were conserved across the Nitrospirae, indicating a common origin. In the second study, a wide variety of MTB genomes were analyzed using core magnetosome proteins and the phylogenetic trees showed MTB clustering together. The authors concluded, like Lefèvre et al., that HGT of magnetosome genes were likely rare events. The simplest conclusion based on these studies is that all MTB originated from a common ancestor. In fact, using commonly accepted molecular clocks, it can be estimated that the original MTB—and presumably the first instance of magnetosome formation—appeared approximately 3.2 billion years ago [10]. An additional implication of this work is that at some point in the past the last common ancestor of the Proteobacteria, Nitrospirae, Omnitrophica, Latescibacteria, and Planctomycetes phyla had the genes necessary for magnetosome formation, or that the last common ancestor of Proteobacteria, Nitrospirae, and Omnitrophica phyla had the genes for magnetite production, specifically. Subsequently, most members of these groups lost the magnetosome genes while the few remaining MTB retained the magnetosome formation genes and some phyla acquired the magnetosome genes through horizontal gene transfer. The environmental conditions and changes that initially favored the evolution and expansion of magnetosome formation genes and later selected against them in the majority of bacteria remain to be elucidated. Perhaps, genetic studies of other model MTB are needed to understand the potential contributions of group-specific genes (such as *mad* and *man* genes) to the evolution and phenotypic diversification of magnetosomes.

The study of uncultured MTB has also been aided through the analysis of gene function in model MTB. Take, for example, the MAI genes *mamE* and *mamO*, which are critical for

biomineralization in both AMB-1 and MSR-1 [35,89]. Both gene products are predicted serine proteases and initial genetic studies concerning their functions concluded that this was indeed the case [90]. However, further biochemical and structural studies revealed that the active site of MamO is not functional and that it is in reality a metal-binding protein that is necessary for the proteolytic activity of MamE [91,92]. Phylogenetic analyses showed that, similar to AMB-1, all proteobacterial MTB encode an active and inactive protease in their magnetosome gene clusters [91]. The active protease is ancestral to all MTB and has been diversified through vertical descent. However, the inactive protease has arisen multiple times in MTB through duplications of the active protease or acquisition via HGT. These insights were only possible through a combination of genetic, genomic, and biochemical studies. They highlight the critical analyses needed in studies where duplication events and diversification of function of similar proteins can blur the accuracy of phylogenetic studies. They also show that the study of a protein in one species of MTB may not clarify the function of a homologous protein in another related organism.

**Section 3: Outlook**

Huge strides have been made in understanding the genetics behind magnetosome formation. While the minimum set of genes required to generate magnetosomes is known, the specific roles of many of these factors remain unknown. Additionally, there are several genes within the MAI that when deleted have subtle or not obvious phenotypes. There are also presumably many genes outside the island which have key, though indirect, roles in magnetosome formation.

Genetic screens provide a high-throughput strategy for uncovering novel genes. Transposon mutagenesis, in particular, has been used multiple times to study the genomes of AMB-1 and MSR-1. In the future, we envision several improvements that can make transposon mutagenesis an even more useful method for genetic investigation of MTB. The latest techniques in transposon mutagenesis involve pooling tens to hundreds of thousands of labeled mutants with a method called random barcoded transposon site-sequencing (RB-TnSeq) [93] (Fig. 4A). This strategy allows for saturated coverage of a bacterial genome and averaged impact of gene loss across multiple mutants. As such, polar effects and individual off-target effects are minimized during phenotyping. However, genes identified in transposon mutagenesis screens still require phenotypic validation with gene deletions. The development of more advanced gene editing technologies, like CRISPR, will be just as valuable for the study of MTB as it has been for other organisms [80,94]. For example, CRISPR interference (CRISPRi) can be used to knockdown multiple genes at a time more readily than traditional methods or to study essential genes by tuning their expression [95,96]. Additionally, stepping aside from transposon mutagenesis and screening instead for point mutants that have conditional phenotypes, act as dominant alleles, or suppress known mutant phenotypes can help to expand our understanding of the genetic networks that participate in magnetosome formation.

The methods for screening after the initial mutagenesis can also be refined. Screens thus far have relied on a simple binary identification of magnetic or non-magnetic cells. The ability to identify mutants on a spectrum of magnetic responses would be highly informative for understanding the process of magnetosome formation (Fig. 4B). It may be possible to use microfluidics for this approach [97,98]. Methods that simply allow for the capture of more magnetic mutants are also key to saturate screens and identify potential negative regulators of magnetosome formation.

Screening methods that allow for the identification of genes with more subtle phenotypes on a spectrum will open the field to studying both genes in the MAI previously thought to have little to no effect on magnetosome formation or genes outside the MAI that are key in magnetosome formation under specific growth conditions. Multiple genes outside the MAI—primarily involved in metabolism—have already been connected to magnetosome formation. For example, the

nitrate reductase genes of the *nap* operon are important for magnetosome formation in MSR-1, even when oxygen is available as the terminal electron acceptor [67]. And the metabolic regulator *crp* has also been tied to magnetosome formation [99]. Different species of MTB migrate to a variety of preferred oxygen concentrations (all under 25μM) using one of three patterns of magneto-aerotaxis [100]. The genetic mechanisms behind aerotactic behavior have begun to be investigated. For example, Popp et al. showed that the chemotaxis operon *cheOp1* was necessary for the aerotactic response in MSR-1 [101].

The insights into metabolism and magnetosome formation are naturally connected to the increasing interest in the field in studying the ecological role of MTB in their natural environments [102–104]. How MTB interact with and adapt to changing conditions will also be an interesting problem from the perspective of geneticists and cell biologists. Most studies on MTB have been done under tightly controlled laboratory conditions, but in nature MTB encounter changes in pH, temperature, oxygen gradients, and nutrient levels. A review by Moisescu et al. summarizes the effects of these changes on magnetosome formation [105]. In addition, the study of environmental conditions may help us understand how extremophile MTB evolved or retained the ability to form magnetosomes in conditions that are not viable for most MTB species [106].

**Conclusion**

The set of genes needed for magnetosome formation has been clearly determined across multiple organisms, and many of their functions have been investigated. However, it is clear that even in the most well-studied MTB, like AMB-1 and MSR-1, the roles of genes that work in tandem with other factors, that participate in multiple aspects of magnetosome formation, or that are only required conditionally have yet to be fully understood. Going forward, more nuanced study of genes involved in magnetosome formation will be key to expanding our knowledge of MTB for basic cell biology, ecology, and biotechnology applications. Additionally, the study of diverse MTB using both targeted genetic analyses and whole genome studies will potentially clarify the functions of many genes, while also adding layers to our picture of MTB.

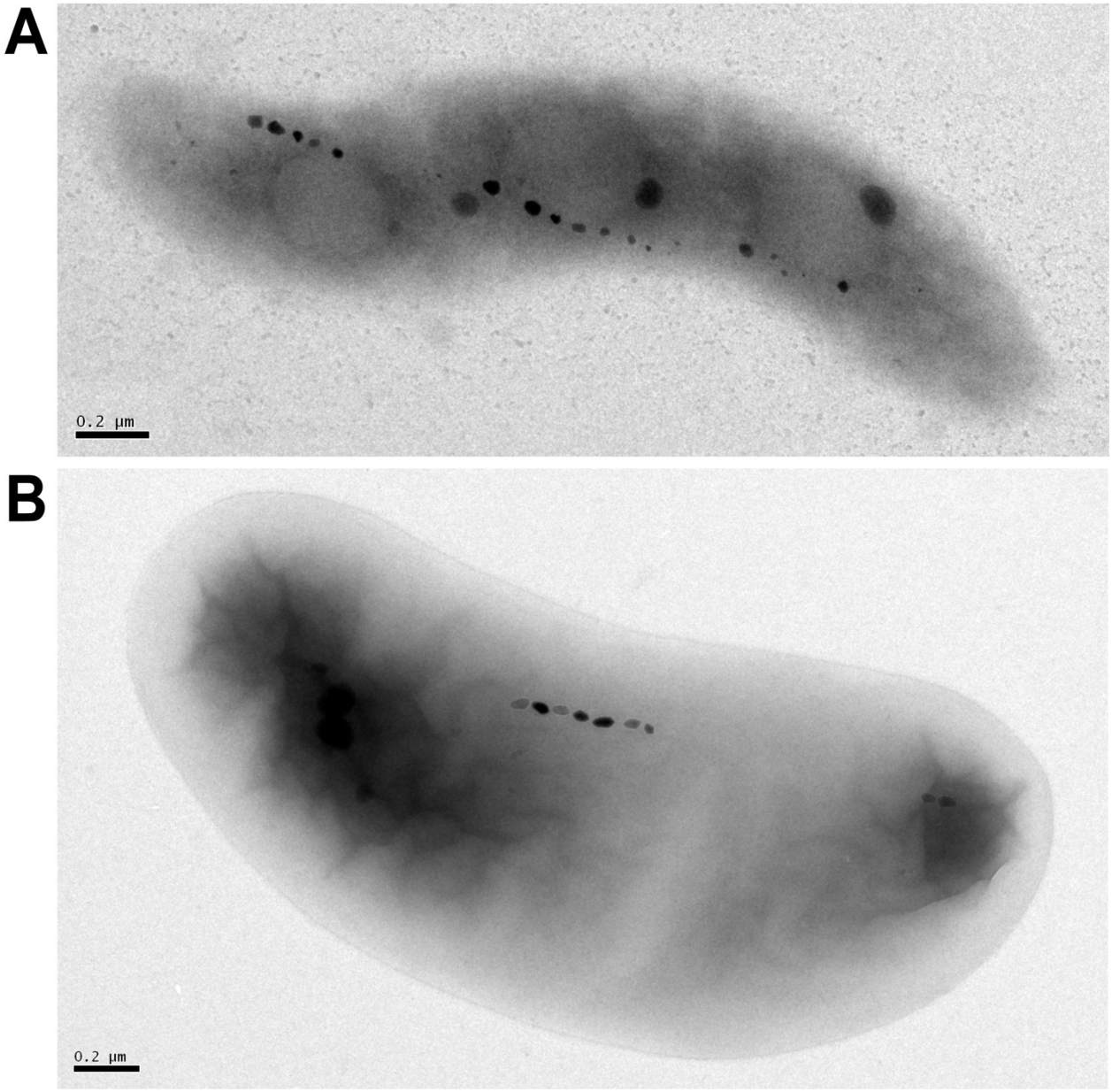


**Fig 1. The magnetotactic bacteria model systems**
(A) TEM image of wild-type AMB-1 cell. (B) TEM image of wild-type RS-1 cell, scale bar 200nm. Reprinted with permission from Rahn-Lee et al. [79].

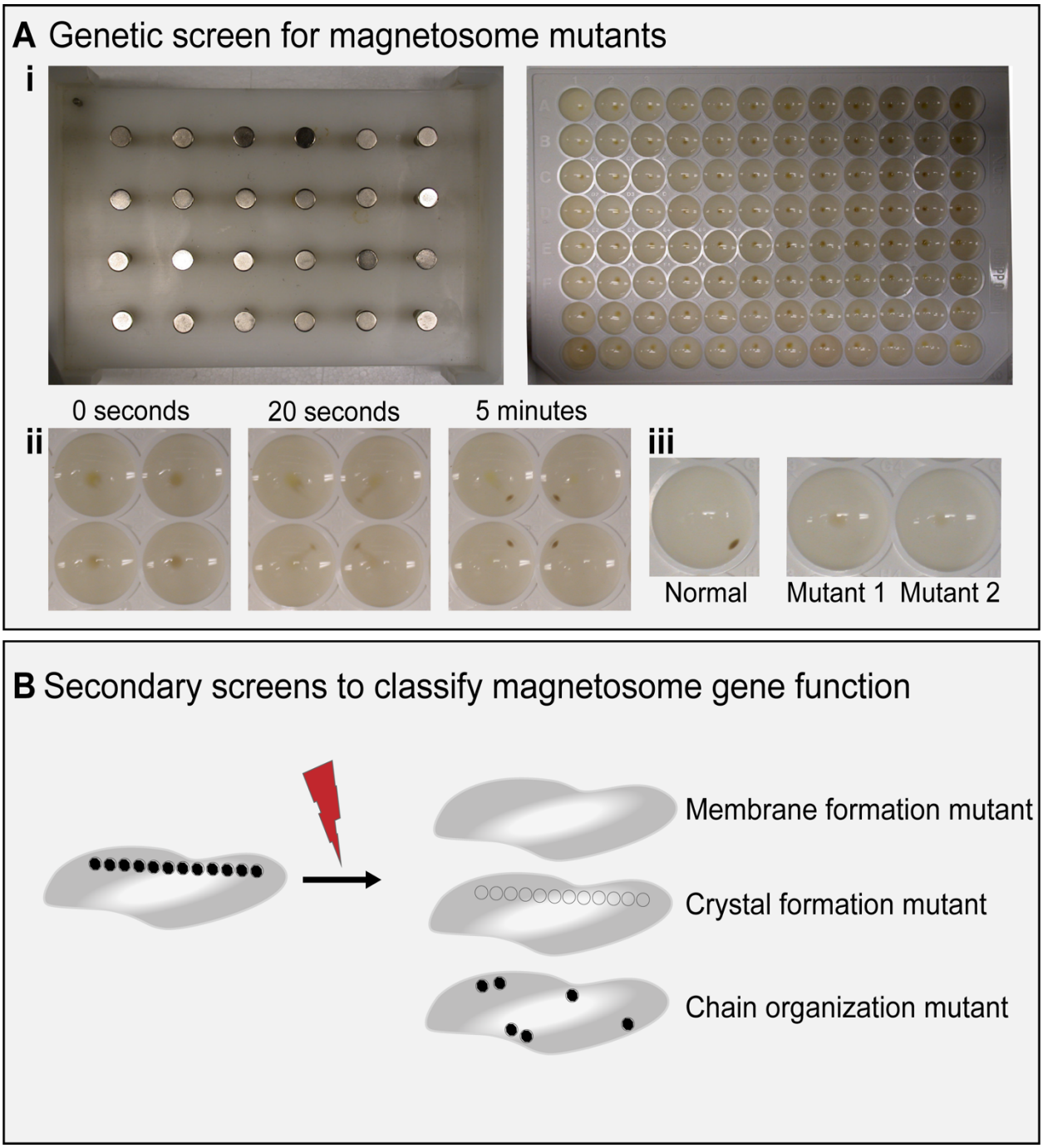


**Fig 2. Magnetic screening technique**
(A)(i) 24-pin magnetic plate (left) and 96-well plate of AMB-1 cells (right) used in Komeili et al. [33]. (ii) Movement of AMB-1 cells on magnetic plate at 0 seconds, 20 seconds, and 5 minutes. (iii) Phenotype of normal magnetic cells (left) and two representative non-magnetic mutants (right). (B) Diagram of secondary screens to classify magnetosome mutants.

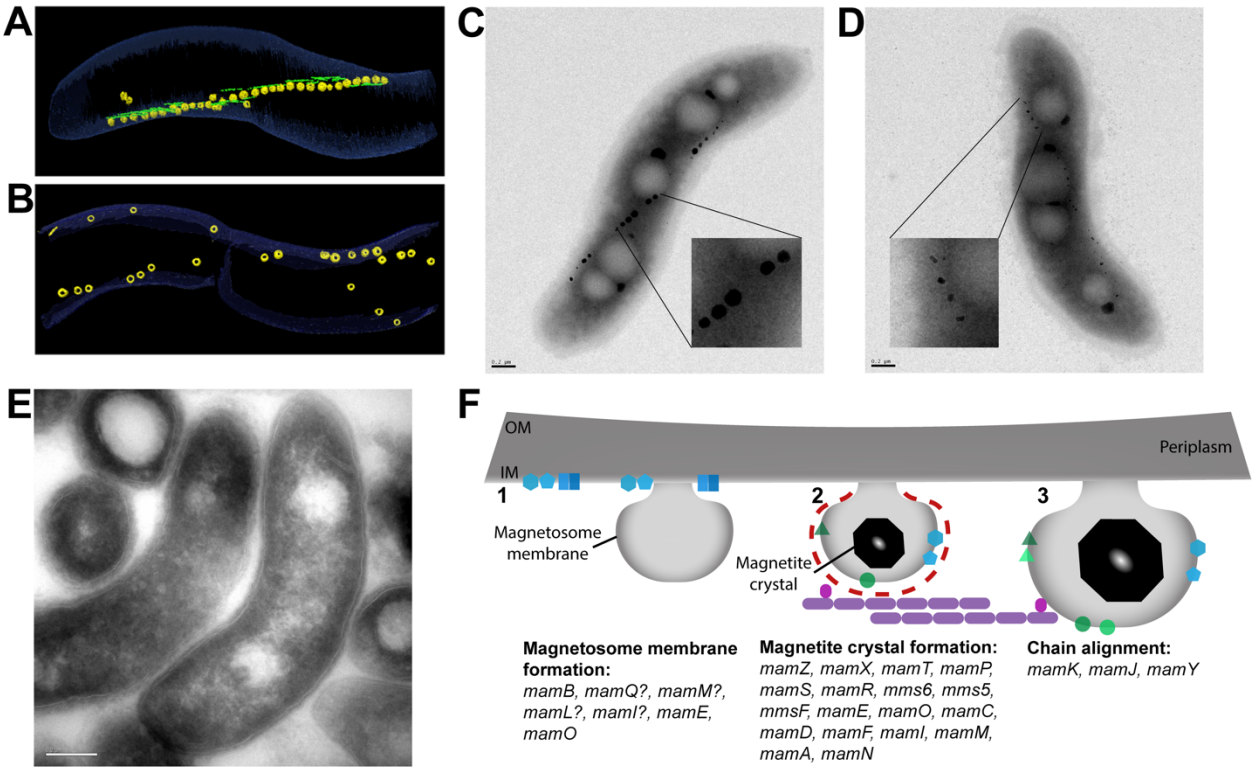


**Fig 3. AMB-1 and MSR-1 strains with defects in magnetosome formation**
(A) Wild-type AMB-1 cell image taken from segmentation of an electron cryotomogram. MamK filaments (green) run parallel to magnetosomes (yellow). (B) Electron cryotomogram image of a Δ*mamK* AMB-1 cell that shows disorganized magnetosomes. Images provided by Komeili. (C) Transmission electron microscopy (TEM) image of a wild-type AMB-1 cell. Scale bar is 0.2μm. Close up of magnetosomes is magnified 6x. (D) Transmission electron microscopy (TEM) image of a Δ*mamT* AMB-1 cell showing small, misshapen magnetosomes. Scale bar is 0.2μm. Close up of magnetosomes is magnified 6x. Image provided by McCausland et al. (E) TEM image of a cryosection of Δ*mamL* AMB-1 cells showing that magnetosome membranes are absent. Scale bar is 0.2μm. Image provided by Komeili. (F) Diagram of the stepwise process of magnetosome formation and the proteins involved from membrane invagination (1) to crystal nucleation (2) to membrane growth and formation of a mature magnetic crystal (3). Genes that have been found to be involved at each step are listed.

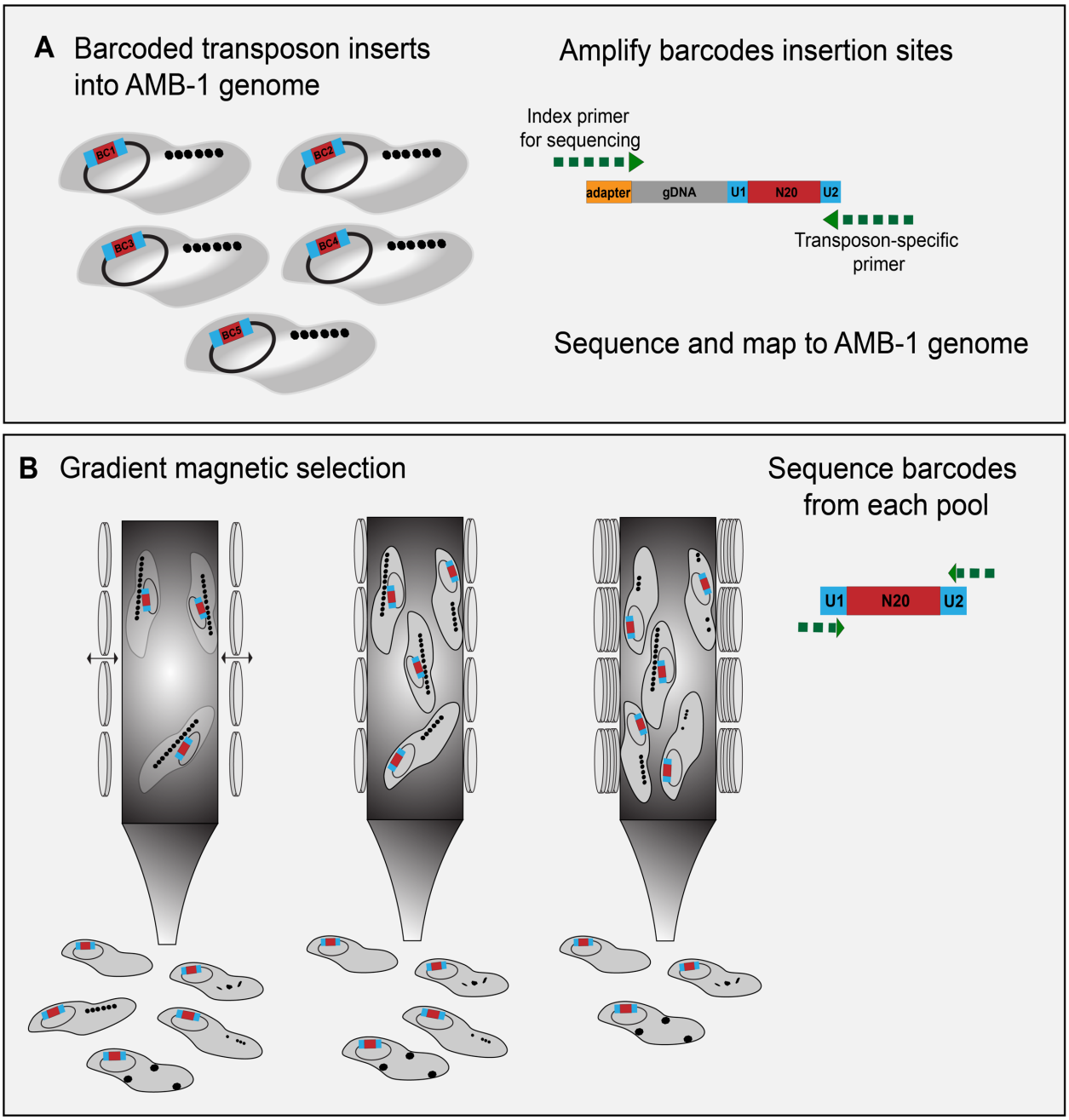


**Fig 4. Barcoded transposon mutagenesis and a potential magnetic screen**
(A) Diagram of barcoded transposon mutagenesis and sequencing (RB-TnSeq) in AMB-1. Each transposon insertion carries a unique 20-nucleotide sequence that acts as a barcode. The mutated strains are pooled and then the barcodes are mapped to their insertion site in the genome. (B) Diagram of magnetic selection with the TnSeq library using different magnetic strengths to select for a range of mutant phenotypes. From left to right, as magnetic strength applied to the column increases, strains with weaker magnetic responses will be able to stick to the column, yielding a gradient of magnetic phenotypes to analyze.

## CHAPTER 2

Global analysis of biomineralization genes in *Magnetospirillum magneticum* AMB-1

Hayley C. McCausland[a], Kelly M. Wetmore[b], and Arash Komeili[a,c]

Department of Molecular and Cell Biology, University of California, Berkeley, USA[a]; Physical Biosciences Division, Lawrence Berkeley National Laboratory, Berkeley, California, USA[b]; Department of Plant and Microbial Biology, University of California, Berkeley, USA[c]

**Abstract:**
Magnetotactic bacteria (MTB) are a phylogenetically diverse group of bacteria remarkable for their ability to biomineralize magnetite ($Fe_3O_4$) or greigite ($Fe_3S_4$) in organelles called magnetosomes. The majority of genes required for magnetosome formation are encoded by a magnetosome gene island (MAI). Most previous genetic studies in MTB have focused on the MAI, using screens to identify key MAI genes or targeted genetics to isolate specific genes and their function in one specific growth condition. This is the first study that has taken an unbiased approach to look at many different growth conditions to reveal key genes both inside and outside the MAI.

Here, we conducted random barcoded transposon mutagenesis (RB-TnSeq) in *Magnetospirillum magneticum* AMB-1. We generated a library of 184,710 unique strains in a wild-type background, generating ~34 mutant strains for each gene. RB-TnSeq also allowed us to determine the essential gene set of AMB-1 under standard laboratory growth conditions. To pinpoint novel genes that are important for magnetosome formation, we subjected the library to magnetic selection screens in varied growth conditions. We compared biomineralization in standard growth conditions to biomineralization in high iron and anaerobic conditions, respectively. Strains with transposon insertions in the MAI gene *mamT* had an exacerbated biomineralization defect under both high iron and anerobic conditions compared to standard conditions, adding to our knowledge of the role of MamT in magnetosome formation. Mutants in an ex-MAI gene, *amb4151,* are more magnetic than wild-type cells under anaerobic conditions. All three of these phenotypes were validated by creating a markerless deletion strain of the gene and evaluating with TEM imaging. Overall, our results indicate that growth conditions affect which genes are required for biomineralization and that some MAI genes may have more nuanced functions than was previously understood.

**Introduction:**
Magnetotactic bacteria (MTB) are a diverse group of bacteria capable of producing intracellular organelles called magnetosomes [1,3–6,107,108] after taking up iron from the surrounding environment. Magnetosomes are membrane-bound compartments in which biomineralization of magnetic crystals of magnetite ($Fe_3O_4$) and/or greigite ($Fe_3S_4$) occurs [3]. Crystals are organized into linear chains along the long axis of the cell, forming a magnetic dipole that allows the cell to orient towards Earth's magnetic fields [8]. MTB inhabit low-oxygen environments and are typically found at the oxic-anoxic transition zone (OATZ) in a water column [3]. Navigation along magnetic field lines is thought to allow cells to efficiently locate the OATZ; a process called magnetoaerotaxis [7].

MTB are ubiquitous in aquatic environments and can account for up to 30% of microbial biomass in some habitats [1]. Because of their presence in water and the large amounts of iron that each cell captures in the process of biomineralization, it is likely that MTB have a large impact on iron cycling in the ocean, potentially taking up anywhere from 1-50% of dissolved iron inputs into the ocean [2]. However, most of what we know about MTB in the environment comes from surveys of species and their numbers in particular habitats. The dynamic responses of MTB, particularly at a genetic level, to fluctuations in the environment remain largely unexplored. A greater understanding of the molecular mechanisms of biomineralization and iron sequestration by MTB in response to changing conditions will inform environmental studies, including the impact that MTB have on iron cycling. Yet, most of our knowledge of the genetics and cell biology of MTB comes from studies done under static conditions that do not accurately reflect the natural environment of MTB grow. Here, we take advantage of the well-studied model organism *Magnetospirillum magneticum* AMB-1 and develop a high throughput genetic strategy to connect genetics to environmental changes.

The genes needed to produce magnetosomes are encoded in magnetosome gene clusters (MGCs). In some species—like the model organisms AMB-1 and *Magnetospirillum gryphiswaldense*—the MGCs are discreet magnetosome gene islands (MAIs). The MAIs in AMB-1 and *Magnetospirillum gryphiswaldense* MSR-1 are well characterized [35,40]. Both organisms have approximately 100 genes in their respective MAIs. However, it was shown by Kolinko et al. that only 31 of the genes in the MSR-1 MAI are necessary and sufficient to synthesize magnetosomes—though even fewer may be required [41]. This implies that the other ~70 genes in the MAI are either unnecessary for the formation of magnetosomes, are redundant with other genes, or are only required under certain growth conditions. There is evidence that some MAI genes are only required for magnetosome formation under certain growth conditions. For example, the genes *mamX* and *ftsZm* are necessary under oxygen-reducing conditions but not nitrate-reducing conditions [64,65].

Genes outside the MSR-1 MAI (ex-MAI genes) have also been connected to magnetosome formation as growth conditions are changed. Deletion of the *nap* operon in MSR-1 resulted in the formation of small, poorly aligned magnetosomes [67], indicating that nitrate metabolism, while not necessary for the growth of MSR-1, is critical in the formation of magnetosomes. The possibility that other genes—both inside and outside the respective MAIs of MSR-1 and AMB-1—are required for magnetosome formation under specific conditions has not been thoroughly examined [32,73,109–111].

Previous genetic studies in magnetotactic bacteria have used either targeted reverse genetics to determine the role of individual genes or operons, or forward genetic screens that focus solely on clear magnetosome mutants. Here, we present a global and readily scalable approach to investigate the genetic requirements of AMB-1. We used a screening technique called

random barcoded transposon site sequencing (RB-TnSeq) [93], which involves generating a pooled library of tens of thousands of transposon mutants. First, we used the winning RB-TnSeq library to determine the essential gene set of AMB-1 in our standard growth conditions, providing a broader view of the lifestyle of this important model organism. Then, we used the RB-TnSeq library to conduct a high-throughput magnetic selection to study the genetic requirements for magnetosome formation under multiple environmental conditions. In particular, we focused on magnetosome formation in varying oxygen and iron concentrations, which have both been shown to influence magnetosome formation [112,113]. Magnetic selection experiments uncovered new functions of known magnetosome genes, while also revealing novel ex-MAI genes that may have a role in magnetosome formation.

**Results:**
**RB-TnSeq libraries reveal the essential gene set of AMB-1**

In order to conduct high-throughput genetic screens in AMB-1, we generated pooled transposon insertion libraries containing thousands of mutants using the transposon mutagenesis technique, RB-TnSeq [93] (Fig.1). A library of ~30 million *mariner* transposon vectors (pKMW3) in the *E. coli* host strain WM3064 was conjugated with AMB-1. After growth on selective plates, all colonies were pooled for sequencing. The location of each transposon was mapped to the AMB-1 genome using Illumina sequencing.

We generated a successful library in WT AMB-1 called magnetotactic bacteria library ML2 (ML2). The library was constructed in our standard laboratory conditions: MG media supplemented with 30μM iron and grown microaerobically. ML2 contained 183,760 unique barcodes (Fig. 2A, B). There were 34.3 hits per protein on average (mean). The read bias (mean:median reads per hit protein) of 1.74 indicates a moderate bias in the library, where no genes are underrepresented by more than two-fold, on average. Since ML2 has a large number of mutant strains with broad coverage of the genome, it was used for downstream biomineralization screens.

Another benefit of making an RB-TnSeq library is that it can be used to determine the putative essential gene set of a strain in the conditions under which it was made (Fig. 2A). Essential genes have very few or no insertions because those mutants should not be viable. Here, we determined the essential gene set of ML2 under standard laboratory conditions. We identified 445 essential genes in the AMB-1 genome—~9.9% of protein coding genes, which is similar to the percentage of essential genes in other RB-TnSeq libraries [114]. The remaining 4216 genes are either non-essential (3774 genes) or were not included in the list of essential genes (472 genes). Those genes that were not included are very similar to other regions of the genome or less than 800 nucleotides. Genes larger than 800 nucleotides were determined to be unlikely to have no insertions by chance [114].

Binning the essential genes into COG categories showed that amino acid metabolism and cell wall structure/biogenesis accounted for the largest proportion of essential genes (16% each) (Fig. 2C). Translation (10% of essential genes) and energy production (9% of essential genes) also contained a large proportion of essential genes. While these categories are expected for essential genes, the individual genes within each category can provide information about what MTB need to grow. For example, a succinate dehydrogenase subunit (*amb3952*) and tartrate dehydrogenase (*amb3176*) are essential under standard conditions, indicating the important role of the TCA cycle in heterotrophic metabolism of AMB-1. Additionally, nitrate reductase subunits (*amb0531* and *amb0533*), nitrate ABC transporter (*amb0534*), and nitrate/sulfonate/bicarbonate ABC transporter ATP-binding protein (*amb0535*) are essential, where nitrate was the only alternative electron acceptor available for respiration.

**Magnetic selection reveals genes important for biomineralization under high iron conditions**

To screen for mutants with defects in biomineralization, we used a magnetic column to separate magnetic from non-magnetic cells in the RB-TnSeq library (Fig. 1B). After thawing an aliquot of ML2 and growing to late log phase ($OD_{400}$ ~0.150), cells were passaged into growth conditions of choice and allowed to grow to stationary phase ($OD_{400}$ ~0.250). Then, each culture was filtered through a magnetic column lined with magnets. Both the non-magnetic and magnetic samples were collected. A sample of the pre-column culture was saved as a control. BarSeq

(sequencing of the unique barcodes) was performed on magnetic, non-magnetic, and pre-column samples and then a magnetic column score (MCS) for each gene was calculated based on the weighted average of each strain's abundance (Fig. 3). It should be noted that BarSeq experiments are usually used to measure growth of each strain, based on a strain's abundance in each experiment. Here, we have adapted the measure of strain fitness to evaluate biomineralization capabilities based on abundance of each strain in pre-column, magnetic, and non-magnetic samples.

To validate the screen, ML2 was run over the column after microaerobic growth in 30μM iron. As there were too few cells in the non-magnetic sample for preparation of gDNA, we reasoned that strains with transposon insertions in magnetosome formation genes would be depleted in the magnetic sample. Thus, a low MCS would correspond to a defect in biomineralization (Fig. 3D). Accordingly, we found that strains with transposon insertions in MAI genes with known roles in magnetosome formation—*mms6, mmsF, mamH, mamE, mamJ, mamK, mamL, mamM, mamN, mamO, mamP, mamA, mamS,* and, mamT—were underrepresented in the populations of magnetic cells (Fig. 3D). It is interesting to note that *mamJ* and mamK, which are involved in magnetosome chain alignment, not biomineralization, also had negative MCS under these conditions. Perhaps, uneven chain segregations in these mutants yields a small but detectable subpopulation which cannot bind to the magnetic column.

The goal of further screens was to identify genes involved in biomineralization when cells are grown in alternative conditions. We focused on genes required for biomineralization under anaerobic conditions and under high iron conditions. Recent work by Amor et al. has shown that the concentration of iron supplied in the growth medium affects both iron uptake and magnetite formation in AMB-1 [2]. As iron concentration is increased in the media, cells take up more iron. Additionally, magnetite crystals in AMB-1 cells increase in size as iron concentration is increased. Previous genomic studies have shown that iron uptake genes are upregulated under magnetosome-forming conditions [18,19, 21]. However, it is not known if there is a genetic response to stimulate increased iron uptake or regulate the size of magnetite crystals in response to iron concentration. Here, we performed a magnetic selection with ML2 after growing cells at standard (30μM) and high (150μM) iron concentrations to uncover genes involved in magnetosome formation when cells are saturated with iron.

After magnetic selection, we compared the MCS from the magnetic populations of the standard and high iron concentrations against each other (Fig. 3B). Most of the MCS either clustered around 0, meaning there was no measurable magnetic defect, or along the slope of 1, meaning there was no difference in magnetic response for that gene between the two iron conditions. There were several genes of interest that were underrepresented (had a magnetic defect) in the magnetic population of each condition. In the standard iron condition, *amb0360* (AMB_RS01830), which is annotated as a hypothetical protein, had a magnetic defect. While there were no protein predictions, *amb0360* does have a homolog in *Magnetospirillum gryphiswaldense* MSR-1 (95.96% identity). One gene, amb4208 (AMB_RS21290) was overrepresented (had a positive MCS) in the high iron condition. It is possible that mutants of this gene are more magnetic than wild-type cells. Again, AMB4208 is a hypothetical protein with homologs in *Magnetospirillum sp.* XM-1 (81.5% identity), ME-1 (80.5% identity), and MSR-1 (75.54% identity).

There were several other genes with magnetic defects in the high iron condition. Of note, there were several MAI genes that were underrepresented in the magnetic population: *mms6, mmsF, mamS,* and *mamT*. MamT is a magnetosome localized protein with a magnetochrome domain (a heme-binding motif unique to magnetosome proteins) and is thought to be involved in redox

chemistry for magnetosome crystal growth [52]. MmsF and MamS are also magnetosome-localized proteins and have been shown to regulate crystal size and morphology [35,45]. The lower magnetic score of these genes in the high iron condition compared to the standard iron condition suggests that they may have a more nuanced function in magnetosome formation than previously thought.

**Magnetic selection reveals genes important for biomineralization under anaerobic conditions**

Both AMB-1 and MSR-1 are capable of growing in microaerobic conditions. However, biomineralization only occurs when oxygen concentrations in the medium are depleted [112]. In the laboratory, AMB-1 is typically grown with a low concentration of oxygen (2-10%) in the culture headspace, with nitrate as an alternative electron acceptor. It is not known if the inability of MTB to form magnetosomes aerobically is simply due to the balance of ferrous and ferric iron required to produce magnetosomes or if there is also a genetic response to turn off magnetosome production at high oxygen concentrations.

Here, we grew ML2 in either microaerobic (test tubes with minimal headspace incubated in a microaerobic chamber) or anaerobic (sealed serum bottles with anaerobic media) conditions and performed a magnetic selection to find genes that are required for magnetosome formation in varying oxygen concentrations. The microaerobic conditions reflect how cells are grown in standard lab conditions.

We compared the MCS from the magnetic populations of the microaerobic and anaerobic samples against each other after magnetic selection (Fig. 3A). Again, most of the MCS either clustered around 0 or along the slope of 1, meaning there was no difference in magnetic response for most genes between the two oxygen conditions. In the microaerobic condition, *amb0360*, again had a magnetic defect, suggesting that it may be important for biomineralization under standard conditions. Another gene, *amb4151* (AMB_RS21005), which is annotated as a hypothetical protein, had a positive MCS in the anaerobic condition, suggesting that mutants of this gene are more magnetic than wild-type cells. *Amb4151* has homologs in *Magnetospirillum sp.* XM-1 (89.07% identity), ME-1 (87.89% identity), and MSR-1 (77.66% identity).

Several MAI genes also had magnetic defects in the anaerobic condition: *amb0936, amb0947, amb1008, amb1009, amb1022*, *mamT*, *mmsF*, and *mamJ*. Again, it was surprising that *mamJ* came up in this screen, as MamJ is known for its role in chain organization, not biomineralization. While both *mamT* and *mmsF* deletion strains have defects in biomineralization [45,52], it is surprising that the MCS is even lower in the high iron condition because magnetosomes are typically larger in size under high iron conditions. These results provide further support that the roles of some MAI genes are conditional.

**Δ*mamT*Δ*R9* plays a greater role for biomineralization in high iron and anaerobic conditions**

In order to validate the results of the screen, we chose to look more closely at a *mamT* deletion in order to confirm that phenotypes seen in the magnetic selection screen also occur when the gene is deleted from a WT background. Here, we used Δ*mamT*Δ*R9,* where region 9 (R9) of the MAI (containing exact duplications of *mamQ,R,B*) was also deleted in order to prevent a recombination event that makes the *mamT* deletion less stable [52]. When grown with 30μM iron, Δ*mamT*Δ*R9* cells produce smaller crystals and have a very low magnetic response

compared to WT cells (Fig. 4A,C). When grown with 150μM iron, TEM images of Δ*mamT*Δ*R9* cells qualitatively look very similar to cells grown with 30μM iron (Fig. 4C). However, the length of the magnetite crystals is decreased in Δ*mamT*Δ*R9* cells in 150μM iron compared to 30μM iron. As described above, it is surprising that magnetosomes would be smaller in the high iron condition. Complementing Δ*mamT*Δ*R9* by integrating *mamT* into the genome restores the WT phenotype in both iron conditions. Again, we validated the phenotype of Δ*mamT*Δ*R9* under anaerobic conditions. When grown anaerobically, Δ*mamT*Δ*R9* magnetite crystals were shorter than both wild-type crystals and Δ*mamT*Δ*R9* under microaerobic conditions (Fig. 4A).

All experiments were repeated in the Δ*R9* strain to confirm that phenotypes seen with Δ*mamT*Δ*R9* were not caused by the R9 deletion (Fig. S1). Δ*R9* cells behaved similarly to WT in that they had larger magnetosomes under both high iron and anaerobic conditions. The MAI gene *mms6* had a biomineralization defect in the 30μM iron condition (-1.59 MCS score), as expected [115] and slightly less of a defect in the 150μM iron condition (-1.29 MCS), so we looked at Δ*mms6* to verify that the magnetic selection was accurate and as a control for Δ*mamT*Δ*R9*. After growing Δ*mms6* in 30μM or 150μM iron, magnetosomes were larger under the high iron conditions, similar to WT (Fig. S2).

These results together suggest that the magnetic selection process is sufficient for pulling out genes that, when disrupted, have a defect in biomineralization. They also show that *mamT*, which was already known to be involved in magnetosome formation may have a more critical role in both high iron and anaerobic conditions.

**Genes outside the MAI may have a role in biomineralization**

It was unexpected to see a gene with a positive MCS in the anaerobic condition, especially a gene outside the MAI, as this could indicate that a novel ex-MAI gene has a role in control of biomineralization. To explore this phenomenon further, we generated a deletion of *amb4151*. Under microaerobic conditions, Δ*amb4151* magnetosomes looked similar to WT magnetosomes (Fig. 5A) and had the same magnetosome length (Fig. 5B). Under anaerobic conditions, WT AMB-1 cells typically produce larger magnetosomes (mean = 37.2 nm, $\sigma$ = 17.0). Δ*amb4151* cells produced larger magnetosomes than WT under anaerobic conditions and appeared to do so more consistently (mean = 53.5 nm, $\sigma$ = 15.8).

**Discussion:**
Previous genetic studies in MTB have relied on transposon mutagenesis screens that required sorting through thousands of individual colonies [22,26,33]. Here, we showed that RB-TnSeq is a streamlined and effective technique for investigating biomineralization in MTB, as the pooled library allows for screening hundreds of thousands of mutants through many growth conditions in a relatively short amount of time. Additionally, the method is incredibly sensitive to small changes in magnetic properties of a mutant. These features allowed us to demonstrate that some known magnetosome genes have differential roles as growth conditions change and that novel genes outside the MAI may have an impact on biomineralization.

There are clear benefits to using RB-TnSeq over traditional methods of mutagenesis. First, the simplicity of sequencing barcodes in each sample allows for streamlined screening and the ability to test many different conditions in a single experiment. Additionally, because the phenotypic score for a gene is averaged across many individual insertions, we can be more confident that genes of interest are worth pursuing. However, RB-TnSeq is not without its challenges. Because all mutants are pooled together it is possible that some phenotypes of some mutants may be masked via transcomplementation by other mutants in the pool. Alternatively, it may be difficult to validate the phenotype after screening. There is a chance that a mutant is influenced by competition in the pool (i.e. the mutants of one gene are outcompeted for nutrient uptake and form smaller magnetosomes) and once the gene is examined on its own, the phenotype may disappear. Biased insertion and polar effects could also cause false positives in some instances. But a phenotype can still be evaluated after the fact with single gene or operon deletions.

In this study, the ML2 (wild-type) library had full coverage of the genome, with over 180,000 strains and approximately 34 transposon insertions per gene. With ML2 we were able to map the essential gene set of AMB-1 under our standard laboratory conditions, which are the conditions under which most genetic studies have been conducted in AMB-1. The essential gene set expands our understanding of the physiology of AMB-1 and allows for comparison to other MTB in either physiological or phylogenetic studies.

We then screened the transposon mutant pool using a magnetic selection. Previous studies in MTB have used similar selection methods (i.e. colony color, response to a magnetic field, magnetic column)[22,26,33,79,116], but the barcode sequencing adds power by quantifying the results. Since MCS is based on a weighted average of all the mutants in a particular gene, a biomineralization phenotype for a particular gene is more reliable. This is particularly important because the biomineralization phenotype for one strain can vary across the population of cells and averaging the scores of multiple mutants strains provides more confidence that the phenotype is real. Additionally, since ML2 is complete library, this allows us to reexamine mutants that were previously discovered with standard techniques.

Importantly, mutants with insertions in MAI genes were depleted from the population of magnetic cells after magnetic selection. This indicated that the screening method reliably detects strains with defects in biomineralization. Interestingly, genes identified in a previous transposon mutagenesis screen by Matsunaga et al. (2005) [32] as being important for biomineralization were not found to have biomineralization defects in this study. Matsunaga et al. created 5762 Tn5 transposon mutants and found 69 mutants with defects in biomineralization, none of which were located in the MAI. It is possible that there were secondary mutations in the Tn5 transposon mutants that were the true cause of the biomineralization defect—for example, spontaneous loss of the MAI. One benefit of RB-TnSeq

is that the phenotype is based on an average of multiple insertions in each gene, making it less likely to falsely link a gene to biomineralization.

We also discovered potential new functions for known magnetosome genes when cells were grown under non-standard conditions (high iron or anaerobic). Of note was *mamT* which is known to be involved in crystal formation but may be more critical under high iron or anaerobic conditions. The *mamT* phenotype is notable because under high iron or anaerobic conditions we expect magnetosomes to get larger, and *mamT* mutants have the opposite phenotype. The effect on magnetosome size was also quite subtle, which highlights the power of the magnetic screen and is ability to identify phenotypes that would have been overlooked otherwise. While we did not investigate the mechanism in this work, perhaps the decreased size of magnetosomes in those two conditions are due to the proposed role of MamT in regulating the balance of iron species within the magnetosome. Further study of MamT under alternative growth conditions could provide further insights into its function.

While some of the genes in the MAI are transposable elements and are unlikely to have a role in magnetosome formation, the screens here showed that many of the genes in the MAI originally thought to have no role in biomineralization—or that have not been studied before—may be important as conditions shift. These genes include: *amb0936*, *amb0947*, *amb0958*, *amb0959*, *amb1009*, *amb1008*, *amb1022, mamJ*, *mamK*, and *mamY*. It is especially surprising that *mamJ* mutants had a biomineralization defect, since the phenotype of *mamJ* is masked by the presence of *limJ* in the magnetosome islet [36]. Additionally, we uncovered genes outside the MAI that may have an impact on magnetosome formation. We found that *amb4151*—annotated as a hypothetical protein—inhibit biomineralization to a small degree. Δ*amb4151* has larger magnetosomes under anaerobic conditions, when compared to WT.

It has been shown that magnetosomes are only made under low oxygen concentrations [112]. However, it is not known if this is simply due to shifting redox conditions or if there is also a genetic response to turn off magnetosome production at high oxygen concentrations. Further study of *amb4151* could be useful to understand the impact of ex-MAI genes on magnetosome formation. Importantly, they suggest that the changes in magnetosome size under shifting iron and oxygen increases are not only due to redox conditions but are also influenced by a genetic response.

The genes highlighted in this study all had nuanced phenotypes, in that each gene deletion had a slight effect on biomineralization. While these genes may not be critical to the formation of magnetosomes, it is still valuable to study their functions. Most, if not all, of the genes that have a large impact on biomineralization or magnetosome formation have already been identified in past screens and reverse genetic studies. Genes with more subtle phenotypes can provide key information on the formation of magnetosomes under different conditions.

While previous studies have suggested that MTB may have a large environmental impact, we know very little about the dynamics of magnetosome formation in natural environments. A greater understanding of the molecular mechanisms of biomineralization can help with understanding how much iron is taken up by MTB and under what conditions. This study shows that RB-TnSeq and screens for biomineralization defects are useful tools to identify genes that influence the response of AMB-1 to changing environmental conditions. There are certainly many applications for this technique to reveal more about growth and biomineralization in MTB. For example, an RB-TnSeq library may be used to find genes important in an oxygen or redox gradient. Or taken a step further, could be used to find mutants in magnetoaerotaxis. Both screens would reveal more about the physiology and lifestyle of magnetotactic bacteria.

**Methods:**

**Growth and culture conditions.** *Magnetospirillum magneticum* AMB-1 was cultured in defined minimal media (MG medium,) supplemented with 1/100 vol of Wolfe's vitamin solution and 30μM ferric malate as previously described [33]. Colonies were grown on solid MG with 0.7% agar. Kanamycin was used at 10μg/mL in solid media and 7μg/mL in liquid media for strains with a kanamycin-resistant cassette integrated into the chromosome or on a plasmid. For microaerobic growth cells were grown in culture tubes or 50mL conical tubes and incubated at 30°C in a microaerobic chamber with 10% oxygen. For anaerobic growth, sealed Balch tubes containing 10mL of MG medium and 20mL of headspace were used. Media was bubbled with $N_2$ gas for 10 min before sealing. Then headspace was flushed with $N_2$ gas for 10 min before autoclaving. Ferric malate and Wolfe's vitamins were added once tubes cooled. All cultures inoculated with a dilution factor of 1:100.

**Library construction + processing**. Detailed description of transposon vector construction is described in Wetmore et al., 2015 [93]. AMB-1 mutant libraries were constructed using APA752 (*mariner* transposon library pKMW3 in WM3064 containing millions of unique 20-nucleotide barcodes). APA752 was transferred to AMB-1 from WM3064 by conjugation: 1L of wild-type AMB-1 culture at OD400 0.230 was conjugated with 100mL of APA752 culture by incubating in a microaerobic (10% oxygen) chamber for 14 hours, then diluted 1:15 and plated on MG/Kan. Plates were incubated in microaerobic jars (7% oxygen) at 30°C for 5 days. Colonies were collected from plates and pooled in liquid MG/Kan, then allowed to grow to late log phase before spinning down 50 mL aliquots and freezing in 1 mL aliquots with 20% glycerol. All libraries were made in standard MG. Some cell pellets from the 50 mL aliquots were set aside for gDNA extraction. To ensure that the library had enough barcodes to indicate complete coverage of the genome, BarSeq PCR followed by Illumina MiSeq sequencing was performed. Libraries determined to be diverse enough were sequenced by Illumina HiSeq in order to map transposon insertions. Illumina library preparation and TnSeq data analysis are described in Wetmore et al., 2015 [93].

**Essential gene analysis.** We used previously published methods to determine the essential gene set of AMB-1 in both standard wild-type and Δ*MAI* strains using the RB-TnSeq libraries [114]. Briefly, read density was determined for each protein-coding gene. Genes that are very similar to other parts of the genome and genes of less than 100 nucleotides were excluded from analysis. Based on the median insertion density and median length of remaining genes, a threshold for gene size included in the essential gene analysis was set for the library by determining how short a gene could be and still be unlikely to have no insertions at all by chance ($P$<0.02, Poisson distribution) [114]. The threshold for ML2 was 800 nucleotides—any genes shorter than that were excluded from the essential gene analysis.

**Competitive mutant magnetic assays.** For each condition, one aliquot of ML2 was thawed and inoculated into 250mL of MG with 7 μg/mL Kanamycin. When the culture recovered to stationary phase—~OD400 0.250 on Ultrospec 2100 pro (Amersham)—cell pellets were collected from 25mL aliquots as time 0 samples. For experiments testing iron concentrations, cells were first washed twice and resuspended in MG without carbon or iron, respectively. Then, cultures were inoculated at 1:100, in triplicate for each condition. For iron experiments, MG was supplemented to either 30μM or 150μM ferric iron using 3mM ferric malate stock. Cultures were balanced with malic acid (18mM (200x) stock). For oxygen experiments with ML2, microaerobic cultures were grown in culture tubes in a microaerobic glove box without shaking and anaerobic cultures were grown in Balch tubes without shaking.

**Magnetic selection.** 15mL of culture from each condition and each triplicate were pelleted as the pre-column sample and frozen at -20°C. For each magnetic selection, an LS column (Miltenyi Biotech) was set up on a ring stand with 6 sets of 2 disc magnets on each side. The remaining 35mL of culture were passaged over the magnetic column via gravity filtration and collected in a 50mL conical (magnetic sample). Then, magnets were removed and column was washed twice with 5mL of MG. Flow-through (non-magnetic sample) was collected. Both magnetic and non-magnetic samples were spun down and cell pellets were frozen at -20°C.

**BarSeq.** Genomic DNA was isolated from library samples using the Qiagen DNeasy Blood & Tissue Kit. gDNA concentration was quantified by NanoDrop. BarSeq PCR was performed using ~200ng of DNA for each sample. Barcodes were amplified using unique, indexed primers, as described in Liu et al., 2021 [117]. Samples were pooled and sequenced using Illumina HiSeq single-end reads.

**BarSeq data analysis and magnetic column abundance calculation.** A detailed description of BarSeq analysis can be found in Wetmore et al., 2015. Briefly, the magnetic column abundance score (MCS) for a gene is calculated from the weighted average of strain MCS. Because these methods were developed for use with growth assays, we added an additional normalization step to account for any growth defects that might influence MCS after passing cells through the magnetic column by subtracting pre-column gene MCS from magnetic and non-magnetic gene MCS.

**Strains**. Δ*mamTΔR9* [52], Δ*mmsF* [45], and Δ*mms6* (Juan Wan) were generated previously. All other gene deletions were made using a two-step recombination method to generate a markerless deletion [33]. Deletion plasmids were constructed using three-piece Gibson assembly. Regions upstream and downstream of the gene of interest were cloned into pAK31 (suicide vector containing the Kanamycin-resistant cassette and *sacB* gene) cut with BamH1 and Spe1. The plasmids were transferred to AMB-1 cells by conjugation and selected on MG/Kanamycin media. Colonies were then grown on MG with 2% sucrose to select for deletion strains. Sucrose-resistant colonies were screened by PCR for the deletion and for the lack of plasmid markers.

Complementation plasmids were constructed using three-piece Gibson assembly. The gene of interest was cloned into pAK22 (replicative plasmid containing the Kanamycin-resistant cassette following a tac promoter) cut with EcoR1 and Spe1. The plasmids were transferred to AMB-1 cells by conjugation and selected on MG/Kanamycin media.

Plasmids

| Name | Origin | Description | Reference |
|---|---|---|---|
| pHM14 | pAK31-derived | Deletion plasmid for *amb4151* | This work |
| pHM19 | pAK22-derived | Complementation plasmid for Δ*amb4151* | This work |
| pAK807 | pAK605-derived | Complementation plasmid for Δ*mamTΔR9* | Patrick Browne (unpublished) |
| pHM20 | pAK31-derived | Deletion plasmid for *amb3952* | This work |

Strains

| Strain | Organism | Description | Reference |
|---|---|---|---|

| | | | |
|---|---|---|---|
| KW… | *E. coli* | mariner RB-TnSeq library | Wetmore et al. |
| AK155 | AMB-1 | Δ*mamT*Δ*R9* | Jones et al. |
| AK57 | AMB-1 | Δ*R9* | Murat et al., 2010 |
| AK104 | AMB-1 | Δ*mmsF* | Murat et al., 2012 [45] |
| AK110 | AMB-1 | Δ*mms6* | Wan et al. (in review) |
| HM02 | AMB-1 | Δ*amb4151* | This work |
| DH5α (λpir) | *E. coli* | Standard molecular cloning strain | |
| WM3064 | *E. coli* | Plasmid conjugation strain | |

Primers

| **Name** | **Sequence** | **Used to generate** |
|---|---|---|
| HM138 | CGAATTCCTGCAGCCCGGGGAAATTCAGAAAATCATAAAATCCACC | Δ*amb4151* |
| HM139 | AAGTCCAGTTCTCTTGCAAATCCGTCGG | Δ*amb4151* |
| HM140 | TTTGCAAGAGAACTGGACTTTACCCTTGCGG | Δ*amb4151* |
| HM141 | CGGTGGCGGCCGCTCTAGAAGACGCCCTTGGCGGTCAG | Δ*amb4151* |
| HM146 | CAATTTCACACAGGAAACAGATGATGATCAGTCACCACGCGGC | pHM19 |
| HM147 | CGGTGGCGGCCGCTCTAGAATCAGGCGTGCACCGGCAG | pHM19 |

**TEM.** Whole AMB-1 cells were imaged by transmission electron microscopy (TEM). To prepare samples for imaging, 1.5mL of stationary phase (~$OD_{400}$ 0.25) culture was pelleted and resuspended in 10μL of MG. Cells were absorbed on glow-discharged, 200-mesh Cu grid with Formvar film and imaged on FEI Technai 12 transmission electron microscope with a Gatan Bioscan (1,000 by 1,000) charge-coupled device (CCD) camera model 792 at an accelerating voltage of 120kV.

**Quantification of crystal size and magnetosome numbers.** TEM images were used to measure crystal size and numbers. The length and width of each crystal was measured along its long axis by hand using ImageJ.

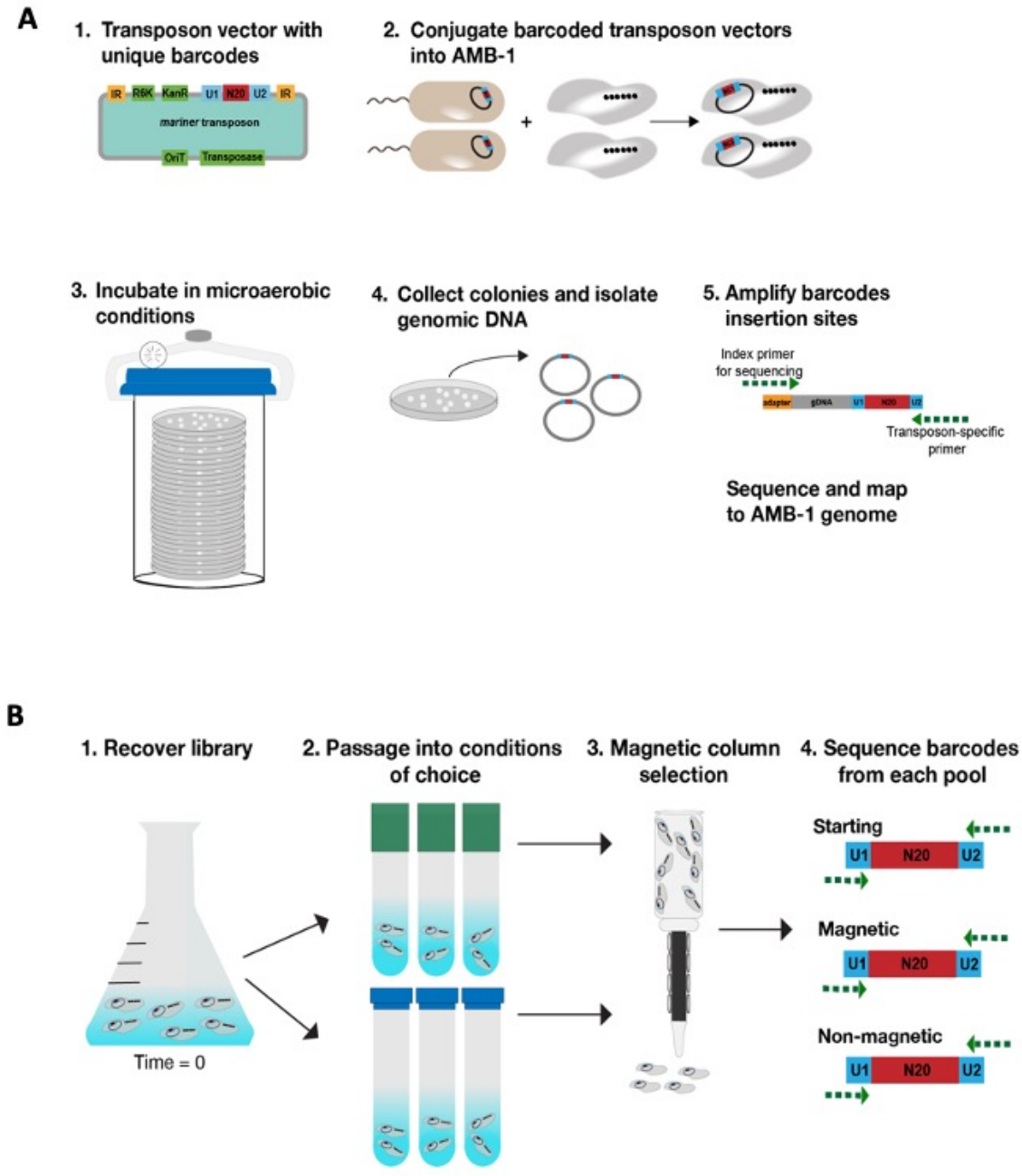


**Figure 1.** RB-TnSeq and magnetic selection. (A) Flow chart of RB-TnSeq library construction and sequencing. 1 (B) Flow chart of magnetic selection using RB-TnSeq library

A

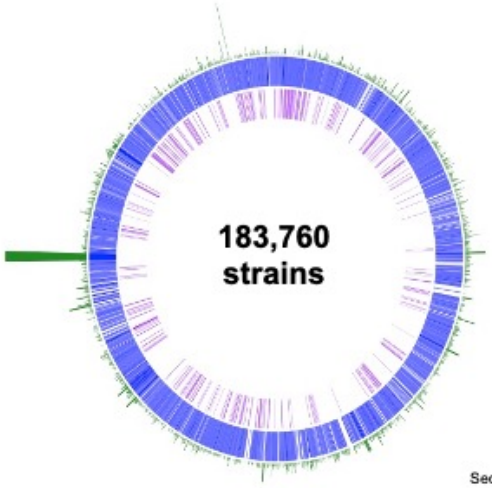


C

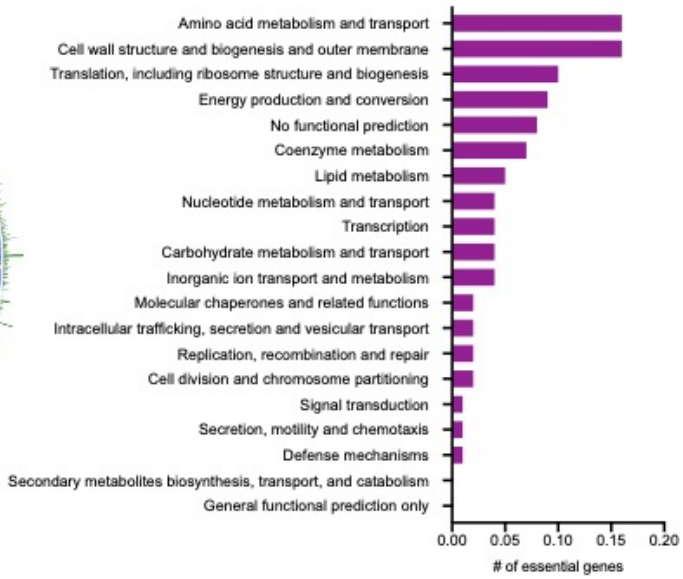


B

| **Library statistics** | |
|---|---|
| No. of strains with unique bar codes | 183,760 |
| **Protein coding genes** | |
| Total no. | 4,489 |
| No. with central insertions | 3,485 |
| Strains per hit gene | 23 (median), 34.3 (mean) |
| **Insertion bias** | |
| % toward coding strand of genes | 50.5 |
| Mean:median no. of reads per gene | 1.74 |

**Figure 2.** RB-TnSeq libraries and essential gene sets (A) Map of WT AMB-1 RB-TnSeq library showing AMB-1 genome (blue), WT essential genes (purple), and transposon insertion loci and densities (green) (B) Summary of library statistics for Magneto ML2. (C) Genes essential to the Magneto ML2 library under standard growth conditions grouped into COG categories

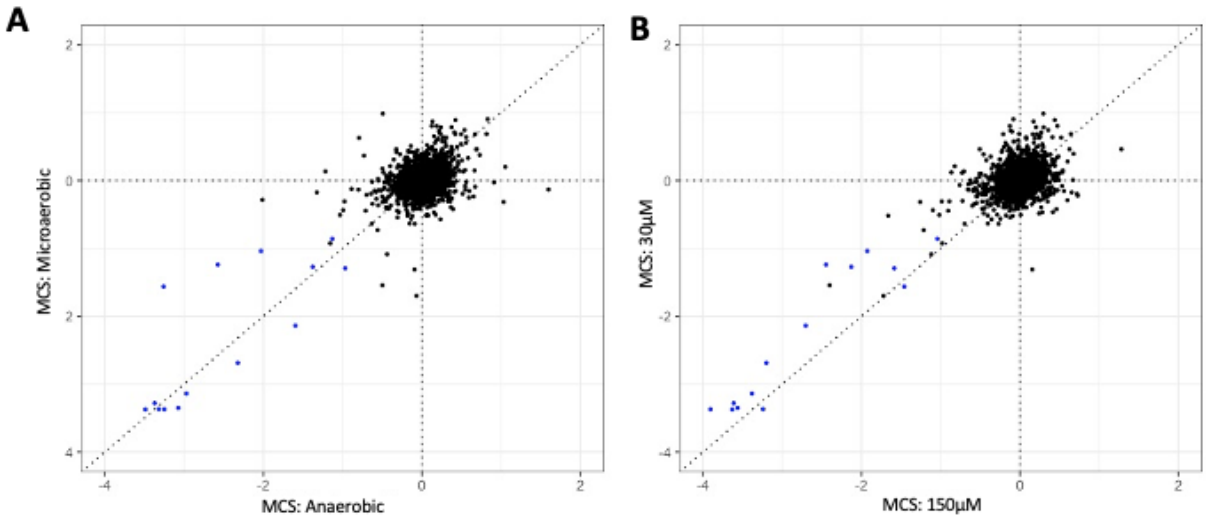


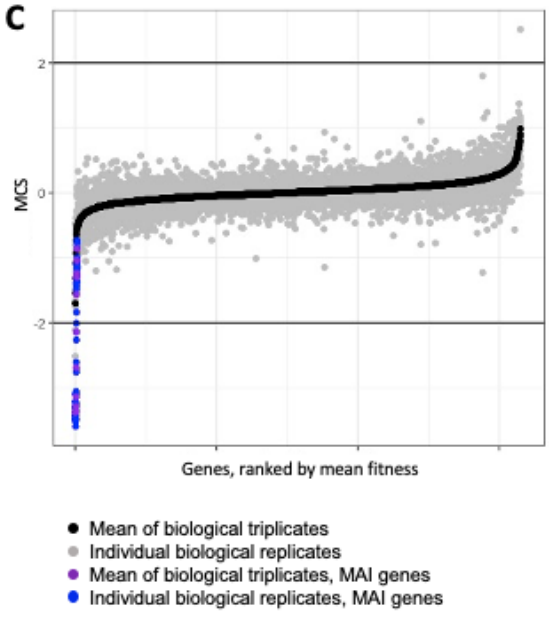


D

| Locus | Protein | Fitness Score |
|---|---|---|
| amb0956 | Mms6 | -1.29 |
| amb0957 | MmsF | -1.04 |
| amb0962 | MamH | -0.86 |
| amb0963 | MamE | -3.38 |
| amb0964 | MamJ | -1.56 |
| amb0965 | MamK | -2.69 |
| amb0966 | MamL | -3.37 |
| amb0967 | MamM | -3.28 |
| amb0968 | MamN | -3.35 |
| amb0969 | MamO | -3.14 |
| amb0970 | MamP | -3.37 |
| amb0971 | MamA | -2.14 |
| amb0975 | MamS | -1.28 |
| amb0976 | MamT | -1.24 |

**Figure 3.** Magnetic fitness of AMB-1 genes (A) Comparison of magnetic fitness scores for AMB-1 grown in microaerobic (<10% oxygen) or anaerobic (0% oxygen) conditions. Each point is the mean gene fitness of three biological replicates. MAI genes with low MCS highlighted in blue (B) Comparison of magnetic fitness scores for AMB-1 grown in 30µM iron or 150µM iron. Each point is the mean gene fitness of three biological replicates. MAI genes with low MCS highlighted in blue (C-D) Magnetosome island gene scores validate the magnetic selection process. (C) Distribution of magnetic fitness scores for WT grown in standard laboratory conditions (microaerobic (<10% oxygen) and 30 µM iron). MAI genes with low MCS highlighted in blue/purple (D) Table highlighting mean fitness scores for MGC genes and their respective proteins

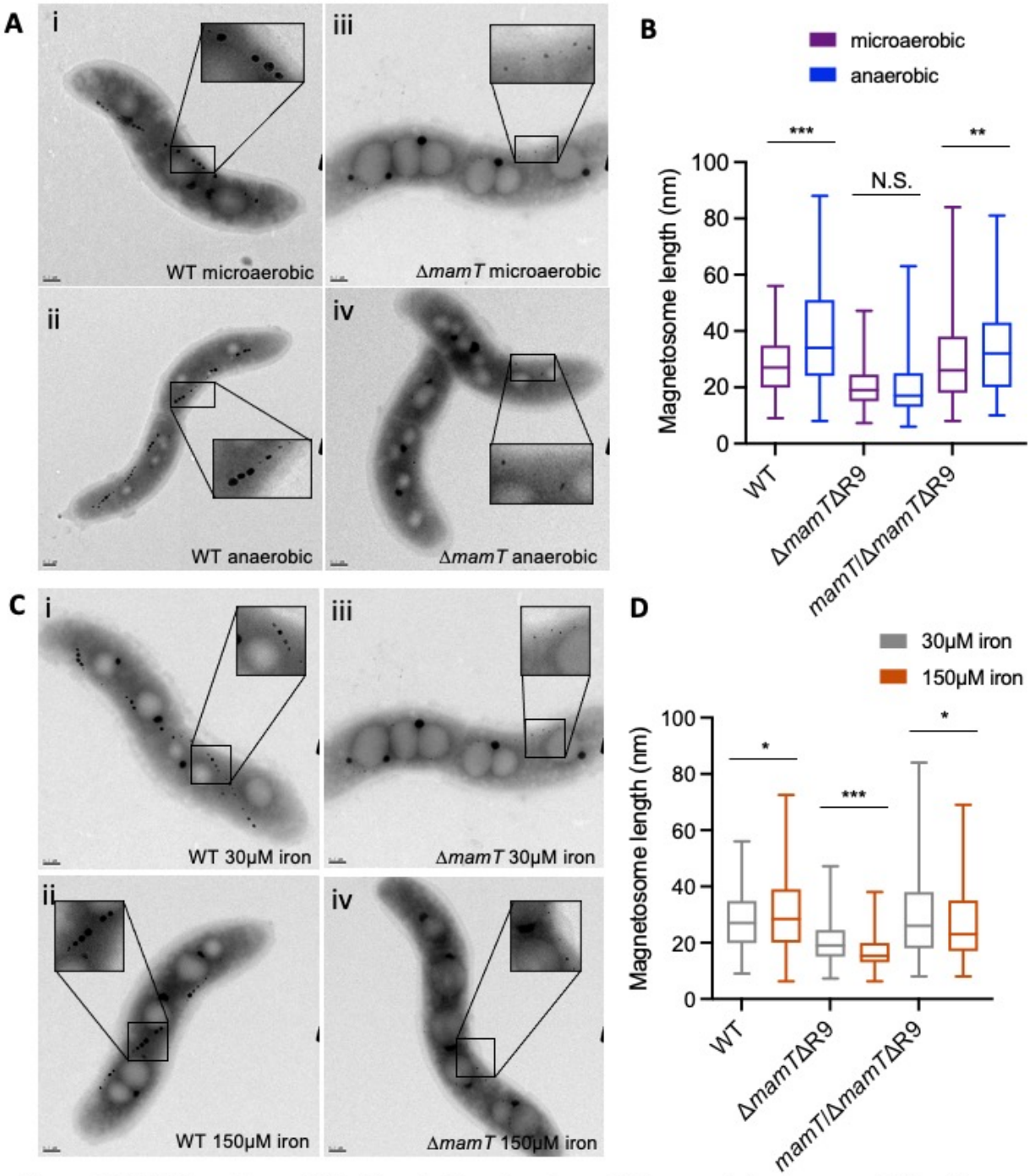


**Figure 4.** Validation of Δ*mamT* biomineralization phenotypes(A) Representative images of WT and Δ*mamT*Δ*R9* in microaerobic (<10% oxygen) or anaerobic (0% oxygen) conditions. (B) Magnetosome length of WT, Δ*mamT*ΔR9, and *mamT*/Δ*mamT*ΔR9 magnetosomes after growth in microaerobic (<10% oxygen) or anaerobic (0% oxygen) conditions. (C) Representative images of WT and Δ*mamT*Δ*R9* in 30μM iron or 150μM iron conditions. (D) Magnetosome length of WT, Δ*mamT*ΔR9, and *mamT*/Δ*mamT*ΔR9 magnetosomes after growth in 30μM iron or 150μM iron.

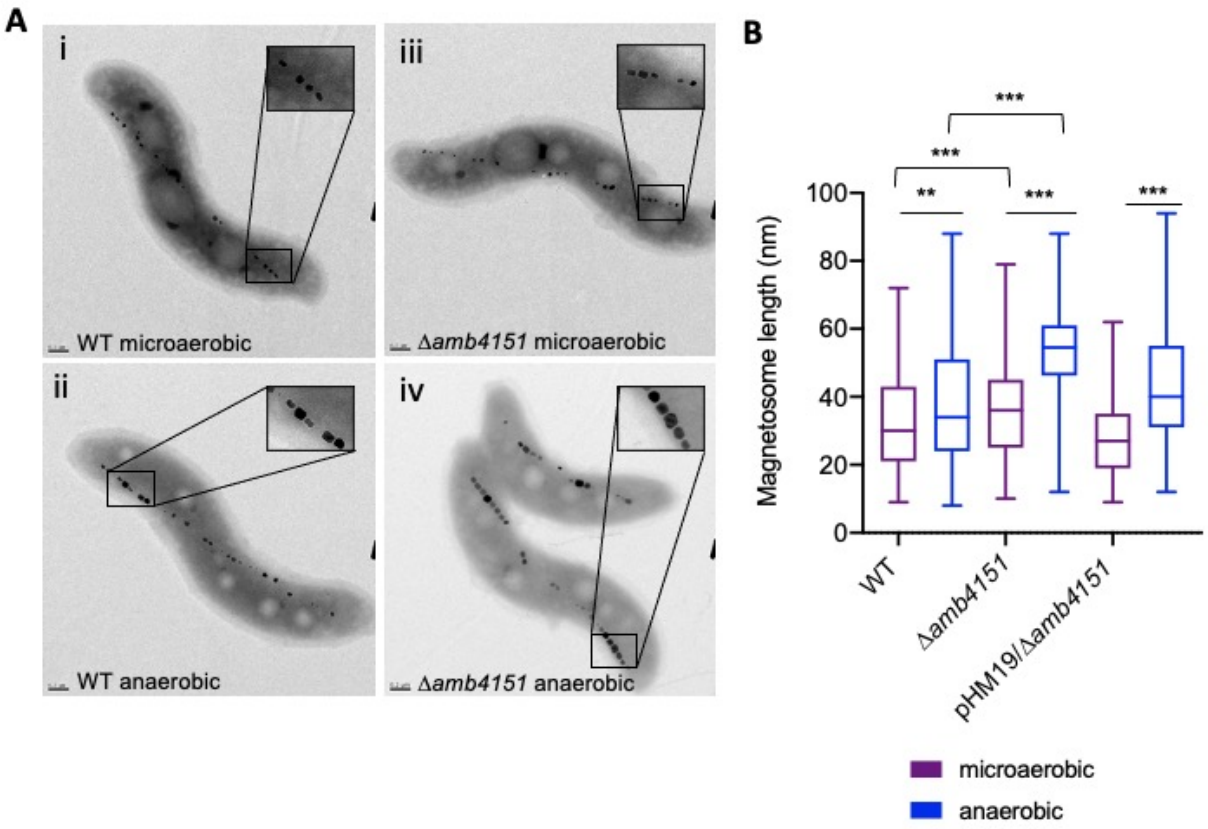


**Figure 5.** Validation of Δ*amb4151* biomineralization phenotypes. (A) Representative transmission electron micrographs of WT and Δ*amb4151* grown in microaerobic (<10% oxygen) and anaerobic (0% oxygen) conditions. i. WT grown in microaerobic conditions ii. WT grown in anaerobic conditions iii. Δ*amb4151* grown in microaerobic conditions iv. Δ*amb4151* grown in anaerobic conditions (B) Magnetosome length of WT, Δ*amb4151*, and *amb4151*/Δ*amb4151* magnetosomes after growth in microaerobic or anaerobic conditions.

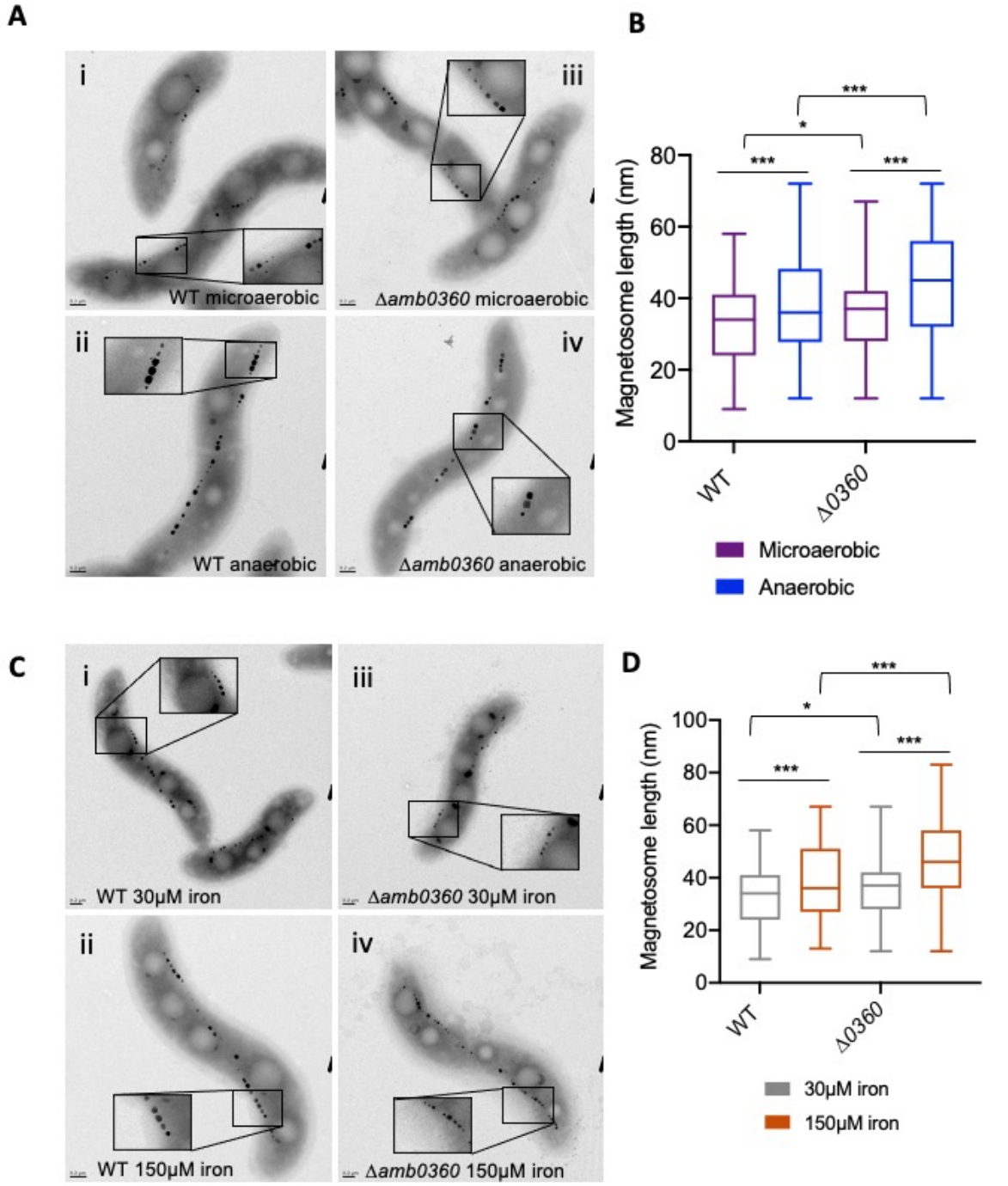


**Figure 6.** Validation of Δ*amb0360* biomineralization defect. (A) Representative transmission electron micrographs of WT and Δ*amb0360* grown in microaerobic (<10% oxygen) and anaerobic (0% oxygen) conditions. (B) Magnetosome length of WT and Δ*amb0360* magnetosomes after growth in microaerobic or anaerobic conditions. (C) Representative transmission electron micrographs of WT and Δ*amb0360* grown in 30 μM or 150 μM iron. (D) Magnetosome length of WT and Δ*amb0360* magnetosomes after growth in 30 μM or 150 μM iron

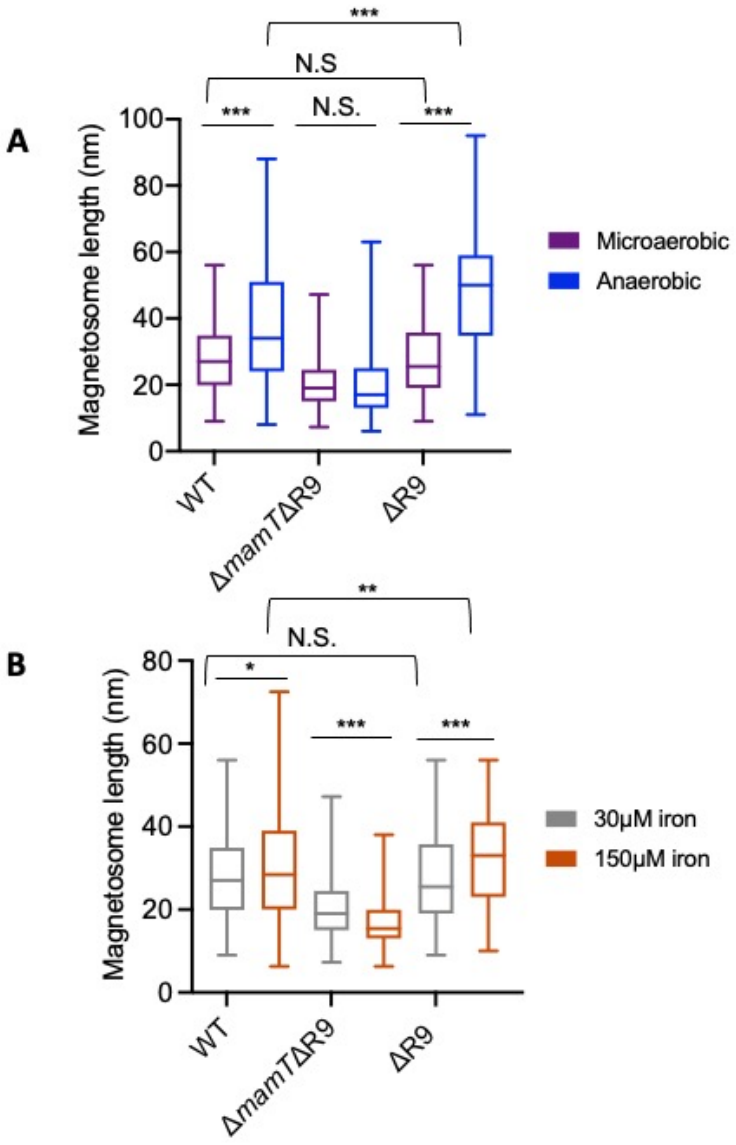


**Figure S1.** Δ*R9* does not impact the Δ*mamT*Δ*R9* phenotype (A) Magnetosome length of WT, Δ*mamT*Δ*R9,* and Δ*R9* magnetosomes after growth in microaerobic (<10% oxygen) or anaerobic (0% oxygen) conditions. (B) Magnetosome length of WT, Δ*mamT*Δ*R9,* and Δ*R9* magnetosomes after growth in 30 μM iron or 150 μM iron conditions.

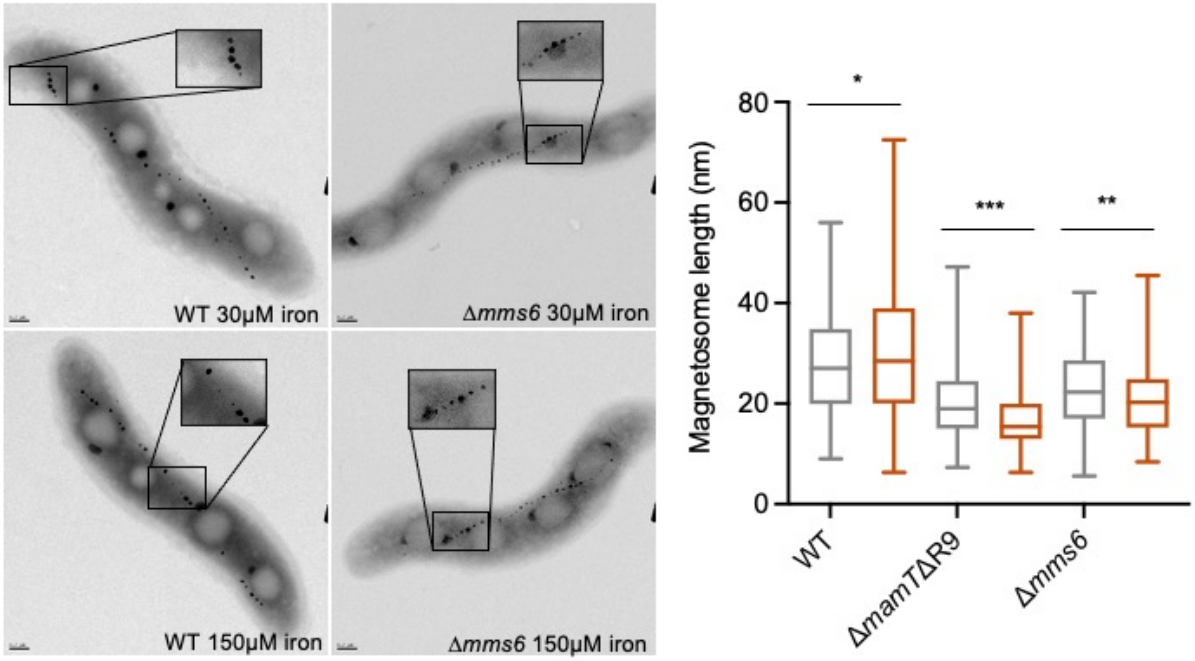


**Figure S2.** Δ*mms6* magnetosomes are longer under high iron conditions. (A) Representative transmission electron micrographs of WT and Δ*mms6* grown in 30 μM or 150 μM iron. (B) Magnetosome length of WT, Δ*mamT*Δ*R9,* and Δ*mms6* magnetosomes after growth in 30 μM iron or 150 μM iron conditions.

Table S1—Test for normality in magnetosome length analysis

| Figure | Strain, Condition | Shapiro-Wilk normality test (P-value) |
|---|---|---|
| Fig. 4B | WT, microaerobic | 0.0054 |
| | WT, anaerobic | <0.0001 |
| | Δ*mamT*Δ*R9*, microaerobic | <0.0001 |
| | Δ*mamT*Δ*R9*, anaerobic | <0.0001 |
| | *mamT*/Δ*mamT*Δ*R9,* microaerobic | <0.0001 |
| | *mamT*/Δ*mamT*Δ*R9,* anaerobic | <0.0001 |
| Fig. 4D | WT, 30 μM | 0.0054 |
| | WT, 150 μM | <0.0001 |
| | Δ*mamT*Δ*R9*, 30 μM | <0.0001 |
| | Δ*mamT*Δ*R9*, 150 μM | <0.0001 |
| | *mamT*/Δ*mamT*Δ*R9*, 30 μM | <0.0001 |
| | *mamT*/Δ*mamT*Δ*R9*, 150 μM | <0.0001 |
| Fig. 5B | WT, microaerobic | <0.0001 |
| | WT, anaerobic | <0.0001 |
| | Δ*amb4151*, microaerobic | 0.002 |
| | Δ*amb4151*, anaerobic | <0.0001 |
| | pHM19/Δ*amb4151,* microaerobic | <0.0001 |
| | pHM19/Δ*amb4151,* anaerobic | <0.0001 |
| Fig. S1A | WT, microaerobic | 0.0054 |
| | WT, anaerobic | <0.0001 |
| | Δ*mamT*Δ*R9*, microaerobic | <0.0001 |
| | Δ*mamT*Δ*R9*, anaerobic | <0.0001 |
| | Δ*R9,* microaerobic | <0.0001 |
| | Δ*R9,* anaerobic | 0.0238 |
| Fig. S1B | WT, 30 μM | 0.0054 |
| | WT, 150 μM | <0.0001 |
| | Δ*mamT*Δ*R9*, 30 μM | <0.0001 |
| | Δ*mamT*Δ*R9*, 150 μM | <0.0001 |
| | Δ*R9*, 30 μM | <0.0001 |
| | Δ*R9*, 150 μM | 0.0003 |

Table S2—Significance difference tests between magnetosome length datasets

| | | **Mann-Whitney U test** | | **t-test** | |
|---|---|---|---|---|---|
| **Figure** | **Strains/Conditions** | **p-value** | **Significant difference** | **p-value** | **Significant difference** |
| Fig. 4B | WT microaerobic & WT anaerobic | 0.030 | * | ---- | ---- |
| | Δ*mamT*Δ*R9* microaerobic & Δ*mamT*Δ*R9* anaerobic | 0.061 | * | ---- | ---- |
| | *mamT*/Δ*mamT*Δ*R9* microaerobic & *mamT*/Δ*mamT*Δ*R9* anaerobic | 0.007 | ** | ---- | ---- |
| | WT microaerobic & Δ*mamT*Δ*R9* microaerobic | <0.0001 | **** | ---- | ---- |

| | | | | | |
|---|---|---|---|---|---|
| | WT anaerobic & Δ*mamT*Δ*R9* anaerobic | <0.0001 | **** | ---- | ---- |
| | WT microaerobic & *mamT*/Δ*mamT*Δ*R9* microaerobic | 0.580 | N.S. | ---- | ---- |
| | WT anaerobic & *mamT*/Δ*mamT*Δ*R9* anaerobic | 0.023 | * | ---- | ---- |
| Fig. 4D | WT 30 μM & WT 150 μM | 0.030 | * | ---- | ---- |
| | Δ*mamT*Δ*R9* 30 μM & Δ*mamT*Δ*R9* 150 μM | <0.0001 | **** | ---- | ---- |
| | *mamT*/Δ*mamT*Δ*R9* 30 μM & *mamT*/Δ*mamT*Δ*R9* 150 μM | 0.041 | * | ---- | ---- |
| | WT 30 μM & Δ*mamT*Δ*R9* 30 μM | <0.0001 | **** | ---- | ---- |
| | WT 150 μM & Δ*mamT*Δ*R9* 150 μM | <0.0001 | **** | ---- | ---- |
| | WT 30 μM & *mamT*/Δ*mamT*Δ*R9* 30 μM | 0.580 | N.S. | ---- | ---- |
| | WT 150 μM & *mamT*/Δ*mamT*Δ*R9* 150 μM | 0.0004 | *** | ---- | ---- |
| Fig. 5B | WT microaerobic & WT anaerobic | 0.0015 | ** | ---- | ---- |
| | Δ*amb4151* microaerobic & Δ*amb4151* anaerobic | <0.0001 | **** | ---- | ---- |
| | pHM19/Δ*amb4151* microaerobic & pHM19/Δ*amb4151* anaerobic | <0.0001 | **** | ---- | ---- |
| | WT microaerobic & Δ*amb4151* microaerobic | 0.007 | ** | ---- | ---- |
| | WT anaerobic & Δ*amb4151* anaerobic | <0.0001 | **** | ---- | ---- |
| | WT microaerobic & pHM19/Δ*amb4151* microaerobic | 0.003 | ** | ---- | ---- |
| | WT anaerobic & pHM19/Δ*amb4151* anaerobic | <0.0001 | **** | ---- | ---- |
| Fig. S1A | Δ*R9* microaerobic & Δ*R9* anaerobic | <0.0001 | **** | ---- | ---- |
| | WT microaerobic & ΔR9 microaerobic | 0.828 | N.S. | ---- | ---- |
| | WT anaerobic & ΔR9 anaerobic | <0.0001 | **** | ---- | ---- |
| Fig. S1B | Δ*R9* 30 μM & Δ*R9* 150 μM | <0.0001 | **** | ---- | ---- |

| | | | | | |
|---|---|---|---|---|---|
| | WT 30 μM & ΔR9 30 μM | 0.828 | N.S. | ---- | ---- |
| | WT 150 μM & ΔR9 150 μM | 0.008 | ** | ---- | ---- |

Significantly different (*P<0.05, **P<$10^{-2}$, ***P<$10^{-3}$, ****P<$10^{-4}$); N.S. not significantly different.

CHAPTER 3

# Nano and Microtechnologies for the Study of Magnetotactic Bacteria

Andy Tay[a], Hayley McCausland[b], Arash Komeili[b,c], and Dino Di Carlo[a]

Department of Bioengineering, University of California, Los Angeles, USA; Department of Molecular and Cell Biology, University of California, Berkeley, USA; Department of Plant and Microbial Biology, University of California, Berkeley, USA

This chapter has been adapted from following, with permission:
Tay A, McCausland H, Komeili A, and DiCarlo D. Nano and Microtechnologies for the Study of Magnetotactic Bacteria. Advanced Functional Materials. 2019. 29, 1904178.

## Abstract

Magnetotactic bacteria (MTB) naturally synthesize magnetic nanoparticles that are wrapped in lipid membranes. These membrane-bound particles, which are known as magnetosomes, are characterized by their narrow size distribution, high colloidal stability, and homogenous magnetic properties. These characteristics of magnetosomes confer them with significant value as materials for biomedical and industrial applications. MTB are also a model system to study key biological questions relating to formation of bacterial organelles, metal homeostasis, biomineralization, and magnetoaerotaxis. The similar size scale of nano and microfluidic systems to MTB and ease of coupling to local magnetic fields make them especially useful to study and analyze MTB. In this Review, a summary of nano- and microtechnologies that are developed for purposes such as MTB sorting, genetic engineering, and motility assays is provided. The use of existing platforms that can be adapted for large-scale MTB processing including microfluidic bioreactors is also described. As this is a relatively new field, future synergistic research directions coupling MTB, and nano- and microfluidics are also suggested. It is hoped that this Review could start to bridge scientific communities and jump-start new ideas in MTB research that can be made possible with nano- and microfluidic technologies.

## Introduction

Magnetotactic bacteria (MTB) are phylogenetically diverse organisms that can biomineralize and assemble linear chains of magnetite ($Fe(II)Fe(III)_2O_4$) or greigite ($Fe(II)Fe(III)_2S_4$) nanoparticles with different shapes and sizes. These nanoparticles which are bound in lipid membranes are known as magnetosomes [3]. Magnetosomes allow MTB to align with the Earth's magnetic field lines and navigate along oxygen gradients in bodies of water through a process referred to as magnetoaerotaxis [61]. MTB provide a model system for studying several important questions in cell biology including cellular organization, the formation of bacterial organelles, and metal homeostasis. It has been found that the formation of magnetosomes is controlled by a specific gene set collectively named as the magnetosome gene cluster (MAI) [61]. Based on how much iron MTB are able to take up from their aquatic environments, it is also possible that MTB can play a significant role in global iron cycling [1].

In addition to being of interest in basic cell biology, magnetosomes hold great promise for use in a variety of applications. Magnetosomes have homogeneous sizes and crystallography, high thermal and colloidal stability, and their surfaces can be functionalized with biocompatible organic molecules [118]. These properties have motivated research using magnetosomes in biomedical applications including targeted drug delivery [119], magnetic resonance imaging (MRI) [120,121], magnetic hyperthermia [122,123], and even neural modulation [124].

Nano and microfluidic approaches hold great promise to transform and accelerate studies of MTB (**Fig. 1**). These technologies utilize devices with fluidic channel dimensions approximately in the range of hundreds of nanometers (nm) to tens of micro-meters (μm) that are suited to precisely control and manipulate fluids. As nano and micro-channels have dimensions in the same length scale as biological cells including MTB, they are able to offer high spatial and temporal control in processes such as cell sorting and the study of cell mobility. For example, microfluidic technologies have been used for repeatable, high-throughput sample processing including cell lysis and nanoparticle functionalization [125,126]. They have also been integrated with other physical forces like magnetism to exploit differences in a particle's magnetic properties for separation [127]. Additionally, high throughput (~1-10 mL/min) microfluidics has been used to monitor cell growth and isolate sub-populations of cells with desirable phenotypes from

bioreactors [128]. Here, we provide a review of existing nano and microfluidic technologies that have been applied to the study and analysis of MTB. As this field is relatively new, we also offer ideas where such precise fluidic control may be applied to advance the MTB field. We hope that this review can encourage synergies among scientists working on MTB and microfluidics to improve our knowledge of this unique class of microorganisms.

## 2.0 Nano and Microfluidics for Cell Analysis

Nano and microfluidic technologies offer several advantages that make them ideal for cell analyses [129]: (1) channels with similar length scale (ranging from a few hundred nm to tens of μm) to particles and cells, which facilitates high spatiotemporal resolution for cell analyses, (2) ease of coupling with other modalities including electrical and magnetic fields to exploit properties of particles and cells for cell lysis, isolation, and purification, and (3) tunable flow rates that offer a range of precision for different cell analysis requirements.

### 2.1 Quantifying the magnetic properties of MTB

MTB are a phylogenetically diverse group of bacteria having different shapes (spirillum, vibrio, fava-bean, cocci, ovoid, and rod) and sizes (length: 1-20 μm, width: 0.2-2.2 μm). Furthermore, different species have also been found to produce different numbers (from <10 to even a thousand) [76], shapes (cubo-octahedral, elongated prismatic, bullet shaped, etc.), and sizes (35-120 nm in diameter) of magnetosomes [120]. There are a few methods to measure the outcomes of biomineralization and the magnetic response of MTB such as alignment to magnetic fields and magnetic content. These techniques include transmission electron microscopy [130], $C_{mag}$ (light scattering in the presence of a magnetic field) measurements [131], and color inspection of brown colonies on agar gel [31]. During transmission electron microscopic imaging, MTB are transferred onto copper grid and can be visualized usually without the use of any contrast agents due to the presence of electron-dense magnetosomes. During $C_{mag}$ measurement, MTB are placed parallel or perpendicular to an external magnetic field and the amount of light absorbance is detected using a spectrophotometer, typically at around 400-600 nm. $C_{mag}$ can be calculated by this equation: $C_{mag} = (A_{400\ nm,\ perpendicular}/A_{400\ nm,\ parallel}) - 1$. Note that the optical density should be at least 0.1 before $C_{mag}$ measurement to ensure that there are sufficient MTB for reproducible readings. Color inspection is a simple technique where the color of MTB colonies is visualized by naked eye. Generally, the darker the color of colonies with the same sizes, it is assumed that the MTB have more magnetosomes. However, these techniques may suffer from limitations such as being non-quantitative, labor intensive, and low throughput (**Table 1**). A few other light-based techniques including optical magnetic imaging [132], fluid cell scanning transmission electron microscopy [133], and confocal Raman micro-spectrometry [134] have been described in the literature but as they typically require expensive set-ups, their use has been relatively limited.

Nano and microfluidic technologies have been developed to separate cells based on cellular properties such as size, deformability, and magnetic content [127]. Recently, Myklatun et al. reported the use of a magnetic microfluidic platform to isolate MTB suspended in a ferrofluid [135]. The team immobilized MTB which had fast flagellar motion using 75$^{o}$C heated media for 15 min but did not demonstrate viability of heat-treated MTB post-separation. While this technology is useful as a single use magnetic separation and quantification of MTB, it is not likely applicable for sorting live MTB due to the use of heated media.

This problem was recently overcome by inhibiting rapid flagellar movement with transient cold, alkaline treatments which preserved cell viability [136]. Next, by exploiting the balance between frictional drag in fluids and magnetic field gradient in a micro-channel, a mixed population of live, wild-type *Magnetospirillum magneticum* (AMB-1) was separated from mutants producing about 2.2x more magnetosomes with efficacy similar to theoretical estimates [137]. The same platform

was also adapted to isolate wild-type *Magnetospirillum gryphiswaldense* (MSR-1) from its Δ*mamAB* mutant counterparts, which do not produce magnetosomes, with sensitivity up to 80% and isolation purity up to 95% as confirmed with a gold standard, fluorescent-activated cell sorter (FACS) technique (**Fig. 2a**) [136]. The magnetic microfluidic platform also offers 25-fold higher throughput than the one fabricated by Myklatun et al. (25,000 cells/min versus 1000 cells/min) [135].

Another application of microfluidic or other micro-magnetic-based separation devices is to distinguish MTB producing magnetosomes of different sizes, shapes, and elemental compositions. This is because these physical properties are known to affect how magnetosomes interact with magnetic fields. For instance, assuming everything being constant, a larger magnetosome is expected to provide more magnetic force than a smaller magnetosome. A magnetosome with higher purity of iron content will also provide more magnetic force than a magnetosome which has lower iron content. These physical properties affect the magnetic volume of magnetosome and hence their interactions with magnetic fields [136,138]. The ability to differentiate magnetosomes in this way will be of great utility in biomedical applications, especially because magnetic nanoparticles with different physical properties, including size, shape and magnetic properties [139] are known to affect biological processes like endocytosis [140] and cytotoxicity [141]. For instance, smaller nanoparticles are more likely to be endocytosed, and hence more likely to induce cytotoxicity when a large quantity is internalized by cells. Furthermore, the composition of the magnetosomes, whether it is magnetite or greigite, can also affect their magnetic and thermal properties for purposes like magnetic hyperthermia [142].

### 2.2 Directed evolution

MTB are fastidious bacteria that grow at an extremely slow rate (a few hr/cell division compared to as fast as 20 min/cell division for *Escherichia (E.) coli*) [41] even in optimized conditions. Kolinko et al. addressed this growth limitation by transferring 30 key genes from MSR-1 to *Rhodospirillum rubrum*, a faster growing photosynthetic prokaryote, showing the possibility of endogenous magnetization in non-magnetic organisms [143]. Liu and colleagues also introduced a mutation upstream of an ATPase gene to generate MSR-1 that overproduced magnetosomes [144]. In addition, Lohβe et al. demonstrated the use of gene amplification to create MSR-1 mutants that produce 2.2 fold more magnetosomes than wild-type cells. These studies are indicative of the rising interest within the community to engineer or evolve organisms that produce magnetosomes more rapidly. Directed evolution offers great implications for studying MTB biology and the use of MTB and magnetosomes. For instance, MTB that over-produce magnetosomes can be cultured in large numbers to harvest magnetosomes for biomedical applications. MTB over-producer mutants may also be more useful than wild-type MTB as micro-robots for drug delivery purposes as they can be more easily manipulated with magnets. Furthermore, by combining directed evolution and genetic dissection, the magnetic gene cascade may be understood to advance the technique of magnetogenetics for wireless magnetic cell manipulation [145].

#### 2.2.1 Selection of MTB over-producers

To demonstrate the use of nano and micro-fabrication technologies for directed evolution of MTB, random chemical mutagenesis and a quantitative magnetic ratcheting technique were combined to select over-producing mutants (**Fig. 2b**) [98]. Existing magnetic methods for cell separation such as magnetic-activated cell sorting (MACS) that accumulates all cells with any magnetic content did not offer sensitivity high enough to differentiate MTB mutants with small differences in magnetosome numbers. Thus, the authors employed a ratcheting system consisting of magnetized permalloy magnetic elements which offer high sensitivity up to ± 5 magnetosomes. AMB-1 was randomly mutated with chemical mutagens to generate mutants with different magnetosome producing abilities followed by selection using the magnetic ratcheting platform.

The mutated AMB-1 can be distinguished based on the balance between the magnetic force on each bacterium and the fluid drag force that each bacterium experiences. Using this strategy, AMB-1 mutants with different number of magnetosomes were generated. For instance, there were mutants without magnetosomes and mutants over-producing ~2 folds more magnetosomes than control AMB-1. The magnetosomes synthesized by the over-producers were also comparable in terms of size, shape, and magnetic properties to those produced by wild-type, control AMB-1.

We also like to highlight that although the working principles i.e. balance between magnetic force and Stokes' drag of magnetic microfluidic platform (see **Section 2.1** and **Fig. 2a**) and magnetic ratcheting system are similar, they offer different levels of precision and throughput. Magnetic microfluidic system provides much higher throughput (25,000 cells/min versus <10,000 cells/min) in quantifying magnetic properties of MTB. On the other hand, the magnetic ratcheting system offers higher quantitative accuracy ($\pm$ 5 magnetosomes versus ($\pm$ 10-15 magnetosomes) for more precision selection of MTB over-producers. A useful future development of the magnetic ratcheting technique is to enable sterile, closed-loop, continual generation of diverse MTB variants with desirable properties to enhance its throughput while preserving its higher precision [35].

### 2.2.2 Genetic engineering

Over a few decades of research, microbiologists have elucidated the roles of the *mamAB* gene cluster in magnetosome formation [29,34,39,45,47,115,146,147]. Other operons, such as *mms6,* that play a role in determining the crystal structure of magnetosomes have also been identified.[148,149] However, it remains a challenge to introduce large plasmid constructs all at one time. For instance, Lohβe et al. doubled the genes in the magnetosome island of MSR-1 to generate mutants producing double the number of magnetosomes [144]. But this was achieved through a laborious process involving random conjugation of MTB with competent *E.coli* for one plasmid construct transfer at a time. Furthermore, this process may be challenging to control and offer variable frequencies depending on the plasmids [150]. There is a biological limitation in the plasmid size (typically less than 50 kilobases (kbp)) that can be transferred through the conjugation pili [150].

Nano and micro-technologies can be used to introduce exogenous materials like plasmid constructs more efficiently into organisms with user-defined conditions. One example is through nano and micro-channel penetration and electroporation [151]. Unlike the use of conjugating *E. coli* or other biological methods, penetration and electroporation makes use of physical forces to locally penetrate through the cell or transiently open pores in the cell wall/membrane for DNA delivery. Bacteria centrifuged at fast speed can be mechanical penetrated onto nano and micro-structures. Electroporation makes use of steep voltage differences to create localized electrical potential differences across cells. This disrupts the cell wall and membrane, causing formation of transient pores for entry of biomolecules such as DNA for transformation [152]. The properties of nano and micro-structures such as length, diameter and voltages can be more easily controlled and optimized by users to achieve increased uniformity in genetic engineering.

Paulo et al. made use of computational simulation to determine the critical electric field just sufficient to induce electroporation and performed microfluidic electroporation to amplify and better control the spatiotemporal properties of the electric field strength [153]. This technique can potentially transform MTB with greater precision in the number of copies of DNA/bacterium as compared to random conjugations with *E. coli,* especially for MTB strains that are difficult to transform. For instance, Okamura et al. made use of bulk liquid electroporation to introduce DNA plasmids into MTB and we speculate that this process could be possibly improved using microfluidic electroporation [154].

Recently, there is also increasing interest in using nano and micro-wires or pillars for direct penetration through cell walls for DNA delivery [155]. Several groups have also developed nanochannel electroporation platforms which integrate localized electric fields to draw large DNA, up to tens of kbp, into cells [156]. These nanochannels are typically a few hundred nm and are larger in magnitudes than plasmids. The use of electric fields facilitates active electrophoretic delivery of negatively-charged DNA; it also reduces the possibility that the nanochannels would be clogged. This can also be useful to genetically or synthetically incorporate magnetic properties to non-magnetic cells as genes of the magnetosome island's operons can be up to tens of thousands of base pairs.

### 2.2.3 Lineage tracking

Microfluidic devices can also facilitate lineage tracking to understand environment-dependent and environment-independent phenotypic variations and cell-fate switching. Such platforms have improved our understanding of stochastic phenotypic changes in bacteria and temporal control of gene circuits encoding for bacterial oscillatory cell fate behaviors [157]. For instance, Wang and co-workers designed a microfluidic device consisting of multiple channels that accommodated only one *E.coli* bacterium at each channel (**Fig. 2c**) [158]. Each newly generated bacterium was flushed by microfluidic flow to the next available channel which allowed easy monitoring of cell shape and size. As *E. coli* and MTB share similar size range, and it will be simple to adapt this device design to separate sister MTB of different generations in their respective micro-channels. For instance, single MTB can be isolated for physical phenotyping and genetic screening to assess the mutational frequency in MTB that is known to affect their magnetic properties [159]. Another potential application of this device is to monitor the production of magnetosomes by MTB over-producers over multiple generations to understand the role of specific genes in phenotypic reversions. It may also find utility in the fundamental understanding of magnetosome splitting between daughter MTB at the single cell level especially because in some MTB strains, there can be uneven magnetosome numbers (e.g. *Magnetospirillum magneticum* AMB-1) or multiple magnetosome chains (e.g. "*Candidatus* Magnetobacterium bavaricum") [160] which complicate equal magnetosome distribution.[160] We note that although most microfluidic platforms are designed to study *E. coli* and other micro-organisms with health implications, they can be conveniently modified to study MTB which has similar size range.

### 2.2.4 Bacterial ecosystems

It is possible that MTB in their natural habitats interact with other micro-organisms through processes like iron and phosphate re-cycling [161]. Microfluidic devices have been employed to construct and replicate environments to elucidate the role of bacterial ecosystems in regulating cellular biology [157]. For instance, Kim and colleagues co-cultured three strains of bacteria. Each strain had a specific role: supplying nitrogen, providing carbon, or degrading antibiotics [162]. The bacteria flourished in the co-culture with finite inter-chamber distance but perished when separated or when positioned too far away for sufficient diffusion of resources. As MTB are able to store iron, a co-culture of MTB may reveal their ecological dynamics with other micro-organisms, especially in iron cycling. Additionally, the ability of MTB to take up toxic, heavy metals such as cobalt and manganese from their natural habitats [163] has intriguing future implications for using MTB as tools for ecological waste water treatment or heavy metal removal.

## 2.3 Single cell analysis

Single-cell analysis has revealed how heterogeneity in cell populations affects cellular functions and responses to stimuli [82]. Single-cell analysis techniques have been applied to understand the similarities in genetic makeup of uncultivated MTB and those that are cultured in order to determine the preferred electron donors and acceptors of uncultivated MTB strains [164]. However, even with knowledge about the genetic makeup of uncultivated MTB, it can be a

laborious and costly process to generate multiple, different media compositions in large (liters) quantities to cultivate newly found MTB strains.

Microfluidics can be helpful to screen a multitude of culture conditions in small volumes (μL to mL). Single-cell droplet microfluidics can generate droplets each encapsulating a single cell for analysis [165]. Using this method, libraries of droplets containing different media conditions can be used to optimize media composition by screening for essential nutrients and elements in a small-volume environment. This automated approach could greatly save on resources and manpower, but also enable signaling molecules to accumulate within a droplet (with sub-nanoliter volumes) at much high concentrations compared to multi well-plates (with tens of microliters to milliliter volumes) approaches. Such techniques may also be useful to progressively isolate MTB mutants that have adapted to different carbon/electron sources for culturing in laboratories.

Currently, droplets are generated in microchannels using water and oil emulsification controlled precisely by flow rate or geometry. However, the magnetic microfluidic droplet generator created by Chen and colleagues can exploit the inherent magnetic properties of MTB to potentially facilitate more accurate downstream analyses with single-cell droplets (**Fig. 2d**) [166]. This microfluidic platform can also be coupled with additional functions for automatic cell lysis, nucleic acid extraction, and polymerase chain reactions for single-cell analysis [167]. Another noteworthy design is by Brouzes et al. who introduced a magnetic microfluidic droplet methods to analyze mRNA in single cells [168]. Using a technique called droplet splitting, a single cell with adsorbed magnetic beads was encapsulated in each droplet. After attracting the magnetized cell to one end of the micro-channel the droplet was cut into two halves. With the volume of the droplet containing the magnetized cell halved, the concentration of mRNA that can be isolated from the cell is doubled, potentially improving the accuracy of downstream analyses. This droplet-splitting strategy can be applied to isolate naturally magnetic MTB in droplets with smaller volume to concentrate samples (DNA/mRNA/proteins) for more sensitive single cell analysis. It can also be useful for high-throughput genetic screening of mutants in order to learn about the functions of specific genes and their roles in magnetosome formation.

**2.4 Mobility**

There is interest in studying the tactic abilities of MTB—magnetotaxis, chemotaxis, phototaxis, and aerotaxis [100,169,170]— because MTB can be used as model organisms to study competing modes of tactic behaviors. There is also potential to use MTB taxis to develop micro-robots for transport and on-chip diagnosis [119,171–173]. Microfluidic devices can be used to advance taxis research. Besides offering better spatiotemporal control of gradients, the transparency of glass or PDMS-based microfluidic devices also facilitate convenient monitoring of biochemical gradients using colored/fluorescent dyes[174]. Such devices have been employed to understand the mobility of bacteria. For instance, Waisbord and co-workers found that *Magnetococcus marinus* in growth media display mobility governed by the balance between magnetic torques and fluctuations of thermal energy [175]. However, in a microchannel devoid of nutrients, *M. marinus* demonstrated run-and-tumble dynamics. This behavior is also observed when *M. marinus* encountered geometrical constraints such as sediments in their natural habitats. Recently, Loehr et al. also demonstrated the possibility of magnetically guiding *M. gryphiswaldense* along lines of instability, revealing a type of mobility not displayed by other bacteria like *E. coli* [176]. Microfluidic flow and mixing can also simulate microparticle suspensions to imitate the presence of agitation [101] to understand how MTB may respond to similar situations in their natural habitats. The data obtained will be useful for modelling of MTB behaviors to create physical models of processes such as magnetotaxis, which can aid in the design of magnetic robots for *in vivo* drug delivery [100].

Aerotaxis refers to directional motion in response to oxygen gradients. Uni-polar, di-polar, and axial magnetoaerotactic behaviors have been observed in different MTB strains by Lefèvre and co-workers, who monitored the motions of MTB in capillary tubes [170]. The team also found that different MTB strains preferred different oxygen levels. Popp et al. looked at the behavior of MSR-1 in oxygen gradients and found that MSR-1 display swimming polarity through oxygen sensory pathways regulated by CheOp1 [7]. Lately, Felfoul et al. described the use of MTB to deliver drug-containing nanoliposomes to tumor hypoxic regions [119]. In the future, microfluidic devices can also be used to enrich MTB with different sensitivity to oxygen gradients for targeted drug delivery to body tissues with different oxygen levels.

Most of the existing literature on the aerotactic behaviors of bacteria made use of distinct bands, corresponding to specific oxygen concentrations, formed by the bacteria in capillary tubes with oxygen gradients [177–179]. However, it is challenging to accurately measure oxygen level in capillary tubes, especially when taking the spatial distribution of the bacteria and the rate of oxygen consumption into account. To overcome this technical limitation, Alder et al. created a microfluidic device with stable linear profiles of oxygen, ranging from 0-0.5% oxygen to up to 16% [180]. The same group also demonstrated the possibility of generating linear, exponential, and non-monotonic shaped oxygen gradients [181], which can be applied to understand both the effects of geometry and oxygen gradients in MTB mobility. For instance, Li and colleagues integrated valves in their microfluidic device and observed that they could induce AMB-1 migration by mixing different concentrations of oxygen and nitrogen gases [182].

Microfluidic chips have also been employed for studying chemotaxis in bacteria. Mao and colleagues first introduced microfluidics into this field by arguing that the conventional capillary assay has limited sensitivity as the chemical concentration gradient becomes shallower with time [173]. However, with a microfluidic device, they were able to maintain steady concentrations of chemo-attractants/repellents at a fixed spot due to constant replenishment. Ahmed et al. later proposed a mathematical model to quantify the chemotactic behaviors of cells in steady, non-linear microfluidic gradients of arbitrary shapes [183]. Englert and co-workers also used flow-based microfluidic systems to generate a steady chemical gradient along the entire channel length as long as flow is maintained [179]. Using devices like these, a wide range of chemical gradients can be created to study the response of MTB to various chemicals of interest. This could be of utility to select MTB attracted to chemical signals secreted by different body tissues or tumors for targeted *in vivo* drug delivery. Other microfluidic devices used to study the thermo- [184] and photo-taxis [185] behaviors of bacteria/algae can also be easily adapted for MTB [186].

## 3.0 Nano and Microfluidics for Industrial Applications

Nano and microfluidic technologies coupled to bioreactors can also be useful for high throughput monitoring of cell growth and magnetosome production rates. Furthermore, they can be integrated with ultrasound or chemical on-chip cell lysis, magnetosome extraction, purification, and functionalization approaches.

### 3.1 Bioreactor

MTB can be cultured in large-scale bioreactors with optimal culture conditions [187,188]. Parallelized microfluidics with multiple devices running simultaneously can offer high throughput sorting at a range of 10-1000 mL/min [128]. This may offer advantages over the use of filters for isolating sub-populations of MTB to minimize clogging/biofouling and repeated need for changing expensive filters [189]. Microfluidic bioreactors may also be used to monitor the response of MTB to environmental changes such as pH, temperature, presence of poly-ethylene-glycol (PEG) [190], oxygen, and shear stresses [191] in real time. Furthermore, micro-scale versions of microfluidic bioreactors can be constructed to monitor how certain processes such as the fluid

dynamics of mixing occur in scaled-up versions [192]. Motivated by the use of multiplexed microfluidic systems for biotechnological purposes, we propose that a highly parallelized magnetic microfluidic system to quantify magnetic contents in MTB may also be used as microfluidic reactors (**Fig. 3a**) [97], highlighting the flexibility of microfluidic devices for use in biotechnology. Mach and Di Carlo also proposed the use of inertial microfluidic platform for scalable blood cell filtration (**Fig. 3b**) [193]. The platform was able to achieve a processing speed of 240 mL/hr. It could be adapted for high throughput magnetic isolation by patterning nano/micro-magnets within the channels and magnetizing them remotely with a large external magnetic field [14].

### 3.2 Magnetosome purification and functionalization

One of the goals of generating MTB over-producers is to harvest their magnetosomes for use in biotechnology or biomedical applications. The current techniques to isolate magnetosomes are ultrasound, chemical, or mechanical lysis followed by collection using a magnet. These methods are time consuming and have user-dependent performance. Furthermore, to recover magnetosomes, substantial wash steps are necessary that increase the loss of magnetosomes [194]. Microfluidics can be coupled with various modalities to construct a μTAS (total analysis system) for on-chip cell lysis, magnetosome extraction, purification, and even functionalization [195]. A μTAS could allow for careful control of cell lysis to avoid any damage to the lipid membranes encapsulating the magnetic nanoparticles and can potentially enhance the recovery of magnetosomes (**Fig. 3c**).

Numerous microfluidic platforms have been described for cell lysis. Bao and Lu made use of electric fields to break up bacterial cells [196]. Lu et al. also made use of electric fields that only disrupt external cell membranes and not membranes of organelles, which is important to prevent aggregation of magnetosomes [197]. Microfluidic platforms can be used to functionalize magnetosomes with antibodies or biocompatible polymers for biological applications (**Fig. 3d**) [198]. The advantages of using such a system in contrast to bulk magnetosome functionalization include saving on expensive reagents like antibodies and obtaining magnetosomes with more uniform and reproducible functionalization [199]. Furthermore, in biomedical applications, functionalization of magnetic nanoparticles with radioactive probes/molecules are usually performed on site [199]. A miniaturized microfluidic system capable of processing 10-25 mL could therefore facilitate timely functionalization of magnetosomes for clinical purposes. However, one caveat is that prototypical microfluidic platforms may not always be compatible with harsher solvents/chemicals used in functionalization [199], and PDMS may need to be substituted with materials such as glass.

## 4.0 Microfluidics for mechano-biology

Geometrical constraints in the natural habitat of MTB can influence the diffusion of nutrients, metabolic waste, and signals that trigger adaptation in the form of growth and mobility. Different microfluidic devices have been fabricated to investigate the role of spatial geometry on the ecological and evolutionary properties of bacteria [200]. Cho et al. showed that *E. coli* oriented and grew to respond to chamber shapes in a microfluidic device to minimize mechanical stresses induced by cell growth and promote efficient nutrient diffusion [201]. Takeuchi et al. also demonstrated the possibility of shaping *E. coli* into patterned shapes [202]. These microfluidic designs may be adapted to explore the mechano-biology of MTB. It will be interesting to understand how the rate of cell division, rate of magnetosome production, and regulation of shape and mobility of MTB are influenced by mechanical forces [203]. How MTB respond to mechanical forces may help inform the design of bioreactor geometry, surface roughness, and stirring rates to influence metabolism or magnetosome production. A recent study also found that the proportion of fine to coarse sand in the environment may influence the dominant species of MTB. Microfluidic devices may be useful for experimental validations of this observation [204].

Microfluidic platforms have also been developed to investigate differences in the stiffness and deformability of bacterial cells such as *E. coli* and their resistance to antibiotics [205]. These platforms offer much higher throughput than conventional tools like optical tweezers and atomic force microscopy [205]. Similar devices can be used to understand whether MTB with different numbers of magnetosomes have different stiffness which may enable high throughput isolation of sub-populations of interest using deformability-based cell cytometry [205].

**5.0 Conclusions and outlook**

Nano and microfluidic technologies are increasingly used for purposes such as single-cell analysis, nanoparticle functionalization, and investigations of cellular processes. Many of the described platforms have been used for cells of relevance to human health applications, like *E. coli*. However, the platforms can be easily adapted for under-studied and useful organisms like MTB through appropriate scaling and creative repurposing. For instance, magnetic microfluidic chips were first described for isolating cancer cells bound to magnetic beads but we have adapted this platform for isolating MTB mutants with different magnetosome numbers. Similar adaptation can be performed to generate microfluidic co-culture systems to understand the ecological roles of MTB. Or microfluidics can be used to analyze MTB behaviors in chemical and oxygen gradients. Microfluidics also has huge potential to improve our understanding of MTB biology and to expand the translational applications of MTB and magnesotomes. For instance, devices for lineage tracking can be used to understand magnetosome splitting during MTB cell division. Microtechnologies can also be used for directed evolution to generate MTB mutants that over-produce magnetosomes for biomedical applications. High throughput microfluidic bioreactors are equally useful for industrial scale culture of MTB and functionalization of magnetosomes. Our review aims to introduce MTB to researchers developing microtechnologies and vice versa. Our goal is that through more conversations between the two communities, there can be new micro-tools to advance our understanding of MTB and to manipulate MTB for scientific applications.

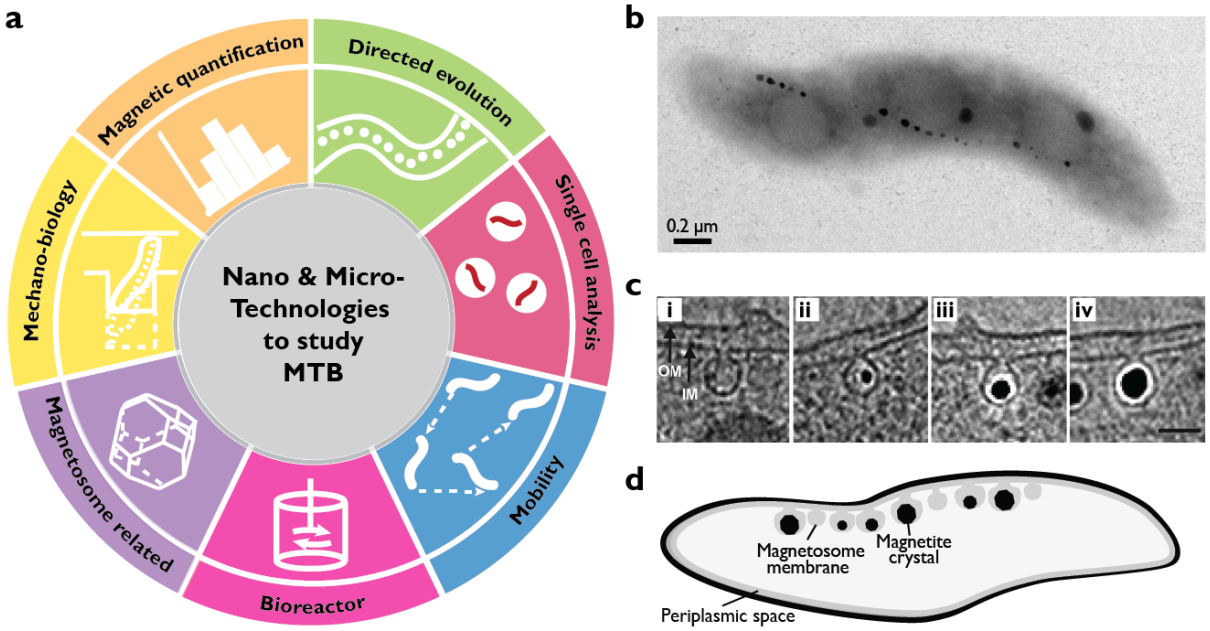


**Fig. 1** Applications of nano/microfluidics to study MTB. (**a**) Ideas include using nano and microfluidics for quantification of magnetic content, directed evolution and single cell analyses. Microfluidics can also be applied for industrial purposes such as on-chip purification and functionalization of magnetosomes. We also anticipate microfluidics technology as useful platforms to study biological processes like magneto-aerotaxis. (**b**) Transmission electron microscopic (TEM) image of a wild-type AMB-1. (**c**) Electron cryotomography of a wild-type AMB-1 magnetosome [206]. Image reproduced with permission from American Association for the Advancement of Science. (**i**) AMB-1 with magnetosome membrane and no magnetite. (**ii**) small magnetite crystal. (**iii**) growing magnetite crystal. (**iv**) full-sized magnetosome. Outer membrane (OM) and inner membrane (IM) are indicated. (**d**) Schematic of wild-type AMB-1 with empty magnetosome, growing magnetite crystals and full-sized magnetosomes.

**Table 1** Techniques for magnetic estimations of MTB

| | **C-mag** [207] | **Color inspection** [208] | **Electron microscope** [209] | **Optical magnetic imaging** [132] | **Magnetic ratcheting** [210] | **Magnetic microfluidic** [211,212] |
|---|---|---|---|---|---|---|
| **Time needed** | Fast (mins) | Slow (~2 weeks) | Slow (~2-3 hr) | Very fast (~s) | Fast (mins) | Fast (mins) |
| **Subjective** | No | Yes | Yes | No | No | No |
| **Automated** | No | No | No | Yes | Semi | Semi |
| **Quantitative** | Yes | No | Yes | Yes | Yes | Yes |
| **Throughput** | N.A. | N.A. | Low | Low | High | High |
| **Possible to re-culture** | Yes | Yes | No | Yes | Yes | Yes |
| **Potential for single cell selection** | No | No | No | No | Yes | Yes |
| **Potential for continuous flow** | N.A. | N.A. | N.A. | N.A. | No | Yes |

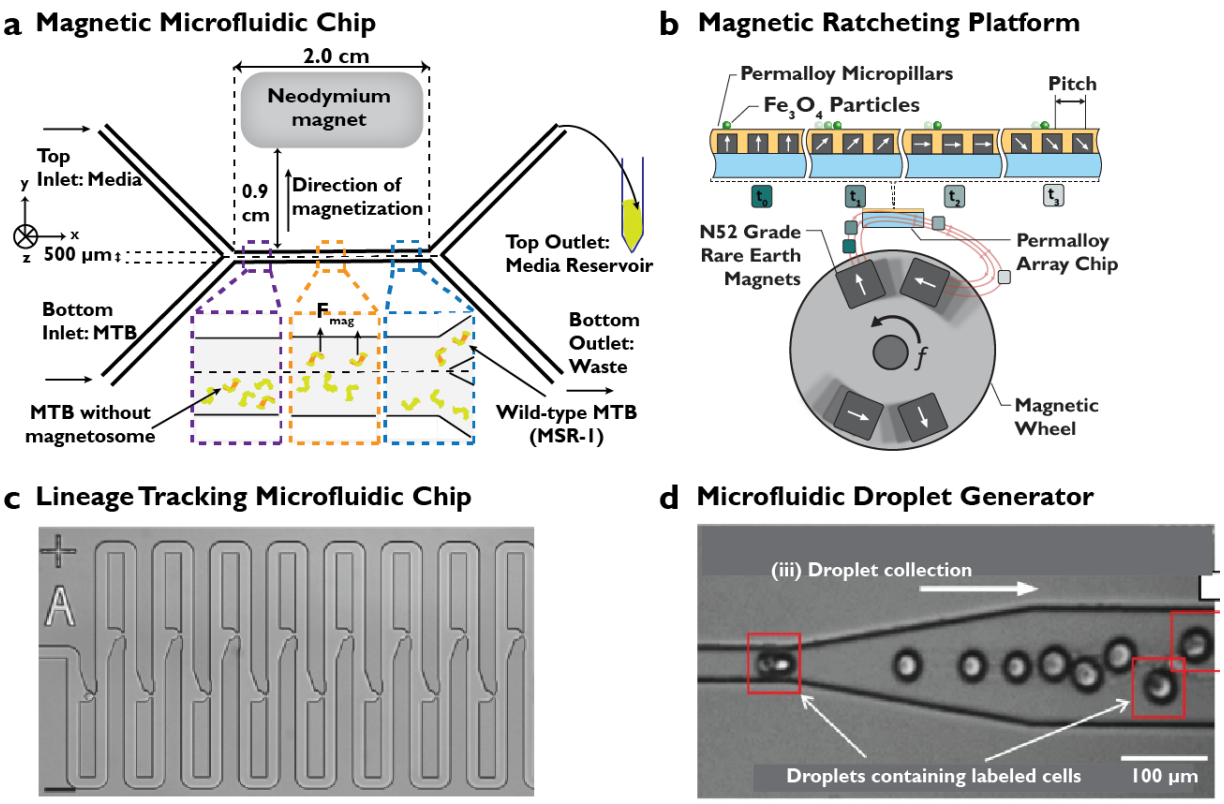


**Fig. 2** Microfluidics for magnetotactic bacteria (MTB) analysis. (**a**) Magnetic microfluidic chip that separates MTB based on their magnetic contents. MTB which are more magnetic are deflected by the magnetic field gradient across the fluid streams and exit through the selection outlet [212]. Reproduced with permission from American Society of Microbiology. (**b**) Magnetic ratcheting platform separates MTB based on the balance between magnetic forces and Stokes' drag. Combining random chemical mutagenesis and this device, AMB-1 over-producers producing 2.2 fold more magnetosomes than wild-type were generated [138]. Reproduced with permission from Wiley. (**c**) Lineages of cells can be tracked with this device as a newly dividing daughter cell is flushed to the next chamber for isolation [158]. Reproduced with permission from Nature Publishing Group. (**d**) Cells encapsulated in droplets can be better separated by magnetic fields due to reduced impact of cell motility [166]. Furthermore, droplets with MTB can be selected based on magnetic content and growth rates. Reproduced with permission from Royal Society of Chemistry.

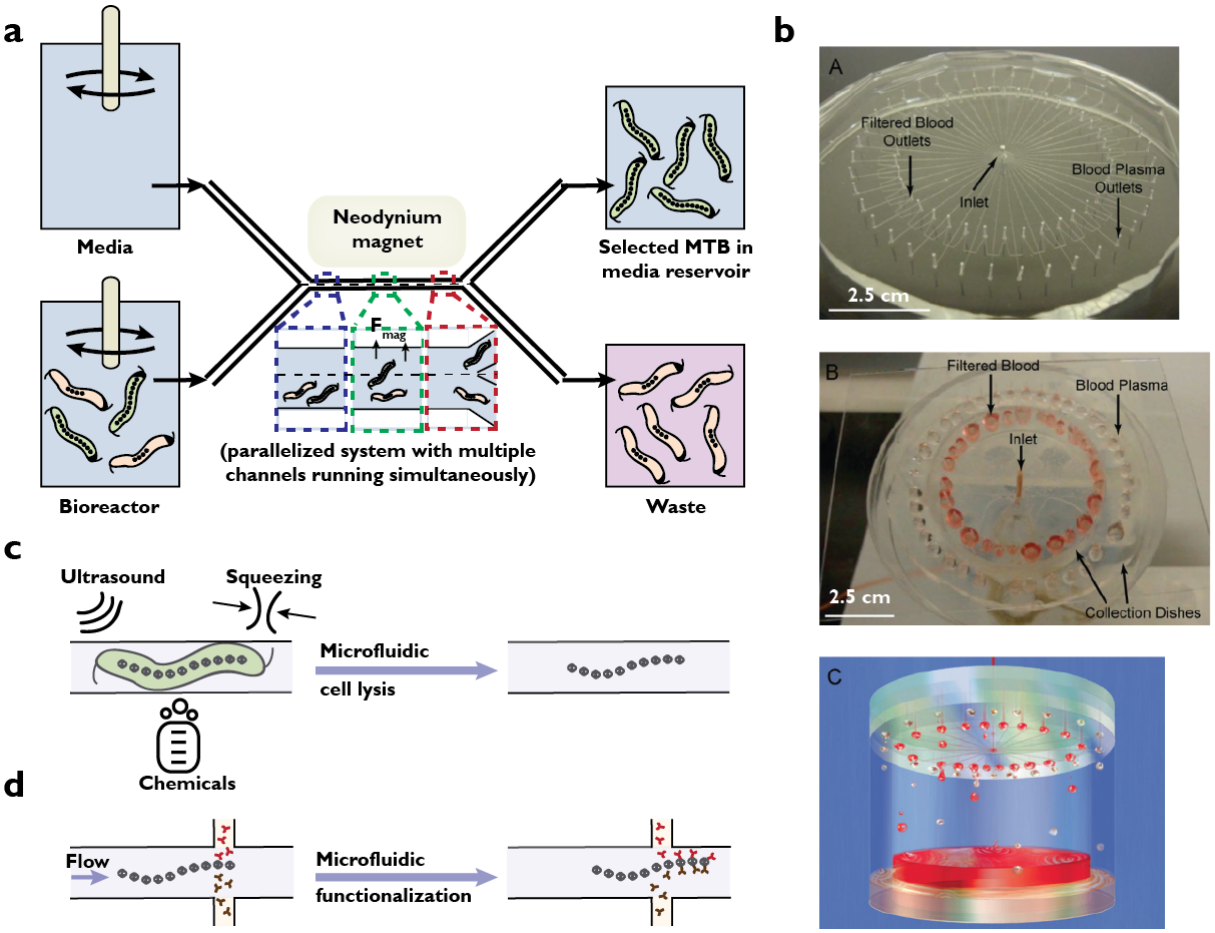


**Fig. 3** Microfluidics for industrial manipulation of MTB. (**a**) A parallelized version of a magnetic microfluidic chip [212] with multiple channels running simultaneously may be coupled to a bioreactor to investigate the effects of supplements in culture media on MTB growth and magnetosome production rate. (**b**) Example of systems incorporating radial microfluidic channels for scalable cell separations. Microfluidic channels can be patterned with nano/micro-magnets remotely magnetized by large external magnetic fields for high through-put MTB processing [213]. Image reproduced with permission from Wiley. (**c**) Microfluidic lysis of MTB with ultrasound, chemicals, or mechanical stresses. By performing cell lysis in microfluidic channels, there is potentially less magnetosome loss than bulk methods such as French-press. (**d**) Microfluidic functionalization of magnetosomes with antibodies or bio-polymers for biotechnological applications. This method helps to reduce waste of costly reagents like antibodies, thus leading to cost-savings. Furthermore, external magnetic fields may be used to orientate magnetosomes for homogenous functionalization.

CHAPTER 4

# Conclusions and future directions for global analysis of biomineralization genes in *Magnetospirillum magneticum* AMB-1

Hayley C McCausland

Department of Molecular and Cell Biology, University of California, Berkeley, USA

## Future Prospects/Directions

### Abstract

The work presented here laid the foundation for the next generation of large-scale genetic studies in MTB and identified new genes of interest to pursue in future studies. There is still much to be learned about genes involved in biomineralization and the behavior of MTB in their natural environment. Further magnetic selections using RB-TnSeq libraries will be useful to identify genes involved in biomineralization under different conditions. Following up on the functions and mechanisms of those genes and proteins will also be an important endeavor. Additionally, it will be valuable to use the power of RB-TnSeq to pursue other important questions in the field of MTB. First, studying genes required for MTB to grow and biomineralize in a natural environment. Second, examining which genes are required at the different stages [42] of growth and magnetosome formation.

### Nuanced roles of magnetosome island genes

An unexpected finding from our magnetic selection screens is that several MAI genes were identified in magnetic selection screens, indicating that they have a different (or more exaggerated) role in biomineralization under certain growth conditions. In particular, *mamT* and *mmsF* mutants had larger biomineralization defects in both anaerobic and high iron conditions, as compared to microaerobic and low iron conditions. MamT and MmsF have been studied in the past, but their exact functions in the process of biomineralization are still unclear. The work presented here showed that MamT does have a more critical role in biomineralization at higher iron concentrations or under anaerobic conditions. Because it has heme domains, it has been proposed that MamT is involved in regulating the balance of ferrous and ferric iron entering the magnetosome, potentially in conjunction with MamP, another magnetochrome protein [52]. The results here support that model, indicating that under conditions in which AMB-1 has an increase in magnetosome formation, the loss of MamT makes it more difficult for proteins, like MamP, that have some redundant function to compensate. Future studies should examine the phenotypes of MamT heme domain mutants under high iron and anaerobic conditions. It will also be important to study the function of MamT heme mutants in conjuction with MamP heme domain mutants.

There were also many genes outside the MGC that appear to be important for biomineralization, both in standard laboratory conditions and under altered growth conditions. Understanding the role these genes play and manipulating them may help with the fine tuning of magnetosome production for different applications. And while the genes identified in the screens presented in this work are annotated as hypothetical proteins that are only present in *Magnetospirilla*, this does not rule out that there are other interesting genes outside the MGC to study.

More important, however, than following up on individual genes will be future studies utilizing the power of the RB-TnSeq library. Now that the tool has been developed for use in AMB-1, we can readily adapt the technique to new screening methods. Two screens that expand on the work presented here—and that would make a significant impact on the field—include studying the formation of magnetosomes over time and observing AMB-1 in a simulated natural environment. Both of these screens would benefit from utilizing some of the microfluidics techniques described in Chapter 3 in order to have a more fine-grained magnetic selection, precisely control the environment, or separate out single cells to examine further.

**Biomineralization genes and environmental adaptation**

It has been shown that magnetosomes are only made under low oxygen concentrations [112]. Previous results have shown that the genes involved in maintaining redox balance in the cell are important for magnetosome formation [67–69,110,214]. However, it hasn't been shown if the redox balance is the direct cause of any biomineralization defects or if there are other genes involved in regulating magnetosome production in response to shifting oxygen concentrations. The results presented in Chapter 2 provide evidence that MTB do have a genetic response—and associated effect on magnetosome production—in response to changing oxygen conditions.

While previous research has shown that genes responsible for regulating the redox balance in the cell are critical for magnetosome formation, little has been done to link the genetic response to the dynamic environmental conditions MTB experience in their natural habitats. In the future, two different studies can build off each other to give a more complete picture of oxygen regulations and magnetosome formation. First, it would be useful conduct another experiment similar to the experiments in Chapter 2 where a magnetic selection as performed after the RB-TnSeq library was grown in microaerobic or anaerobic conditions. The new experiment would involve more tightly controlled oxygen conditions—growing the cells with 0%, 1%, 2%, and 5% oxygen—which will allow us to know precisely at what level of oxygen certain genes are needed for biomineralization. The second study would seek to mimic natural environmental conditions by growing an RB-TnSeq library in an oxygen gradient and determining which genes are important for biomineralization, which genes provide a fitness advantage, and which mutants migrate to a preferred oxygen concentration. The one caveat with this study is that the library would need to be created in an AMB-1 strain that is capable of swimming (our lab strain does not swim). These studies combined would provide valuable insight into how MTB respond to their environment.

**Genes required throughout the magnetosome formation process**

As described earlier, magnetosome formation is a step-wise process and many of the MAI genes involved in those steps have already been identified. Others are known to be involved in magnetosome formation, but it is not clear at which step exactly. Magnetosome formation requires increased iron uptake, protein trafficking, and membrane remodeling. Therefore, it is possible that there are genes outside the MAI that are important for magnetosome formation at different stages in the process. We could use RB-TnSeq to provide a more fine-grained picture of each step in the magnetosome formation process.

This study would involve growing the RB-TnSeq library without any iron, passaging the library, and then adding iron. Samples would be taken at time points every few hours in order to observe the formation of magnetosomes [90]. A magnetic selection would be performed on each sample to determine which mutants are underrepresented in the magnetic fraction. Some troubleshooting would be required to establish a magnetic selection that is sensitive to determine the difference between magnetosomes that do not form and magnetosomes that have stalled at a certain step in the process. However, having multiple time points may help confirm which genes are involved, as mutants that inhibit magnetosome formation in early stages will be depleted at all time points. This technique is advantageous compared to transcriptomic and proteomic studies. We know that MAI genes are constitutively expressed and it is likely that other genes involved in the magnetosome formation process are also expressed, regardless of whether or not the cell is building magnetosomes. An RB-TnSeq screen would allow us to go beyond transcription and translation to phenotype.

## APPENDIX

Potential growth conditions for AMB-1 using alternative electron acceptors and carbon sources

### Introduction:

Studies in MSR-1 have shown that phenotypes for some biomineralization genes are only revealed under specific growth conditions [64,67]. Those studies have focused on altering the electron acceptor available to MSR-1 for respiration. To date, no studies have experimented with electron acceptors other than nitrate and oxygen or changed the available electron donors. When AMB-1 was first cultured in the lab by Matsunaga et al. (1991), it was determined that it can grow with twelve different carbon sources [23]. Other than the Matsunaga et al. study, no experiments with alternative electron acceptors or donors in AMB-1 have been published. We tested growth of AMB-1 with several electron acceptor and donor pairs, in order to determine the full range of conditions permissive for biomineralization. This would allow for more detailed studies on how AMB-1 responds to its environment. The data presented here is not exhaustive and could be supplemented further.

### Results:

In order to explore the ability of AMB-1 to grow and biomineralize on alternative electron acceptors and donors, we selected a few acceptor/donor pairs: nitrate and succinate, fumarate and pyruvate, and fumarate and acetate (Table 1). The nitrate/succinate pair is essentially a simplified version of standard MG media. As such, it was not surprising that cells were able to grow in microaerobic conditions with nitrate/succinate media. Anaerobic growth was not tested with the nitrate/succinate media, though it is likely that cells would be able to grow and biomineralize under those conditions. As expected, cells were able to grow on ammonium/succinate media under microaerobic conditions and not under anaerobic conditions, where no electron acceptor is available. However, it is surprising that AMB-1 has a low Cmag value in the ammonium/succinate condition, since MSR-1 is able to biomineralize well when ammonium is used in place of nitrate as a nitrogen source [67].

AMB-1 cells were able to grow when fumarate was provided as an electron acceptor, but biomineralization was weak. In the fumarate/acetate growth condition, the maximum density of cells was also decreased. Adding nitrate back to the fumarate/pyruvate condition led to an increase in the Cmag, though cultures still did not reach typical WT Cmag values. And under anaerobic conditions, nitrate was necessary for both growth and biomineralization, indicating that AMB-1 does not use fumarate as an electron acceptor.

Proteomics data [215] showed that three proteins that encode for a tetrathionate reductase (Amb3286, Amb3287, and Amb3288) were present on the magnetosome membrane in a strain of AMB-1 with a catalytically inactive form of the magnetosome protein MamE (*mamE$^{PD}$)* [90]. This suggested that AMB-1 might be able to grow using tetrathionate as an electron acceptor. We tested growth and biomineralization of AMB-1 with tetrathionate, both microaerobically and anaerobically. The results suggest that AMB-1 is able to grow using tetrathionate as an electron acceptor, though it grows to a higher density when oxygen is also available as an electron acceptor. Cells are only able to weakly biomineralize when grown anaerobically with tetrathionate. Further study is necessary to determine the importance of tetrathionate reductases on the magnetosome membrane.

Overall, these data indicate that nitrate and oxygen are the primary electron acceptors for growth and biomineralization in AMB-1. It might be more fruitful for further experiments with growth conditions to focus on carbon sources or iron sources, as indicated in Matsunaga et al.

**Table 1**

| **Media** | **Microaerobic growth** | | **Anaerobic growth** | |
|---|---|---|---|---|
| | OD400 Max | Cmag Max | OD400 Max | Cmag Max |
| MG | 0.250 | 1.60 | 0.270 | 2.10 |
| Nitrate/Succinate | 0.250 | 1.60 | -- | -- |
| Ammonium/Succinate | 0.200 | 1.20 | 0.050 | 1.08 |
| Fumarate/Pyruvate | 0.200 | 1.10 | 0.060 | 1.12 |
| Fumarate/Pyruvate + Nitrate | 0.190 | 1.30 | 0.190 | 1.70 |
| Fumarate/Acetate | 0.142 | 1.10 | -- | -- |
| Tetrathionate/Succinate | 0.280 | 1.34 | 0.116 | 1.13 |

**Methods:**

**Growth and culture conditions**

As a control, *Magnetospirillum magneticum* AMB-1 was cultured in MG medium (as described in Ch. 2) supplemented with 1/100 vol of Wolfe's vitamin solution and 30μM ferric malate. To test alternative media conditions, a base media without any carbon sources, nitrogen sources, or electron donors was used (Table 2). Stocks of additional components at 100x concentration (molar equivalent to any electron or carbon sources in MG, pH 6.9) were made (Table 3) and added before inoculating cultures. For conditions that did not include sodium nitrate in the media, ammonium chloride was added as a nitrogen source.

Microaerobic growth cells were grown in culture tubes or 50mL conical tubes and incubated at 30°C in a microaerobic chamber with 10% oxygen. For anaerobic growth, sealed Balch tubes containing 10mL of MG medium and 20mL of headspace were used. Media was bubbled with $N_2$ gas for 10 min before sealing. Then headspace was flushed with $N_2$ gas for 10 min before autoclaving. Ferric malate and Wolfe's vitamins were added once tubes cooled. All cultures inoculated with a dilution factor of 1:100.

Table 2—Base media recipe

| **Media component** | **Amount per L** |
|---|---|
| L-ascorbic acid | 0.035 g |
| Sodium thiosulfate | 0.1 g |
| Potassium phosphate monobasic | 0.68 g |
| Wolfe's mineral solution | 5 mL |

Table 3—Nitrogen and carbon sources, 100x stocks

| **Media component** | **100x Concentration** |
|---|---|
| Succinic acid | 3M |
| Sodium pyruvate | 3M |
| Tartaric acid | 2.5M |
| Tetrathionate dihydrite | 1.4M |

| | |
|---|---|
| Sodium nitrate | 1.4M |
| Fumaric acid | 1.4M |
| Ammonium chloride | 1.4M |
| Sodium acetate | 0.85M |

REFERENCES


1. Lin W, Bazylinski DA, Xiao T, Wu L-F, Pan Y. Life with compass: diversity and biogeography of magnetotactic bacteria. Environ Microbiol. 2014;16(9):2646–58.

2. Amor M, Tharaud M, Gélabert A, Komeili A. Single-cell determination of iron content in magnetotactic bacteria: implications for the iron biogeochemical cycle. Environ Microbiol.

3. Lefèvre CT, Bazylinski DA. Ecology, Diversity, and Evolution of Magnetotactic Bacteria. Microbiol Mol Biol Rev MMBR. 2013 Sep;77(3):497–526.

4. Grant CR, Wan J, Komeili A. Organelle Formation in Bacteria and Archaea. Annu Rev Cell Dev Biol. 2018 Oct 6;34(1):217–38.

5. Rahn-Lee L, Komeili A. The magnetosome model: insights into the mechanisms of bacterial biomineralization. Front Microbiol. 2013;4.

6. Lin W, Pan Y, Bazylinski DA. Diversity and ecology of and biomineralization by magnetotactic bacteria. Environ Microbiol Rep. 2017;9(4):345–56.

7. Frankel RB, Bazylinski DA, Johnson MS, Taylor BL. Magneto-aerotaxis in marine coccoid bacteria. Biophys J. 1997 Aug;73(2):994–1000.

8. Blakemore R. Magnetotactic bacteria. Science. 1975 Oct 24;190(4212):377–9.

9. Kopp RE, Kirschvink JL. The identification and biogeochemical interpretation of fossil magnetotactic bacteria. Earth-Sci Rev. 2008 Jan 1;86(1):42–61.

10. Lin W, Paterson GA, Zhu Q, Wang Y, Kopylova E, Li Y, et al. Origin of microbial biomineralization and magnetotaxis during the Archean. Proc Natl Acad Sci U S A. 2017 28;114(9):2171–6.

11. Lin W, Kirschvink JL, Paterson GA, Bazylinski DA, Pan Y. On the origin of microbial magnetoreception. Natl Sci Rev.

12. Jimenez-Lopez C, Romanek CS, Bazylinski DA. Magnetite as a prokaryotic biomarker: A review. J Geophys Res Biogeosciences. 2010 Jun;115(G2):n/a-n/a.

13. Yan L, Da H, Zhang S, López VM, Wang W. Bacterial magnetosome and its potential application. Microbiol Res. 2017 Oct 1;203:19–28.

14. Alphandéry E. Applications of magnetosomes synthesized by magnetotactic bacteria in medicine. Front Bioeng Biotechnol. 2014;2:5.

15. Vargas G, Cypriano J, Correa T, Leão P, Bazylinski DA, Abreu F. Applications of Magnetotactic Bacteria, Magnetosomes and Magnetosome Crystals in Biotechnology and Nanotechnology: Mini-Review. Mol Basel Switz. 2018 Sep 24;23(10).

16. Fukuda Y, Okamura Y, Takeyama H, Matsunaga T. Dynamic analysis of a genomic island in Magnetospirillum sp. strain AMB-1 reveals how magnetosome synthesis developed. FEBS Lett. 2006 Feb 6;580(3):801–12.

17. Schübbe S, Kube M, Scheffel A, Wawer C, Heyen U, Meyerdierks A, et al. Characterization of a spontaneous nonmagnetic mutant of Magnetospirillum gryphiswaldense reveals a large deletion comprising a putative magnetosome island. J Bacteriol. 2003 Oct;185(19):5779–90.

18. Ullrich S, Kube M, Schübbe S, Reinhardt R, Schüler D. A hypervariable 130-kilobase genomic region of Magnetospirillum gryphiswaldense comprises a magnetosome island which undergoes frequent rearrangements during stationary growth. J Bacteriol. 2005 Nov;187(21):7176–84.

19. Lefèvre CT, Trubitsyn D, Abreu F, Kolinko S, Jogler C, de Almeida LGP, et al. Comparative genomic analysis of magnetotactic bacteria from the Deltaproteobacteria provides new insights into magnetite and greigite magnetosome genes required for magnetotaxis. Environ Microbiol. 2013 Oct;15(10):2712–35.

20. Lin W, Zhang W, Zhao X, Roberts AP, Paterson GA, Bazylinski DA, et al. Genomic expansion of magnetotactic bacteria reveals an early common origin of magnetotaxis with lineage-specific evolution. ISME J. 2018 Jun;12(6):1508.

21. Blakemore RP, Maratea D, Wolfe RS. Isolation and pure culture of a freshwater magnetic spirillum in chemically defined medium. J Bacteriol. 1979 Nov;140(2):720–9.

22. Matsunaga T, Nakamura C, Burgess JG, Sode K. Gene transfer in magnetic bacteria: transposon mutagenesis and cloning of genomic DNA fragments required for magnetosome synthesis. J Bacteriol. 1992 May;174(9):2748–53.

23. Matsunaga T, Sakaguchi T, Tadakoro F. Magnetite formation by a magnetic bacterium capable of growing aerobically. Appl Microbiol Biotechnol. 1991 Aug 1;35(5):651–5.

24. Schleifer KH, Schüler D, Spring S, Weizenegger M, Amann R, Ludwig W, et al. The Genus Magnetospirillum gen. nov. Description of Magnetospirillum gryphiswaldense sp. nov. and Transfer of Aquaspirillum magnetotacticum to Magnetospirillum magnetotacticum comb. nov. Syst Appl Microbiol. 1991 Oct 1;14(4):379–85.

25. Nakamura C, Burgess JG, Sode K, Matsunaga T. An Iron-regulated Gene, magA, Encoding an Iron Transport Protein of Magnetospirillum sp. Strain AMB-1. J Biol Chem. 1995 Nov 24;270(47):28392–6.

26. Wahyudi AT, Takeyama H, Matsunaga T. Isolation of Magnetospirillum magneticum AMB-1 mutants defective in bacterial magnetic particle synthesis by transposon mutagenesis. Appl Biochem Biotechnol. 2001;91–93:147–54.

27. Schübbe S, Williams TJ, Xie G, Kiss HE, Brettin TS, Martinez D, et al. Complete Genome Sequence of the Chemolithoautotrophic Marine Magnetotactic Coccus Strain MC-1. Appl Env Microbiol. 2009 Jul 15;75(14):4835–52.

28. Smalley MD, Marinov GK, Bertani LE, DeSalvo G. Genome Sequence of Magnetospirillum magnetotacticum Strain MS-1. Genome Announc. 2015 Apr 2;3(2).

29. Grünberg K, Wawer C, Tebo BM, Schüler D. A large gene cluster encoding several magnetosome proteins is conserved in different species of magnetotactic bacteria. Appl Environ Microbiol. 2001 Oct;67(10):4573–82.

30. Schübbe S, Würdemann C, Peplies J, Heyen U, Wawer C, Glöckner FO, et al. Transcriptional organization and regulation of magnetosome operons in Magnetospirillum gryphiswaldense. Appl Environ Microbiol. 2006 Sep;72(9):5757–65.

31. Schultheiss D, Schüler D. Development of a genetic system for Magnetospirillum gryphiswaldense. Arch Microbiol. 2003 Feb;179(2):89–94.

32. Matsunaga T, Okamura Y, Fukuda Y, Wahyudi AT, Murase Y, Takeyama H. Complete genome sequence of the facultative anaerobic magnetotactic bacterium Magnetospirillum sp. strain AMB-1. DNA Res Int J Rapid Publ Rep Genes Genomes. 2005;12(3):157–66.

33. Komeili A, Vali H, Beveridge TJ, Newman DK. Magnetosome vesicles are present before magnetite formation, and MamA is required for their activation. Proc Natl Acad Sci U S A. 2004 Mar 16;101(11):3839–44.

34. Grünberg K, Müller E-C, Otto A, Reszka R, Linder D, Kube M, et al. Biochemical and proteomic analysis of the magnetosome membrane in Magnetospirillum gryphiswaldense. Appl Environ Microbiol. 2004 Feb;70(2):1040–50.

35. Murat D, Quinlan A, Vali H, Komeili A. Comprehensive genetic dissection of the magnetosome gene island reveals the step-wise assembly of a prokaryotic organelle. Proc Natl Acad Sci U S A. 2010 Mar 23;107(12):5593–8.

36. Rioux J-B, Philippe N, Pereira S, Pignol D, Wu L-F, Ginet N. A second actin-like MamK protein in Magnetospirillum magneticum AMB-1 encoded outside the genomic magnetosome island. PloS One. 2010 Feb 10;5(2):e9151.

37. Abreu N, Mannoubi S, Ozyamak E, Pignol D, Ginet N, Komeili A. Interplay between two bacterial actin homologs, MamK and MamK-Like, is required for the alignment of magnetosome organelles in Magnetospirillum magneticum AMB-1. J Bacteriol. 2014 Sep;196(17):3111–21.

38. Wang X, Wang Q, Zhang W, Wang Y, Li L, Wen T, et al. Complete Genome Sequence of Magnetospirillum gryphiswaldense MSR-1. Genome Announc. 2014 Mar 13;2(2).

39. Lohße A, Borg S, Raschdorf O, Kolinko I, Tompa É, Pósfai M, et al. Genetic Dissection of the mamAB and mms6 Operons Reveals a Gene Set Essential for Magnetosome Biogenesis in Magnetospirillum gryphiswaldense. J Bacteriol. 2014 Jul;196(14):2658–69.

40. Lohße A, Ullrich S, Katzmann E, Borg S, Wanner G, Richter M, et al. Functional Analysis of the Magnetosome Island in Magnetospirillum gryphiswaldense: The mamAB Operon Is Sufficient for Magnetite Biomineralization. PLoS ONE [Internet]. 2011 Oct 17 [cited 2019 Feb 7];6(10). Available from: https://www.ncbi.nlm.nih.gov/pmc/articles/PMC3197154/

41. Kolinko I, Lohße A, Borg S, Raschdorf O, Jogler C, Tu Q, et al. Biosynthesis of magnetic nanostructures in a foreign organism by transfer of bacterial magnetosome gene clusters. Nat Nanotechnol. 2014 Mar;9(3):193–7.

42. Cornejo E, Subramanian P, Li Z, Jensen GJ, Komeili A. Dynamic Remodeling of the Magnetosome Membrane Is Triggered by the Initiation of Biomineralization. mBio. 2016 Mar 2;7(1):e01898-15.

43. Raschdorf O, Forstner Y, Kolinko I, Uebe R, Plitzko JM, Schüler D. Genetic and Ultrastructural Analysis Reveals the Key Players and Initial Steps of Bacterial Magnetosome Membrane Biogenesis. PLOS Genet. 2016 Jun 10;12(6):e1006101.

44. Uebe R, Junge K, Henn V, Poxleitner G, Katzmann E, Plitzko JM, et al. The cation diffusion facilitator proteins MamB and MamM of Magnetospirillum gryphiswaldense have distinct and complex functions, and are involved in magnetite biomineralization and magnetosome membrane assembly. Mol Microbiol. 2011 Nov;82(4):818–35.

45. Murat D, Falahati V, Bertinetti L, Csencsits R, Körnig A, Downing K, et al. The magnetosome membrane protein, MmsF, is a major regulator of magnetite biomineralization in Magnetospirillum magneticum AMB-1. Mol Microbiol. 2012 Aug;85(4):684–99.

46. Siponen MI, Legrand P, Widdrat M, Jones SR, Zhang W-J, Chang MCY, et al. Structural insight into magnetochrome-mediated magnetite biomineralization. Nature. 2013 Oct 31;502(7473):681–4.

47. Rawlings AE, Bramble JP, Walker R, Bain J, Galloway JM, Staniland SS. Self-assembled MmsF proteinosomes control magnetite nanoparticle formation in vitro. Proc Natl Acad Sci. 2014 Nov 11;111(45):16094–9.

48. Kashyap S, Woehl TJ, Liu X, Mallapragada SK, Prozorov T. Nucleation of Iron Oxide Nanoparticles Mediated by Mms6 Protein in Situ. ACS Nano. 2014 Sep 23;8(9):9097–106.

49. Amemiya Y, Arakaki A, Staniland SS, Tanaka T, Matsunaga T. Controlled formation of magnetite crystal by partial oxidation of ferrous hydroxide in the presence of recombinant magnetotactic bacterial protein Mms6. Biomaterials. 2007 Dec;28(35):5381–9.

50. Yamagishi A, Tanaka M, Lenders JJM, Thiesbrummel J, Sommerdijk NAJM, Matsunaga T, et al. Control of magnetite nanocrystal morphology in magnetotactic bacteria by regulation of mms7 gene expression. In: Scientific reports. 2016.

51. Arakaki A, Yamagishi A, Fukuyo A, Tanaka M, Matsunaga T. Co-ordinated functions of Mms proteins define the surface structure of cubo-octahedral magnetite crystals in magnetotactic bacteria. Mol Microbiol. 2014 Aug;93(3):554–67.

52. Jones SR, Wilson TD, Brown ME, Rahn-Lee L, Yu Y, Fredriksen LL, et al. Genetic and biochemical investigations of the role of MamP in redox control of iron biomineralization in Magnetospirillum magneticum. Proc Natl Acad Sci U S A. 2015 Mar 31;112(13):3904–9.

53. Scheffel A, Gruska M, Faivre D, Linaroudis A, Plitzko JM, Schüler D. An acidic protein aligns magnetosomes along a filamentous structure in magnetotactic bacteria. Nature. 2006 Mar;440(7080):110–4.

54. Komeili A, Li Z, Newman DK, Jensen GJ. Magnetosomes are cell membrane invaginations organized by the actin-like protein MamK. Science. 2006 Jan 13;311(5758):242–5.

55. Draper O, Byrne ME, Li Z, Keyhani S, Barrozo JC, Jensen G, et al. MamK, a bacterial actin, forms dynamic filaments in vivo that are regulated by the acidic proteins MamJ and LimJ. Mol Microbiol. 2011 Oct;82(2):342–54.

56. Toro-Nahuelpan M, Müller FD, Klumpp S, Plitzko JM, Bramkamp M, Schüler D. Segregation of prokaryotic magnetosomes organelles is driven by treadmilling of a dynamic actin-like MamK filament. BMC Biol. 2016 12;14(1):88.

57. Ozyamak E, Kollman J, Agard DA, Komeili A. The bacterial actin MamK: in vitro assembly behavior and filament architecture. J Biol Chem. 2013 Feb 8;288(6):4265–77.

58. Toro-Nahuelpan M, Giacomelli G, Raschdorf O, Borg S, Plitzko JM, Bramkamp M, et al. MamY is a membrane-bound protein that aligns magnetosomes and the motility axis of helical magnetotactic bacteria. Nat Microbiol. 2019 Jul 29;

59. Katzmann E, Scheffel A, Gruska M, Plitzko JM, Schüler D. Loss of the actin-like protein MamK has pleiotropic effects on magnetosome formation and chain assembly in Magnetospirillum gryphiswaldense. Mol Microbiol. 2010;77(1):208–24.

60. Taoka A, Kiyokawa A, Uesugi C, Kikuchi Y, Oestreicher Z, Morii K, et al. Tethered Magnets Are the Key to Magnetotaxis: Direct Observations of Magnetospirillum magneticum AMB-1 Show that MamK Distributes Magnetosome Organelles Equally to Daughter Cells. mBio. 2017 08;8(4).

61. Uebe R, Schüler D. Magnetosome biogenesis in magnetotactic bacteria. Nat Rev Microbiol. 2016 13;14(10):621–37.

62. Barber-Zucker S, Zarivach R. A Look into the Biochemistry of Magnetosome Biosynthesis in Magnetotactic Bacteria. ACS Chem Biol. 2017 20;12(1):13–22.

63. Schüler D. Genetics and cell biology of magnetosome formation in magnetotactic bacteria. FEMS Microbiol Rev. 2008;32(4):654–72.

64. Raschdorf O, Müller FD, Pósfai M, Plitzko JM, Schüler D. The magnetosome proteins MamX, MamZ and MamH are involved in redox control of magnetite biomineralization in Magnetospirillum gryphiswaldense. Mol Microbiol. 2013 Sep;89(5):872–86.

65. Müller FD, Raschdorf O, Nudelman H, Messerer M, Katzmann E, Plitzko JM, et al. The FtsZ-Like Protein FtsZm of Magnetospirillum gryphiswaldense Likely Interacts with Its Generic Homolog and Is Required for Biomineralization under Nitrate Deprivation. J Bacteriol. 2014 Feb 1;196(3):650–9.

66. Ding Y, Li J, Liu J, Yang J, Jiang W, Tian J, et al. Deletion of the ftsZ-Like Gene Results in the Production of Superparamagnetic Magnetite Magnetosomes in Magnetospirillum gryphiswaldense. J Bacteriol. 2010 Feb;192(4):1097–105.

67. Li Y, Katzmann E, Borg S, Schüler D. The Periplasmic Nitrate Reductase Nap Is Required for Anaerobic Growth and Involved in Redox Control of Magnetite Biomineralization in Magnetospirillum gryphiswaldense. J Bacteriol. 2012 Sep 15;194(18):4847–56.

68. Li Y, Raschdorf O, Silva KT, Schüler D. The Terminal Oxidase cbb3 Functions in Redox Control of Magnetite Biomineralization in Magnetospirillum gryphiswaldense. J Bacteriol. 2014 Jul;196(14):2552–62.

69. Li Y, Sabaty M, Borg S, Silva KT, Pignol D, Schüler D. The oxygen sensor MgFnr controls magnetite biomineralization by regulation of denitrification in Magnetospirillum gryphiswaldense. BMC Microbiol. 2014 Jun 10;14(1):153.

70. Fillat MF. The FUR (ferric uptake regulator) superfamily: Diversity and versatility of key transcriptional regulators. Arch Biochem Biophys. 2014 Mar 15;546:41–52.

71. Uebe R, Voigt B, Schweder T, Albrecht D, Katzmann E, Lang C, et al. Deletion of a fur-like gene affects iron homeostasis and magnetosome formation in Magnetospirillum gryphiswaldense. J Bacteriol. 2010 Aug;192(16):4192–204.

72. Rong C, Huang Y, Zhang W, Jiang W, Li Y, Li J. Ferrous iron transport protein B gene (feoB1) plays an accessory role in magnetosome formation in Magnetospirillum gryphiswaldense strain MSR-1. Res Microbiol. 2008 Oct;159(7–8):530–6.

73. Suzuki T, Okamura Y, Calugay RJ, Takeyama H, Matsunaga T. Global Gene Expression Analysis of Iron-Inducible Genes in Magnetospirillum magneticum AMB-1. J Bacteriol. 2006 Mar;188(6):2275–9.

74. Taoka A, Umeyama C, Fukumori Y. Identification of iron transporters expressed in the magnetotactic bacterium Magnetospirillum magnetotacticum. Curr Microbiol. 2009 Feb;58(2):177–81.

75. Wang Q, Wang M, Wang X, Guan G, Li Y, Peng Y, et al. Iron Response Regulator Protein IrrB in Magnetospirillum gryphiswaldense MSR-1 Helps Control the Iron/Oxygen Balance, Oxidative Stress Tolerance, and Magnetosome Formation. Appl Environ Microbiol. 2015 Dec;81(23):8044–53.

76. Lin W, Deng A, Wang Z, Li Y, Wen T, Wu L-F, et al. Genomic insights into the uncultured genus “Candidatus Magnetobacterium” in the phylum Nitrospirae. ISME J. 2014 Dec;8(12):2463–77.

77. Sakaguchi T, Burgess JG, Matsunaga T. Magnetite formation by a sulphate-reducing bacterium. Nature. 1993 Sep;365(6441):47.

78. Sakaguchi T, Arakaki A, Matsunaga T. Desulfovibrio magneticus sp. nov., a novel sulfate-reducing bacterium that produces intracellular single-domain-sized magnetite particles. Int J Syst Evol Microbiol. 2002 Jan;52(1):215–21.

79. Rahn-Lee L, Byrne ME, Zhang M, Sage DL, Glenn DR, Milbourne T, et al. A Genetic Strategy for Probing the Functional Diversity of Magnetosome Formation. PLOS Genet. 2015 Jan 8;11(1):e1004811.

80. Grant CR, Rahn-Lee L, LeGault KN, Komeili A. Genome Editing Method for the Anaerobic Magnetotactic Bacterium Desulfovibrio magneticus RS-1. Appl Env Microbiol. 2018 Nov 15;84(22):e01724-18.

81. Byrne ME, Ball DA, Guerquin-Kern J-L, Rouiller I, Wu T-D, Downing KH, et al. Desulfovibrio magneticus RS-1 contains an iron- and phosphorus-rich organelle distinct from its bullet-shaped magnetosomes. Proc Natl Acad Sci. 2010 Jul 6;107(27):12263–8.

82. Kolinko S, Richter M, Glöckner F-O, Brachmann A, Schüler D. Single-cell genomics of uncultivated deep-branching magnetotactic bacteria reveals a conserved set of magnetosome genes. Environ Microbiol. 2016 Jan;18(1):21–37.

83. Descamps ECT, Monteil CL, Menguy N, Ginet N, Pignol D, Bazylinski DA, et al. Desulfamplus magnetovallimortis gen. nov., sp. nov., a magnetotactic bacterium from a brackish desert spring able to biomineralize greigite and magnetite, that represents a novel lineage in the Desulfobacteraceae. Syst Appl Microbiol. 2017 Jul;40(5):280–9.

84. Monteil CL, Perrière G, Menguy N, Ginet N, Alonso B, Waisbord N, et al. Genomic study of a novel magnetotactic Alphaproteobacteria uncovers the multiple ancestry of magnetotaxis. Environ Microbiol. 2018 Dec;20(12):4415–30.

85. Lefèvre CT, Menguy N, Abreu F, Lins U, Pósfai M, Prozorov T, et al. A cultured greigite-producing magnetotactic bacterium in a novel group of sulfate-reducing bacteria. Science. 2011 Dec 23;334(6063):1720–3.

86. DeLong EF, Frankel RB, Bazylinski DA. Multiple Evolutionary Origins of Magnetotaxis in Bacteria. Science. 1993;259(5096):803–6.

87. Abreu F, Cantão ME, Nicolás MF, Barcellos FG, Morillo V, Almeida LG, et al. Common ancestry of iron oxide- and iron-sulfide-based biomineralization in magnetotactic bacteria. ISME J. 2011 Oct;5(10):1634–40.

88. Lefèvre CT, Trubitsyn D, Abreu F, Kolinko S, Almeida LGP de, Vasconcelos ATR de, et al. Monophyletic origin of magnetotaxis and the first magnetosomes. Environ Microbiol. 2013;15(8):2267–74.

89. Yang W, Li R, Peng T, Zhang Y, Jiang W, Li Y, et al. mamO and mamE genes are essential for magnetosome crystal biomineralization in Magnetospirillum gryphiswaldense MSR-1. Res Microbiol. 2010 Oct;161(8):701–5.

90. Quinlan A, Murat D, Vali H, Komeili A. The HtrA/DegP family protease MamE is a bifunctional protein with roles in magnetosome protein localization and magnetite biomineralization. Mol Microbiol. 2011 May;80(4):1075–87.

91. Hershey DM, Ren X, Melnyk RA, Browne PJ, Ozyamak E, Jones SR, et al. MamO Is a Repurposed Serine Protease that Promotes Magnetite Biomineralization through Direct Transition Metal Binding in Magnetotactic Bacteria. PLoS Biol. 2016 Mar;14(3):e1002402.

92. Hershey DM, Browne PJ, Iavarone AT, Teyra J, Lee EH, Sidhu SS, et al. Magnetite Biomineralization in Magnetospirillum magneticum Is Regulated by a Switch-like Behavior in the HtrA Protease MamE. J Biol Chem. 2016 19;291(34):17941–52.

93. Wetmore KM, Price MN, Waters RJ, Lamson JS, He J, Hoover CA, et al. Rapid Quantification of Mutant Fitness in Diverse Bacteria by Sequencing Randomly Bar-Coded Transposons. mBio. 2015 Jul 1;6(3):e00306-15.

94. Chen H, Zhang S-D, Chen L, Cai Y, Zhang W-J, Song T, et al. Efficient Genome Editing of Magnetospirillum magneticum AMB-1 by CRISPR-Cas9 System for Analyzing Magnetotactic Behavior. Front Microbiol. 2018 Jul 17;9.

95. Peters JM, Colavin A, Shi H, Czarny TL, Larson MH, Wong S, et al. A Comprehensive, CRISPR-based Functional Analysis of Essential Genes in Bacteria. Cell. 2016 Jun 2;165(6):1493–506.

96. Peters JM, Koo B-M, Patino R, Heussler GE, Hearne CC, Qu J, et al. Enabling genetic analysis of diverse bacteria with Mobile-CRISPRi. Nat Microbiol. 2019 Feb;4(2):244–50.

97. Tay A, Pfeiffer D, Rowe K, Tannenbaum A, Popp F, Strangeway R, et al. High-Throughput Microfluidic Sorting of Live Magnetotactic Bacteria. Appl Env Microbiol. 2018 Sep 1;84(17):e01308-18.

98. Tay A, McCausland H, Komeili A, Carlo DD. Nano and Microtechnologies for the Study of Magnetotactic Bacteria. Adv Funct Mater. 2019;29(38):1904178.

99. Wen T, Guo F, Zhang Y, Tian J, Li Y, Li J, et al. A novel role for Crp in controlling magnetosome biosynthesis in Magnetospirillum gryphiswaldense MSR-1. Sci Rep. 2016 Feb 16;6:21156.

100. Lefèvre CT, Bennet M, Landau L, Vach P, Pignol D, Bazylinski DA, et al. Diversity of magneto-aerotactic behaviors and oxygen sensing mechanisms in cultured magnetotactic bacteria. Biophys J. 2014 Jul 15;107(2):527–38.

101. Popp F, Armitage JP, Schüler D. Polarity of bacterial magnetotaxis is controlled by aerotaxis through a common sensory pathway. Nat Commun. 2014 Nov 14;5:5398.

102. Simmons SL, Sievert SM, Frankel RB, Bazylinski DA, Edwards KJ. Spatiotemporal distribution of marine magnetotactic bacteria in a seasonally stratified coastal salt pond. Appl Environ Microbiol. 2004 Oct;70(10):6230–9.

103. Flies CB, Jonkers HM, de Beer D, Bosselmann K, Böttcher ME, Schüler D. Diversity and vertical distribution of magnetotactic bacteria along chemical gradients in freshwater microcosms. FEMS Microbiol Ecol. 2005 Apr 1;52(2):185–95.

104. Liu J, Zhang W, Du H, Leng X, Li J-H, Pan H, et al. Seasonal changes in the vertical distribution of two types of multicellular magnetotactic prokaryotes in the sediment of Lake Yuehu, China. Environ Microbiol Rep. 2018;10(4):475–84.

105. Moisescu C, Ardelean II, Benning LG. The effect and role of environmental conditions on magnetosome synthesis. Front Microbiol. 2014 Feb 11;5.

106. Bazylinski DA, Lefèvre CT. Magnetotactic bacteria from extreme environments. Life Basel Switz. 2013 Mar 26;3(2):295–307.

107. Monteil CL, Lefevre CT. Magnetoreception in Microorganisms. Trends Microbiol [Internet]. 2019 Nov 18 [cited 2019 Nov 30];0(0). Available from: https://www.cell.com/trends/microbiology/abstract/S0966-842X(19)30267-7

108. McCausland HC, Komeili A. Magnetic genes: Studying the genetics of biomineralization in magnetotactic bacteria. PLOS Genet. 2020 Feb 13;16(2):e1008499.

109. Wang Q, Liu J-X, Zhang W-J, Zhang T-W, Yang J, Li Y. Expression patterns of key iron and oxygen metabolism genes during magnetosome formation in Magnetospirillum gryphiswaldense MSR-1. FEMS Microbiol Lett. 2013 Oct 1;347(2):163–72.

110. Wang X, Wang Q, Zhang Y, Wang Y, Zhou Y, Zhang W, et al. Transcriptome analysis reveals physiological characteristics required for magnetosome formation in Magnetospirillum gryphiswaldense MSR-1. Environ Microbiol Rep. 2016;8(3):371–81.

111. Wang Q, Wang X, Zhang W, Li X, Zhou Y, Li D, et al. Physiological characteristics of Magnetospirillum gryphiswaldense MSR-1 that control cell growth under high-iron and low-oxygen conditions. Sci Rep. 2017 05;7(1):2800.

112. Heyen U, Schüler D. Growth and magnetosome formation by microaerophilic Magnetospirillum strains in an oxygen-controlled fermentor. Appl Microbiol Biotechnol. 2003 Jun 1;61(5):536–44.

113. Amor M, Tharaud M, Gélabert A, Komeili A. Single-cell determination of iron content in magnetotactic bacteria: implications for the iron biogeochemical cycle. bioRxiv. 2019 Feb 5;541953.

114. Price MN, Wetmore KM, Waters RJ, Callaghan M, Ray J, Liu H, et al. Mutant phenotypes for thousands of bacterial genes of unknown function. Nature. 2018 May 16;557(7706):503–9.

115. Tanaka M, Mazuyama E, Arakaki A, Matsunaga T. MMS6 protein regulates crystal morphology during nano-sized magnetite biomineralization in vivo. J Biol Chem. 2011 Feb 25;286(8):6386–92.

116. Silva KT, Schüler M, Mickoleit F, Zwiener T, Müller FD, Awal RP, et al. Genome-Wide Identification of Essential and Auxiliary Gene Sets for Magnetosome Biosynthesis in Magnetospirillum gryphiswaldense. mSystems [Internet]. 2020 Dec 22 [cited 2020 Nov 19];5(6). Available from: https://msystems.asm.org/content/5/6/e00565-20

117. Liu H, Shiver AL, Price MN, Carlson HK, Trotter VV, Chen Y, et al. Functional genetics of human gut commensal Bacteroides thetaiotaomicron reveals metabolic requirements for growth across environments. Cell Rep. 2021 Mar 2;34(9):108789.

118. Mickoleit F, Borkner CB, Toro-Nahuelpan M, Herold HM, Maier DS, Plitzko JM, et al. In Vivo Coating of Bacterial Magnetic Nanoparticles by Magnetosome Expression of Spider Silk-Inspired Peptides. Biomacromolecules. 2018 Mar 12;19(3):962–72.

119. Felfoul O, Mohammadi M, Taherkhani S, de Lanauze D, Zhong Xu Y, Loghin D, et al. Magneto-aerotactic bacteria deliver drug-containing nanoliposomes to tumour hypoxic regions. Nat Nanotechnol. 2016 Nov;11(11):941–7.

120. Araujo ACV, Abreu F, Silva KT, Bazylinski DA, Lins U. Magnetotactic bacteria as potential sources of bioproducts. Mar Drugs. 2015 Jan 16;13(1):389–430.

121. Mahmoudi M, Tachibana A, Goldstone AB, Woo YJ, Chakraborty P, Lee KR, et al. Novel MRI Contrast Agent from Magnetotactic Bacteria Enables In Vivo Tracking of iPSC-derived Cardiomyocytes. Sci Rep. 2016 Jun 6;6:26960.

122. Chen C, Chen L, Yi Y, Chen C, Wu L-F, Song T. Killing of Staphylococcus aureus via Magnetic Hyperthermia Mediated by Magnetotactic Bacteria. Appl Environ Microbiol. 2016 Feb 12;82(7):2219–26.

123. Chen C, Wang S, Li L, Wang P, Chen C, Sun Z, et al. Bacterial magnetic nanoparticles for photothermal therapy of cancer under the guidance of MRI. Biomaterials. 2016 Oct;104:352–60.

124. Tay A, Kunze A, Murray C, Di Carlo D. Induction of Calcium Influx in Cortical Neural Networks by Nanomagnetic Forces. ACS Nano. 2016 Jan 28;

125. Lu H, Schmidt M a, Jensen KF. A microfluidic electroporation device for cell lysis. Lab Chip. 2005;5(1):23–9.

126. Gomez L, Sebastian V, Irusta S, Ibarra A, Arruebo M, Santamaria J. Scaled-up production of plasmonic nanoparticles using microfluidics: From metal precursors to functionalized and sterilized nanoparticles. Lab Chip. 2014;

127. Xia N, Hunt TP, Mayers BT, Alsberg E, Whitesides GM, Westervelt RM, et al. Combined microfluidic-micromagnetic separation of living cells in continuous flow. Biomed Microdevices. 2006 Dec;8(4):299–308.

128. Warkiani ME, Tay AKP, Guan G, Han J. Membrane-less microfiltration using inertial microfluidics. Sci Rep. 2015 Jul 8;5:11018.

129. Bhagat AAS, Bow H, Hou HW, Tan SJ, Han J, Lim CT. Microfluidics for cell separation. Med Biol Eng Comput. 2010 Oct;48(10):999–1014.

130. Bazylinski DA, Garratt-Reed AJ, Frankel RB. Electron microscopic studies of magnetosomes in magnetotactic bacteria. Microsc Res Tech. 1994;27(5):389–401.

131. Zhao L, Wu D, Wu L-F, Song T. A simple and accurate method for quantification of magnetosomes in magnetotactic bacteria by common spectrophotometer. J Biochem Biophys Methods. 2007 Apr 10;70(3):377–83.

132. Le Sage D, Arai K, Glenn DR, DeVience SJ, Pham LM, Rahn-Lee L, et al. Optical magnetic imaging of living cells. Nature. 2013 Apr 25;496(7446):486–9.

133. Woehl TJ, Kashyap S, Firlar E, Perez-Gonzalez T, Faivre D, Trubitsyn D, et al. Correlative electron and fluorescence microscopy of magnetotactic bacteria in liquid: toward in vivo imaging. Sci Rep. 2014 Jan;4:6854.

134. Eder SHK, Gigler AM, Hanzlik M, Winklhofer M. Sub-micrometer-scale mapping of magnetite crystals and sulfur globules in magnetotactic bacteria using confocal raman micro-spectrometry. PLoS ONE. 2014;9(9).

135. Myklatun A, Cappetta M, Winklhofer M, Ntziachristos V, Westmeyer GG. Microfluidic sorting of intrinsically magnetic cells under visual control. Sci Rep. 2017;7(1):6942.

136. Tay A, Pfeiffer D, Rowe K, Tannenbaum A, Popp F, Strangeway R, et al. High-throughput microfluidic sorting of live magnetotactic bacteria. Appl Environ Microbiol. 2018 Jun 29;AEM.01308-18.

137. Tay AKP. Acute and Chronic Neural Stimulation via Mechano-Sensitive Ion Channels. Springer; 2017. 129 p.

138. Tay A, Murray C, Di Carlo D. Phenotypic Selection of Magnetospirillum magneticum (AMB-1) Overproducers Using Magnetic Ratcheting. Adv Funct Mater. 2017 Sep 5;1703106.

139. Liang X, Shi H, Jia X, Yang Y, Liu X. Dispersibility, Shape and Magnetic Properties of Nano-$Fe_3O_4$ Particles. Mater Sci Appl. 2011;02(11):1644–53.

140. Vácha R, Martinez-Veracoechea FJ, Frenkel D. Receptor-mediated endocytosis of nanoparticles of various shapes. Nano Lett. 2011 Dec 14;11(12):5391–5.

141. Brunner TJ, Wick P, Manser P, Spohn P, Grass RN, Limbach LK, et al. In vitro cytotoxicity of oxide nanoparticles: comparison to asbestos, silica, and the effect of particle solubility. Environ Sci Technol. 2006 Jul 15;40(14):4374–81.

142. Hou Y, Xu Z, Sun S. Controlled synthesis and chemical conversions of FeO nanoparticles. Angew Chem - Int Ed. 2007;46(33):6329–32.

143. Liu J, Ding Y, Jiang W, Tian J, Li Y, Li J. A mutation upstream of an ATPase gene significantly increases magnetosome production in Magnetospirillum gryphiswaldense. Appl Microbiol Biotechnol. 2008;81(3):551–8.

144. Lohße A, Kolinko I, Raschdorf O, Uebe R, Borg S, Brachmann A, et al. Overproduction of magnetosomes by genomic amplification of biosynthetic gene clusters in a magnetotactic bacterium. Appl Environ Microbiol. 2016 Mar 11;

145. Badran AH, Liu DR. In vivo continuous directed evolution. Curr Opin Chem Biol. 2015 Feb;24:1–10.

146. Arakaki A, Webb J, Matsunaga T. A novel protein tightly bound to bacterial magnetic particles in Magnetospirillum magneticum strain AMB-1. J Biol Chem. 2003 Mar 7;278(10):8745–50.

147. Yin X, Stotzky G. Gene transfer among bacteria in natural environments. Adv Appl Microbiol. 1997;45:153–212.

148. Tanaka M, Mazuyama E, Arakaki A, Matsunaga T. MMS6 protein regulates crystal morphology during nano-sized magnetite biomineralization in vivo. J Biol Chem. 2011 Feb 25;286(8):6386–92.

149. Murat D, Falahati V, Bertinetti L, Csencsits R, Körnig A, Downing K, et al. The magnetosome membrane protein, MmsF, is a major regulator of magnetite biomineralization in Magnetospirillum magneticum AMB-1. Mol Microbiol. 2012 Aug;85(4):684–99.

150. Zhao X, Huang X, Wang X, Wu Y, Eisfeld AK, Schwind S, et al. Nanochannel Electroporation as a Platform for Living Cell Interrogation in Acute Myeloid Leukemia. Adv Sci. 2015;2(12).

151. Dower WJ, Miller JF, Ragsdale CW. High efficiency transformation of E.coli by high voltage electroporation. Nucleic Acids Res. 1988;

152. Garcia P a, Ge Z, Moran JL, Buie CR. Microfluidic Screening of Electric Fields for Electroporation. Sci Rep. 2016;6(August 2015):21238.

153. Okamura Y, Takeyama H, Sekine T, Sakaguchi T, Wahyudi AT, Sato R, et al. Design and application of a new cryptic-plasmid-based shuttle vector for Magnetospirillum magneticum. Appl Environ Microbiol. 2003 Jul;69(7):4274–7.

154. Shalek AK, Robinson JT, Karp ES, Lee JS, Ahn D-R, Yoon M-H, et al. Vertical silicon nanowires as a universal platform for delivering biomolecules into living cells. Proc Natl Acad Sci. 2010;107(5):1870–5.

155. Cao Y, Hjort M, Chen H, Birey F, Leal-Ortiz SA, Han CM, et al. Nondestructive nanostraw intracellular sampling for longitudinal cell monitoring. Proc Natl Acad Sci. 2017;201615375.

156. Wu F, Dekker C. Nanofabricated structures and microfluidic devices for bacteria: from techniques to biology. Chem Soc Rev. 2015;1:268–80.

157. Kimmerling RJ, Lee Szeto G, Li JW, Genshaft AS, Kazer SW, Payer KR, et al. A microfluidic platform enabling single-cell RNA-seq of multigenerational lineages. Nat Commun. 2016;7:10220.

158. Kolinko I, Jogler C, Katzmann E, Schüler D. Frequent mutations within the genomic magnetosome island of magnetospirillum gryphiswaldense are mediated by RecA. J Bacteriol. 2011;193(19):5328–34.

159. Jogler C, Niebler M, Lin W, Kube M, Wanner G, Kolinko S, et al. Cultivation-independent characterization of “Candidatus Magnetobacterium bavaricum” via ultrastructural, geochemical, ecological and metagenomic methods. Environ Microbiol. 2010;

160. Staniland SS, Moisescu C, Benning LG. Cell division in magnetotactic bacteria splits magnetosome chain in half. J Basic Microbiol. 2010;50(4):392–6.

161. Kim HJ, Boedicker JQ, Choi JW, Ismagilov RF. Defined spatial structure stabilizes a synthetic multispecies bacterial community. Proc Natl Acad Sci U S A. 2008;105(47):18188–93.

162. Tanaka M, Knowles W, Brown R, Hondow N, Arakaki A, Baldwin S, et al. Biomagnetic recovery of selenium: Bioaccumulating of selenium granules in magnetotactic bacteria. Appl Environ Microbiol. 2016 Apr 22;AEM.00508-16-.

163. Zare RN, Kim S. Microfluidic platforms for single-cell analysis. Annu Rev Biomed Eng. 2010 Aug 15;12:187–201.

164. Mazutis L, Gilbert J, Ung WL, Weitz DA, Griffiths AD, Heyman JA. Single-cell analysis and sorting using droplet-based microfluidics. Nat Protoc. 2013 May;8(5):870–91.

165. Chen A, Byvank T, Chang W-J, Bharde A, Vieira G, Miller BL, et al. On-chip magnetic separation and encapsulation of cells in droplets. Lab Chip. 2013;13(6):1172–81.

166. Chen L, Manz A, Day PJR. Total nucleic acid analysis integrated on microfluidic devices. Lab Chip. 2007;7(11):1413–23.

167. Brouzes E, Kruse T, Kimmerling R, Strey HH. Rapid and continuous magnetic separation in droplet microfluidic devices. Lab Chip. 2015;15(3):908–19.

168. Khalil ISM, Tabak AF, Hageman T, Ewis M, Pichel M, Mitwally ME, et al. Near-surface effects on the controlled motion of magnetotactic bacteria. In: 2017 IEEE International Conference on Robotics and Automation (ICRA). IEEE; 2017. p. 5976–82.

169. Rismani Yazdi S, Nosrati R, Stevens CA, Vogel D, Davies PL, Escobedo C. Magnetotaxis Enables Magnetotactic Bacteria to Navigate in Flow. Small. 2018 Feb 1;14(5):1702982.

170. Ma Q, Chen C, Wei S, Chen C, Wu LF, Song T. Construction and operation of a microrobot based on magnetotactic bacteria in a microfluidic chip. Biomicrofluidics. 2012;6(2).

171. Kaehr B, Shear JB. High-throughput design of microfluidics based on directed bacterial motility. Lab Chip. 2009;9(207890):2632–7.

172. Martel S, Mohammadi M, Felfoul O, Zhao Lu, Pouponneau P. Flagellated magnetotactic bacteria as controlled MRI-trackable propulsion and steering systems for medical nanorobots operating in the human microvasculature. Int J Robot Res. 2009;

173. Ahmed T, Shimizu TS, Stocker R. Microfluidics for bacterial chemotaxis. Integr Biol. 2010;2(11–12):604.

174. Waisbord N, Lefèvre C, Bocquet L, Ybert C, Cottin-Bizonne C. Environment-dependent swimming strategy of Magnetococcus marinus under magnetic field. 2016 Mar 1;

175. Loehr J, Pfeiffer D, Schüler D, Fischer TM. Magnetic guidance of the magnetotactic bacterium Magnetospirillum gryphiswaldense. Soft Matter. 2016 Mar 14;

176. Rusconi R, Garren M, Stocker R. Microfluidics Expanding the Frontiers of Microbial Ecology. Annu Rev Biophys. 2014;43(1):65–91.

177. Smith MJ, Sheehan PE, Perry LL, O'Connor K, Csonka LN, Applegate BM, et al. Quantifying the magnetic advantage in magnetotaxis. Biophys J. 2006 Aug 1;91(3):1098–107.

178. Bennet M, McCarthy A, Fix D, Edwards MR, Repp F, Vach P, et al. Influence of magnetic fields on magneto-aerotaxis. PLoS ONE. 2014;

179. Adler M, Erickstad M, Gutierrez E, Groisman A. Studies of bacterial aerotaxis in a microfluidic device. Lab Chip. 2012;12(22):4835–47.

180. Adler M, Polinkovsky M, Gutierrez E, Groisman A. Generation of oxygen gradients with arbitrary shapes in a microfluidic device. Lab Chip. 2010;10(3):388–91.

181. Li N, Luo C, Zhu X, Chen Y, Ouyang Q, Zhou L. Microfluidic generation and dynamically switching of oxygen gradients applied to the observation of cell aerotactic behaviour. In: Microelectronic Engineering. 2011. p. 1698–701.

182. Mao H, Cremer PS, Manson MD. A sensitive, versatile microfluidic assay for bacterial chemotaxis. Proc Natl Acad Sci U S A. 2003 Apr 29;100(9):5449–54.

183. Englert DL, Manson MD, Jayaraman A. Investigation of bacterial chemotaxis in flow-based microfluidic devices. Nat Protoc. 2010 May;5(5):864–72.

184. Kim JYH, Kwak HS, Sung YJ, Choi H Il, Hong ME, Lim HS, et al. Microfluidic high-throughput selection of microalgal strains with superior photosynthetic productivity using competitive phototaxis. Sci Rep. 2016;6:21155.

185. Chen C, Ma Q, Jiang W, Song T. Phototaxis in the magnetotactic bacterium Magnetospirillum magneticum strain AMB-1 is independent of magnetic fields. Appl Microbiol Biotechnol. 2011;90(1):269–75.

186. Silva KT, Leão PE, Abreu F, López JA, Gutarra ML, Farina M, et al. Optimization of magnetosome production and growth by the magnetotactic vibrio Magnetovibrio blakemorei strain MV-1 through a statistics-based experimental design. Appl Environ Microbiol. 2013;79(8):2823–7.

187. Ali I, Peng C, Khan ZM, Naz I. Yield cultivation of magnetotactic bacteria and magnetosomes: A review. J Basic Microbiol. 2017 Apr 1;

188. Vyawahare S, Griffiths AD, Merten CA. Miniaturization and parallelization of biological and chemical assays in microfluidic devices. Chem Biol. 2010 Oct 29;17(10):1052–65.

189. Shimoshige H, Kobayashi H, Mizuki T, Nagaoka Y, Inoue A, Maekawa T. Effect of Polyethylene Glycol on the Formation of Magnetic Nanoparticles Synthesized by Magnetospirillum magnetotacticum MS-1. PloS One. 2015;10(5):e0127481.

190. Li J, Pan Y. AMB-1: Implications for Biologically Controlled Mineralization. Geomicrobiol J. 2012;29(4):362–73.

191. Micheletti M, Lye GJ. Microscale bioprocess optimisation. Curr Opin Biotechnol. 2006 Dec;17(6):611–8.

192. Mach AJ, Di Carlo D. Continuous scalable blood filtration device using inertial microfluidics. Biotechnol Bioeng. 2010 Oct 1;107(2):302–11.

193. Tseng P, Judy JW, Di Carlo D. Magnetic nanoparticle-mediated massively parallel mechanical modulation of single-cell behavior. Nat Methods. 2012;9(11):1113–9.

194. Nevill JT, Cooper R, Dueck M, Breslauer DN, Lee LP. Integrated microfluidic cell culture and lysis on a chip. Lab Chip. 2007 Dec;7(12):1689–95.

195. Bao N, Lu C. A microfluidic device for physical trapping and electrical lysis of bacterial cells. Appl Phys Lett. 2008;92(21).

196. Valencia PM, Farokhzad OC, Karnik R, Langer R. Microfluidic technologies for accelerating the clinical translation of nanoparticles. Nat Nanotechnol. 2012 Oct;7(10):623–9.

197. Lu H, Schmidt MA, Jensen KF. A microfluidic electroporation device for cell lysis. Lab Chip. 2005 Jan;5(1):23–9.

198. Gomez L, Sebastian V, Irusta S, Ibarra A, Arruebo M, Santamaria J. Scaled-up production of plasmonic nanoparticles using microfluidics: from metal precursors to functionalized and sterilized nanoparticles. Lab Chip. 2014 Jan 21;14(2):325–32.

199. Cho H, J??nsson H, Campbell K, Melke P, Williams JW, Jedynak B, et al. Self-organization in high-density bacterial colonies: Efficient crowd control. PLoS Biol. 2007;5(11):2614–23.

200. Kimmerling RJ, Lee Szeto G, Li JW, Genshaft AS, Kazer SW, Payer KR, et al. A microfluidic platform enabling single-cell RNA-seq of multigenerational lineages. Nat Commun. 2016 Jan 6;7:10220.

201. Takeuchi S, DiLuzio WR, Weibel DB, Whitesides GM. Controlling the shape of filamentous cells of Escherichia coli. Nano Lett. 2005 Sep;5(9):1819–23.

202. Männik J, Driessen R, Galajda P, Keymer JE, Dekker C. Bacterial growth and motility in sub-micron constrictions. Proc Natl Acad Sci U S A. 2009 Sep 1;106(35):14861–6.

203. Xu C, Zhang W, Pan H, Du H, Xiao T. Distribution and diversity of magnetotactic bacteria in sediments of the Yellow Sea continental shelf. J Soils Sediments. 2018 Jul 10;18(7):2634–46.

204. Sun X, Weinlandt WD, Patel H, Wu M, Hernandez CJ. A microfluidic platform for profiling biomechanical properties of bacteria. Lab Chip. 2014 Jul 21;14(14):2491–8.

205. Tse HTK, Gossett DR, Moon YS, Masaeli M, Sohsman M, Ying Y, et al. Quantitative diagnosis of malignant pleural effusions by single-cell mechanophenotyping. Sci Transl Med. 2013 Nov 20;5(212):212ra163.

206. Komeili A, Li Z, Newman DK, Jensen GJ. Magnetosomes are cell membrane invaginations organized by the actin-like protein MamK. Science. 2006 Jan 13;311(5758):242–5.

207. Zhao L, Wu D, Wu L-F, Song T. A simple and accurate method for quantification of magnetosomes in magnetotactic bacteria by common spectrophotometer. J Biochem Biophys Methods. 2007 Apr 10;70(3):377–83.

208. Murray C, Pao E, Tseng P, Aftab S, Kulkarni R, Rettig M, et al. Quantitative Magnetic Separation of Particles and Cells Using Gradient Magnetic Ratcheting. Small Weinh Bergstr Ger. 2016 Apr 13;12(14):1891–9.

209. Bazylinski DA, Garratt-Reed AJ, Frankel RB. Electron microscopic studies of magnetosomes in magnetotactic bacteria. Microsc Res Tech. 1994 Apr 1;27(5):389–401.

210. Fossum S, Crooke E, Skarstad K. Organization of sister origins and replisomes during multifork DNA replication in Escherichia coli. EMBO J. 2007 Oct 31;26(21):4514–22.

211. Myklatun A, Cappetta M, Winklhofer M, Ntziachristos V, Westmeyer GG. Microfluidic sorting of intrinsically magnetic cells under visual control. Sci Rep. 2017 Jul 31;7(1):6942.

212. Tay A, Pfeiffer D, Rowe K, Tannenbaum A, Popp F, Strangeway R, et al. High-Throughput Microfluidic Sorting of Live Magnetotactic Bacteria. Appl Environ Microbiol. 2018 Sep 1;84(17):e01308-18.

213. Tseng P, Judy JW, Di Carlo D. Magnetic nanoparticle-mediated massively parallel mechanical modulation of single-cell behavior. Nat Methods. 2012 Nov;9(11):1113–9.

214. Zhang Y, Wen T, Guo F, Geng Y, Liu J, Peng T, et al. The Disruption of an OxyR-Like Protein Impairs Intracellular Magnetite Biomineralization in Magnetospirillum gryphiswaldense MSR-1. Front Microbiol. 2017;8:208.

215. Browne PJ. Regulation of Biomineralization in Magnetotactic Bacteria [Internet] [Ph.D.]. [United States -- California]: University of California, Berkeley; [cited 2021 Jul 26]. Available from: http://www.proquest.com/dissertations/docview/2031162629/abstract/DEE9BD8C6BC64D47PQ/1